AFFIDAVIT

I declare that I have authored this thesis independently, that I have not used other than the declared sources/resources, and that I have explicitly indicated all material which has been quoted either literally or by content from the sources used. The text document uploaded to TUGRAZonline is identical to the present master‘s thesis dissertation.

13.05.2015

Date

Signature

DANKSAGUNG

An erster Stelle möchte ich mich bei meiner Familie und besonders bei meinen Eltern Gudrun und Edgar Albrecht für die großzügige und bedingungslose Unterstützung während meiner gesamten Ausbildungszeit bedanken. Euer Vertrauen hat mir viel Kraft gegeben. Danke!

Ganz besonders bedanke ich mich bei meinen Betreuern dieser Masterarbeit Ass.Prof. Dr. Harald Pichler und Dr. Barbara Petschacher für die ausgezeichnete Betreuung und Begleitung und die vielen fruchtbaren Diskussionen.
Mein besonderer Dank gilt Holly Stolterfoht, die mich stets hilfsbereit bei meinen Aufgaben unterstützt hat. Ich danke auch Dr. Martin Lehmann für die gute Zusammenarbeit. Ohne das gute Zusammenwirken aller Beteiligten wäre diese Arbeit nicht möglich gewesen. Der kollegiale Umgang innerhalb des Projekt-Teams und der gesamten Pichler-Gruppe war stets harmonisch und ich werde immer gerne an diese Zeit zurück denken.

Ich danke Prof. Dr. Erich Leitner und seinem Team für die GC-MS Messungen meiner Sterol-Proben.

Danksagen will ich auch allen ACIB- und Instituts-Kollegen für die schöne Zeit und die wertvollen Gespräche.

Allen mir nahestehenden Personen, Freunden und Studienkollegen danke ich für die schöne Zeit in Graz.

ABSTRACT

Functionality of numerous membrane proteins relies on the presence of specific sterols in the membrane. Sterol-O-Acyltransferases (SOATs) play key roles in cellular sterol homeostasis due to formation of steryl esters and are being investigated for decades as potential drug targets against atherosclerosis, cancer and Alzheimer's disease. SOATs have multiple transmembrane domains, so we reasoned that sterols are not only used as substrates but on top of that also function as important structural interaction partners. The main sterol found in membranes depends on the organism. For example, cholesterol is present in mammals, whereas ergosterol is formed in yeast. Here, a set of modified yeast strains is introduced for *in vivo* investigation of SOAT substrate preferences in different sterol environments. For that purpose, *Saccharomyces cerevisiae* was re-programmed to produce more than 99% cholesterol, ensuring a sterol environment more similar to mammals. Next, the activities of seven microbial and mammalian SOATs were compared, upon expressing them in a CEN.PK2 *are1are2* knockout strain background producing either ergosterol or mammalian sterols. The results suggest that the two isoenzymes SOAT1 and SOAT2 of *Rattus norvegicus* are very substrate selective for different sterols. SOAT1 prefers to acylate ergosterol, whereas SOAT2 is highly active on cholesterol and acylates only trace amounts of ergosterol.

KURZFASSUNG

Die Funktionalität vieler Membranproteine wird durch bestimmte Sterole in der Membran beeinflusst. Sterol-O-Acyltransferasen (SOATs) spielen eine Schlüsselrolle bei der Regulierung des zellulären Sterol-Haushalts durch die Bildung von Sterylester und werden deshalb seit Jahrzehnten als mögliche Angriffsziele für Arzneimittel gegen Arteriosklerose, Krebs und Alzheimer untersucht. SOATs haben mehrere Transmembran-Domänen, sodass wir annehmen können, dass Sterole sowohl als Substrat, als auch als wichtige strukturelle Interaktionspartner fungieren. Hier wird ein neues Hefe-System vorgestellt, mit dessen Hilfe die Substratpräferenzen von SOATs in verschiedenen Sterol-Umgebungen *in vivo* untersucht werden können. Ergosterol wird normalerweise in Hefe gebildet, während Cholesterin in Säugetieren vorkommt. Um die Sterol-Umgebung an jene von Säugetieren anzugleichen wurde die Hefe *Saccharomyces cerevisiae* so umprogrammiert, dass sie über 99% Cholesterin produziert. In dieser Studie wurde die Aktivität von sieben SOATs aus Mikroben und Säugern in CEN.PK2 *are1are2* Knockout-Stämmen verglichen, die entweder Ergosterol, oder diverse tierische Sterole produzieren. Die erzielten Resultate deuten darauf hin, dass die Isoenzyme SOAT1 und SOAT2 von *Rattus norvegicus* hohe Selektivität für unterschiedliche Sterole zeigen; SOAT1 bevorzugt Ergosterol, während SOAT2 hauptsächlich Cholesterin und nur Spuren von Ergosterol acyliert.

CONTENTS

1 INTRODUCTION

1.1 Function and structure of sterols

In this study, we focus on one category of extraordinary bio-molecules, namely sterols. We examine their characteristics and potential for enhancing heterologous expression of specific integral membrane enzymes from higher eukaryotes in yeast. Sterols are major lipid compounds in eukaryotes and are involved in multiple cellular functions such as the permeability and curvature of membranes (Mullner and Daum 2004; Lucero and Robbins 2004), endocytosis through interaction with sphingolipids (Souza and Pichler 2007) and signal transduction (Cherezov et al. 2007; Head et al. 2013). Also, sterols are important for activity of various membrane proteins in terms of protein sorting through formation of membrane lipid rafts (Umebayashi and Nakano 2003), stabilizing proteins structurally (Gimpl and Fahrenholz 2002; Hirz et al. 2013) and sterols even serve as interaction partners for regulating channel, transporter and receptor functions (Gimpl et al. 1997; Opekarova and Tanner 2003; Levitan et al. 2014). With great power comes great responsibility and terrible diseases arise when regulation mechanisms of sterol homeostasis fail. Numerous reviews describe critical roles of cholesterol on severe medical issues (Porter& Herman 2011; Kanungo et al. 2013).

What are the features of these special compounds? Sterols are bulky but relatively flat amphiphilic compounds, consisting of a variable side chain attached to sterane, an aliphatic tetracyclic system composed of three 6-carbon rings and one 5-carbon ring (Figure 1). In addition, sterols have a small polar entity namely a hydroxyl group at the 3-position of the A-ring. Introduction and reduction of double bonds influence the three-dimensional structure depending on the location where the modification occurs (Figure 2). Desaturation at C8(9) between ring B and C for example gives zymosterol a planar ring conformation, whereas other sterols with desaturation at positions C5 or C7 have a slightly more twisted conformation. Double bonds within the side chain give a more rigid structure while fully reduced side chains are very flexible. Also conjugated systems can exist as shown for ergosterol and 7-dehydrocholesterol.

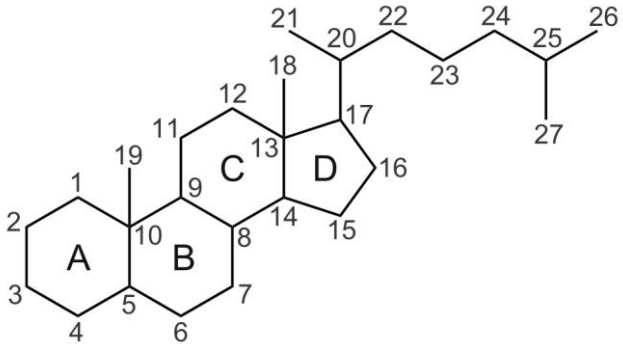

Figure 1: Structure of cholestane. Formula from wikipedia.org. For guidelines on lipid annotation see Fahy et al. (2005).

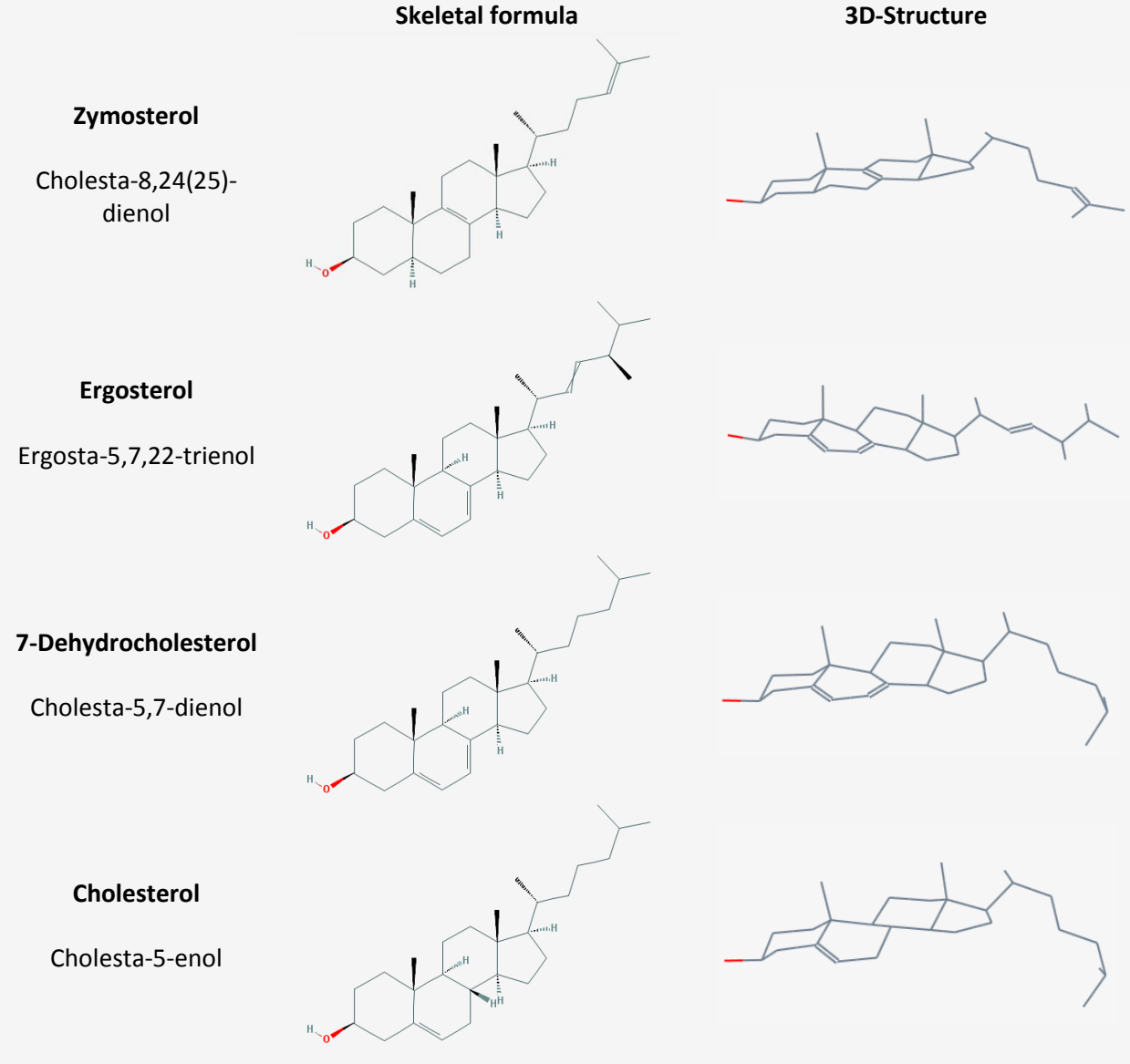

Figure 2: Structural differences of selected sterols. Images taken from NCBI PubChem Compound Database (CID=92746, 439550, 439423, 5997).

1.2 Sterol pathway engineering

Plants produce so-called phytosterols, for instance campesterol, sitosterol, and stigmasterol. By contrast, mammals contain mainly cholesterol, whereas fungi including yeast contain ergosterol. It is not surprising that the huge diversity of naturally occurring sterols has an important influence on functional expression of membrane proteins from higher eukaryotes in yeast. So there is a huge demand to further analyze protein-sterol/lipid interactions for basic research and pharmaceutical purposes (Wriessnegger and Pichler 2013). Moreover, sterols themselves are industrially relevant for the production of vitamins and steroid hormones. So it is beneficial to use simple model organisms like yeast for inexpensive production and ease in manipulation.

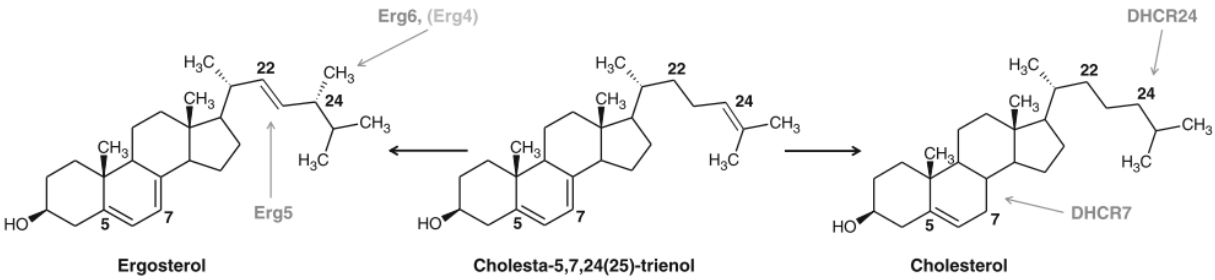

Figure 3: Sterol engineering strategy. Ergosterol or cholesterol formation from cholesta-5,7,24(25)-trienol. Taken from Hirz et al. (2013)

A tremendous effort has been made to determine sterol structures and the enzymes responsible for their synthesis. Native biosynthetic pathways, recently reviewed for mammals (Acimovic and Rozman 2013) and yeast (Kristan and Rižner 2012), lead to different end products but share conserved reaction steps and precursors. Published in the year 2011, Souza et al. used this circumstance to re-program *S. cerevisiae* to stably produce cholesterol (≈ 96%) instead of ergosterol (Figure 3) by exchanging yeast C-24 methyl-transferase and C-22 desaturase for mammalian C-7 and C-24 reductases. Later on, a *P. pastoris* cholesterol strain was successfully applied for improved expression of a complex integral membrane protein, namely a human Na,K-ATPase isoform (Hirz et al. 2013).

1.3 Protein-Sterol Interaction

Due to the amphiphilic nature of sterols, their polar heads face the membrane surface, while the rest is embedded inside the membrane. Thus, interaction between sterols and proteins predominantly occurs through transmembrane domains (TMDs) that cross the lipid bilayer. The molecular basis for allosteric regulation and protein stability is still subject to extensive research. As summarized by Fantini and Barrantes (2013), certain kinds of residues have been identified to be important (Figure 4). Basic amino acids like lysine and arginine interact with the polar hydroxyl-group that face the membrane surface. Aromatic side chains of tyrosine and phenylalanine can stack onto the sterane ring structure through CH-π interactions and branched aliphatic residues like isoleucine, valine or leucine can interpenetrate the rough side of the sterol and its aliphatic chain through van der Waals interactions. Motifs like the Cholesterol Recognition/interaction Amino acid Consensus sequence (CRAC) can help with the search for possible sterol interaction domains (Li and Papadopoulos 1998). Scanning for a pattern like (L/V)-X_{1-5}-(Y/F)-X_{1-5}-(K/R) or *vice versa* is limited to only secondary structure analysis, although sterol binding can also involve multiple protein TMDs.

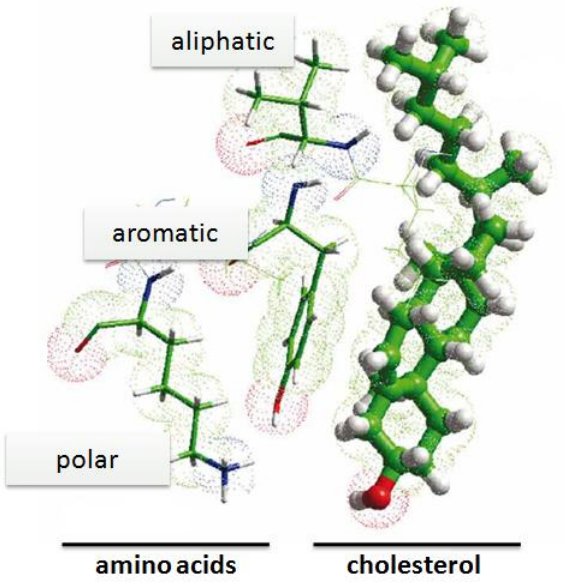

Figure 4: Molecular protein-sterol interactions. Amino acid residues involved in cholesterol interaction. Adapted from Fantini & Barrantes (2013).

1.4 Microbial and mammalian Sterol-O-Acyltransferases

Sterol-O-Acyltransferases (SOATs), also abbreviated as ACATs (Acyl-CoA:cholesterol acyltransferases) or AREs (ACAT related enzymes), are embedded in the endoplasmic reticulum (ER) membrane and play key roles in cellular sterol homeostasis. Therefore, SOATs are potential drug targets for therapeutic intervention against Alzheimer's disease (Murphy et al. 2013) and cancer (Yue et al. 2014). Tremendous effort has been made in search and development of specific SOAT inhibitors (Alegret et al., 2004; US 8283378 B2 patent from 2012), some are already commercially available (Santa Cruz Biotechnology, Inc.) and several Inhibitors have been successfully tested on models (Lee et al. 2015; Masumoto et al. 2015). Whether or not the inhibition of SOATs has positive effects on preventing atherosclerosis is subject of a fierce and controversial debate for quite some time (Fazio et al. 2005; Rong et al. 2005; Farese 2006; Chang et al. 2009).

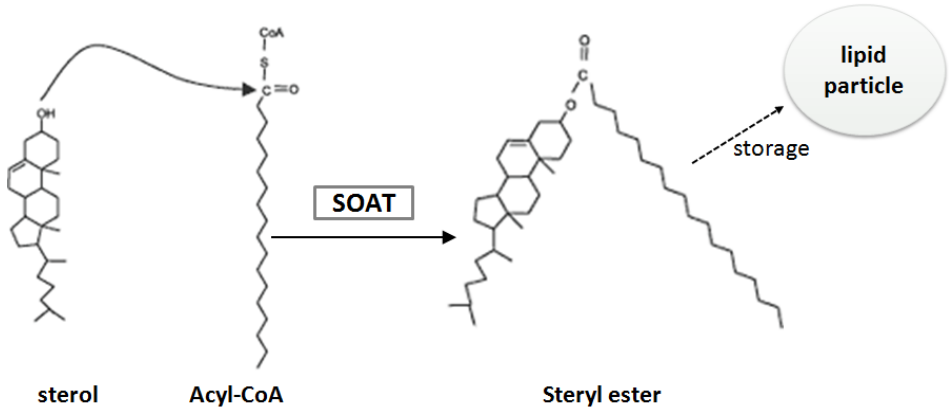

Figure 5: SOAT catalyzed formation of steryl esters. Modified from Alegret et al. (2004).

Conserved from yeast to mammals, SOATs are capable of acylating sterols at their free 3' OH-group with an activated fatty acyl-CoA resulting in the formation of steryl esters (SE), which then are stored in cytoplasmic lipid particles (Figure 5) together with triacylglycerols as energy reservoir or stock of membrane building blocks (Chang et al. 2006; Daum et al. 2007). SE can be hydrolyzed in case of low levels of free membrane sterols, while high levels of free sterols or free fatty acids promote SE synthesis through transcriptional or post-translational mechanisms (Wagner et al. 2009; Seo et al. 2001; Chang et al. 1997; Zhang et al. 2014). Typically, a pair of SOAT isofoms exists in eukaryotic cells and their conservation at the nucleotide level suggests common evolution arising from gene duplications (Oelkers et al. 1998). All of them share highly conserved sequences shown to be important for enzymatic activity and likely to be substrate binding sites. One of which, the FYxDWWN region, is conserved among other members of the membrane-bound-O-acyltransferase (MBOAT) family and it is predicted to be important for fatty acyl-CoA binding. The second conserved pattern is SOAT specific and thus possibly involved in sterol binding (Oelkers et al. 1998). So far, no crystal structures exist for any of the MBOAT proteins and their topologies are still under investigation (Pagac et al. 2011).

1.5 Aim of this study

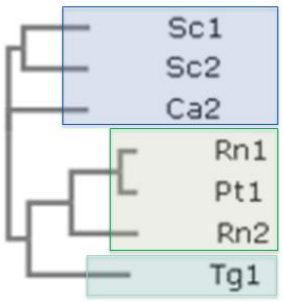

Figure 6: Selected SOATs. For details see Figure 19.

SOATs are integral membrane proteins located in the endoplasmic reticulum and are directly in contact with different kinds of lipids that could affect their structural integrity. It is conceivable, that SOATs with multiple trans-membrane domains (TMDs) also interact structurally with the free sterols besides using them as a substrate. In that case, expression level and/or activity of the tested SOATs possibly would be increased, if the preferred sterol is present in the lipid composition of the yeast membranes. A change in activity alone could also be a result of higher specificity for a certain sterol. Therefore, sterols which serve as good substrates not necessarily have the same structural features as the sterol species that improve expression and folding. The role of allosteric regulators has been reported mainly for mammalian SOATs testing several sterols and sterol like compounds *in vitro* (Chang et al. 2010; Rogers et al. 2014). So there is a need for better *in vivo* investigation including a greater diversity of SOATs to find generalities or discover interesting specifics which could be relevant for the industrial production of pharmaceutics, specific sterols, vitamins and steroid hormones. In order to efficiently produce great amounts of highly valued compounds like the vitamin D3 precursor 7-dehydrocholesterol (7-DHC) in yeast, expression of a very active and stable sterol O-acyltransferase with specificity for the desired substrate is required. The strategy we pursued here was the exploration of heterologous SOATs from microbes and mammals (Figure 19). A set of seven SOATs originating from five different organisms were compared *in vivo* upon expression in *S. cerevisiae* CEN.PK2 *are1are2* knockout strains with modified sterol composition. Then, SOAT activity was determined by measuring free sterol and steryl esters content after 65 h of cultivating yeasts producing mainly ergosterol (ERG), 7-dehydrocholesterol (7-DHC) or cholesterol (CLR). Therefore to test influence of structural interactions, a new strain producing more than 99 % cholesterol (of total sterols) was established in addition to previously engineered sterol modified strains, ensuring a sterol environment more similar to mammalian ER membranes. In the course of this, we used a novel method for screening cholesterol-producing transformants employing the benefit of the sterol structure specific interaction of natamycin. Both sterol-modified strains exhibited an extended lag-phase, yet they grew to similar cell densities as the ERG-strain. So far, our data suggest that the two isoenzymes SOAT1 (Rn1) and SOAT2 (Rn2) of *Rattus norvegicus* are substrate-selective for different sterols. Rn1 prefers the acylation of ergosterol, whereas Rn2 is highly active on cholesterol or 7-DHC and acylates only trace amounts of ergosterol. It has been reported that the two SOATs from *S. cerevisiae* also have non-equivalent substrate specificities, Are2p preferring ergosterol and Are1p also esterifying precursors of ergosterol (Zweytick et al., 2000). Our data complement these findings for the redundant rat enzymes. Furthermore, we find unexpected shifts in SOAT activity for zymosterol.

2 MATERIALS AND METHODS

2.1 Materials

2.1.1 Instruments and devices

Table 1: Alphabetically ordered list of instruments and devices used in this study

Label	Supplier
Centrifuge 5415R	Eppendorf, Germany
Centrifuge 5810R	Eppendorf, Germany
Electrophoresis gel chambers	PowerPac™ Basic + Sub-Cell GT, Biorad, USA
Electroporation: Cuvettes (2 mm gap)	Molecular BioProducts Inc., USA
Electroporation: MicroPulserTM	BIO-RAD, USA
Eppendorf tubes	Greiner bio-one International AG
Falcon tubes	Greiner bio-one International AG
Flasks 250 mL	Simax
G:Box HR	Syngene, UK
GC caps	VWR International, GmbH
GC gripper	VWR International, GmbH
GC vials	VWR International, GmbH
GC/MS column: Agilent 19091S-433UI HP-5ms Ultra Inert, 50 m, 0.25 mm, 0.25 µm	Agilent Technologies
GC/MS dedector: HP 5973 Mass Selective Detector	Agilent Technologies
GC/MS: HP 6890 Series GC Systems	Agilent Technologies, Austria
Glass beads	Carl Roth GmbH + Co KG
Glass bottles	Schott/ Duran, Ilmabor TGI
Hamilton syringe EY40.1	Carl Roth GmbH + Co KG
HPLC	Agilent Technologies
HPLC column: YMC-Pack *Pro* C18 RS	YMC Co., Ltd, Japan
HPLC detector UV/MS	Agilent Technologies
Incubator (30°C and 37°C)	Binder GmbH
Labofuge 400 R centrifuge	Heraeus/Thermo Scientific
Laminar flow chamber BSB4A	Gelaire Flow Laboratories
MF Membrane filters, 0.025 µm VSWP	Millipore, USA
Vortex-Genie 2	Scientific Industries Inc, USA
N_2 Evaporator	VLM GmbH Bielefeld
NanoDrop 2000c spectrophotometer	Thermo Scientific
NuPAGE®SDS Gels: 4-12% Bis-Tris Gel (1mm x 15 wells and 1.5 mm x 10 wells)	Invitrogen Life Technologies Corp.
Optima LE-80 Ultracentrifuge	Beckman Coulter Inc.
PCR machines	GeneAmp® PCR System 2700, Applied Biosystems, USA
PCR tubes	Greiner bio-one International AG
Petri dishes	Greiner bio-one International AG
Photometer	BioPhotometer, Eppendorf, Germany
Pipette tips	Greiner bio-one International AG
Pipettes:	
Proline	Biohit
Pipetman P20N; P200N; P1000N	Gilson Inc., USA
Eppendorf research 0.5-10 µL	Eppendorf, Germany
Pyrex® tubes	Pyrex, Incorp.
Scanner	HP scanjet 4370
Thermomixer	Eppendorf, Germany
TLC chambers	CAMAG
TLC scanner	CAMAG
TLC silica plates: aluminium sheets 20 x 20 cm, silica gel 60	Merck GmbH.
Transferpettor (200-1000 µL; 10-50 µL)	Brand GmbH, Germany

UV-cuvettes	Greiner bio-one International AG
Vibrax	Vibrax VXR basic, IKA GmbH& Co KG, Germany

2.1.2 Reagents

Table 2: Alphabetically ordered list of compounds, reagents and proteins used in this study

Compound label	Supplier
7-Dehydrocholesterol	DSM (in-kind contribution)
Acetic acid	Carl Roth GmbH + Co KG
Acetone	Carl Roth GmbH + Co KG
Agar	BD Bacto-Becton, Dickinson and Company
Agarose	Biozym Scientific GmbH
Antibody: Goat Anti-Mouse IgG, (H+L), (min x HnBvHs Sr Prot), Peroxidase Conjugated, # 31432	Thermo Scientific
Antibody: Goat anti-rabbit IgG, horseradish peroxidase conjugated	Sigma-Aldrich Corp.
Antibody: Mouse Anti-Flag, IgG	
Antibody: Mouse Anti-GAPDH IgG, monoclonal, HRP conjugate, # MA5-15738-HRP	Thermo Scientific
Antibody:Rabbit Anti-SOAT1(human) IgG, polyclonal, ab93477	Abcam, UK
Chloroform	Carl Roth GmbH + Co KG
Cholesta-5,7,24-trienol	DSM (in-kind contribution)
Cholesterol	Sigma-Aldrich Corp.
Cholesteryl acetate	Sigma-Aldrich Corp.
Cholesteryl oleate	Sigma-Aldrich Corp.
Deionised water	Fresenius Kabi Austria GmbH
Diethylether	Carl Roth GmbH + Co KG
Dipotassium hydrogen phosphate	Carl Roth GmbH + Co KG
dNTPs	Fermentas Thermo Fisher Scientific Inc.
Ergosterol	Sigma-Aldrich Corp.
Ethanol	Australco Handels GmbH
Ethylacetate	Carl Roth GmbH + Co KG
FD Green Buffer	Fermentas Thermo Fisher Scientific Inc.
FD Restriction enzymes	Fermentas Thermo Fisher Scientific Inc.
Gene Jet Plasmid Miniprep Kit	Fermentas Thermo Fisher Scientific Inc.
Gene Ruler DNA Ladder Mix	Fermentas Thermo Fisher Scientific Inc.
Geneticin (G418 Sulfate)	Invitrogen Life Technologies Corporation
Glucose monohydrate	Carl Roth GmbH + Co KG
Glycerol	Carl Roth GmbH + Co KG
HCl	Carl Roth GmbH + Co KG
L-Adenine	Carl Roth GmbH + Co KG
Lanosterol	Sigma-Aldrich Corp.
L-Histidine	Carl Roth GmbH + Co KG
Lithiumacetate	Fluka/Sigma-Aldrich Corp.
L-Leucine	Carl Roth GmbH + Co KG
L-Lysine	Carl Roth GmbH + Co KG
Loading Dye (6x)	Fermentas Thermo Fisher Scientific Inc.
L-Tyrosine	Carl Roth GmbH + Co KG
Magnesium chloride	Carl Roth GmbH + Co KG
Manganese chloride	Carl Roth GmbH + Co KG
Maxima Hot Start Green PCR Master Mix (2x)	Fermentas Thermo Fisher Scientific Inc.
Methanol	Carl Roth GmbH + Co KG
N'O'-bis(trimethylsilyl)-trifluoracetamid	Sigma-Aldrich Corp.
Nitrogen	House pipe
Nitrogen base without amino acids	Difco Becton, Dickinson and Company
NuPAGE LDS 4x sample buffer	Invitrogen Life Technologies Corporation

NuPAGE MES running buffer 20x	Invitrogen Life Technologies Corporation
NuPAGE sample reducing agent 10x	Invitrogen Life Technologies Corporation
NuPAGE transfer buffer	Invitrogen Life Technologies Corporation
PageRuler Prestained Protein Ladder	Fermentas Thermo Fisher Scientific Inc.
PEG 3500	Thermo Scientific
Petrol ether	Carl Roth GmbH + Co KG
Phusion DNA polymerase	Finnzymes Thermo Fisher Scientific Inc.
Phusion HF buffer	Finnzymes Thermo Fisher Scientific Inc.
Ponceau S	Amersham Life Science
Potassium dihydrogen phosphate	Carl Roth GmbH + Co KG
Potassium hydroxide	Carl Roth GmbH + Co KG
Pyridine	Carl Roth GmbH + Co KG
Pyrogallol	Carl Roth GmbH + Co KG
Sigma Fast™ Protease Inhibitor Tablet	Sigma-Aldrich Corp.
Single stranded carrier DNA (fish sperm)	Roche Diagnostics, GmbH
Skim-milk powder (Eiweiß 90)	DM Drogerie Markt GmbH
Sodium acetate	Carl Roth GmbH + Co KG
Sodium chloride	Carl Roth GmbH + Co KG
Sodium hydroxide	Carl Roth GmbH + Co KG
Sorbitol	Carl Roth GmbH + Co KG
Sulfuric acid	Carl Roth GmbH + Co KG
SuperSignal West Femto Maximum Sensitivity Substrate Kit, # 34094	Thermo Scientific
SuperSignal West Pico Chemiluminescent Substrate Kit	Thermo Scientific
T4 DNA Ligase	Thermo Scientific
T4 DNA ligase buffer 10x	Thermo Scientific
Trichloroacetic acid	Carl Roth GmbH + Co KG
Trifluoroacetic Acid (TFA), LC-MS Grade (Pierce), # 85183	Thermo Scientific
Triolein	Sigma-Aldrich Corp.
Tris	Carl Roth GmbH + Co KG
Tryptophan	Carl Roth GmbH + Co KG
Tween20	Carl Roth GmbH + Co KG
Western blot membrane	Sartorius AG, nitrocellulose blotting membrane
Wizard Gel Slice and PCR Product Preparation	Promega Corp.
Yeast extract	Carl Roth GmbH + Co KG
Zymolyase (from *A. luteus*)	Seikagaku Biobusiness, Corp.
Zymosterol	DSM (in-kind contribution)

2.1.3 Media and Buffers

Table 3 Media and components used for this work

Label	Conc.	Compound
LB	10 g/L	tryptone
	5 g/L	yeast extract
	5 g/L	NaCl
	20 g/L	agar (optional)
		water
	(1 mL/L)	ampicillin stock solution (1000x) (optional)
SD-ura	6.7 g/L	bacto yeast nitrogen base without amino acids
	20 g/L	glucose
	20 g/L	agar (optional)
	0.2 g/L	SD-ura dropout powder mix
	4 mL	sterile filtered tryptophan 250x stock (10 mg/L)
		→ Final amino acid concentration: each 40 mg/L
SD-ura-trp dropout mix	2 g	of each amino acids: Adenine, leucine, lysine, histidine, tyrosine
SOC	20 g/L	bacto tryptone
	0.58 g/L	NaCl, 2 g/L $MgCl_2$, 0.16 g/L KCl, 2.46 g/L $MgSO_4$
	5 g/L	bacto yeast extract
	3.46 g/L	dextrose
YPD	10 g/L	bacto yeast extract
	20 g/L	peptone
	20 g/L	glucose
	(20 g/L)	agar (optional)
	(1 mL/L)	10 mM geneticin (G418) stock solution (1000x) (optional)
	(1 mL/L)	6 mM natamycin (100x) (optional)

2.1.4 Strains

Table 4: *Saccharomyces cerevisiae* strains

Strain	Major modification	Genotype	Source
ERG "COS 5"	*are1are2*	CEN.PK2 *MATa ura3 trp1 his3 leu2 MAL2 SUC2 are1:: HIS3 are2::TRP1*	Corinna Odar
7DHC "10A"	*are1are2erg5erg6::S24R*	CEN.PK2 *MATa ura3 trp1 his3 leu2 MAL2 SUC2 are1:: HIS3 are2::TRP1 erg5::LEU2, erg6::S24R-HPH*	Holly Stolterfoht
CLR "BA-C"	*are1are2erg5::S7Rerg6::S24R*	CEN.PK2 *MATa ura3 trp1 his3 leu2 MAL2 SUC2 are1:: HIS3 are2::TRP1 erg5::S7R erg6::S24R-HPH*	This study

Table 5: Electrocompetent *Escherichia coli* strain.

Name	Genotype	Source
TOP 10 F'	F´{lacI^q Tn10 (Tet^R)} mcrA Δ(mrr-hsdRMS-mcrBC) Φ80lacZΔM15 ΔlacX74 recA1 araD139 Δ(ara-leu)7697 galUgalKrpsL endA1 nupG	Invitrogen

2.1.5 Sequences

SOAT sequences were selected by Regina Leber based on literature describing their successful expression in yeast.

Table 6: SOAT protein sequences. Native DNA and codon-optimized sequences are listed in the digital appendix.

	Sequence
Sc1	MTETKDLLQDEEFLKIRRLNSAEANKRHSVTYDNVILPQESMEVSPRSSTTSLVEPVESTEGVESTEAERVAGKQEQ EEEYPVDAHMQKYLSHLKSKSRSRFHRKDASKYVSFFGDVSFDPRPTLLDSAINVPFQTTFKGPVLEKQLKNLQLTK TKTKATVKTTVKTTEKTDKADAPPGEKLESNFSGIYVFAWMFLGWIAIRCCTDYYASYGSAWNKLEIVQYMTTDLFT IAMLDLAMFLCTFFVVFVHWLVKKRIINWKWTGFVAVSIFELAFIPVTFPIYVYYFDFNWVTRIFLFLHSVVFVMKS HSFAFYNGYLWDIKQELEYSSKQLQKYKESLSPETREILQKSCDFCLFELNYQTKDNDFPNNISCSNFFMFCLFPVL VYQINYPRTSRIRWRYVLEKVCAIIGTIFLMMVTAQFFMHPVAMRCIQFHNTPTFGGWIPATQEWFHLLFDMIPGFT VLYMLTFYMIWDALLNCVAELTRFADRYFYGDWWNCVSFEEFSRIWNVPVHKFLLRHVYHSSMGALHLSKSQATLFT FFLSAVFHEMAMFAIFRRVRGYLFMFQLSQFVWTALSNTKFLRARPQLSNVVFSFGVCSGPSIIMTLYLTL
Sc2	MDKKKDLLENEQFLRIQKLNAADAGKRQSITVDDEGELYGLDTSGNSPANEHTATTITQNHSVVASNGDVAFIPGTA TEGNTEIVTEEVIETDDNMFKTHVKTLSSKEKARYRQGSSNFISYFDDMSFEHRPSILDGSVNEPFKTKFVGPTLEK EIRRREKELMAMRKNLHHRKSSPDAVDSVGKNDGAAPTTVPTAATSETVVTVETTIISSNFSGLYVAFWMAIAFGAV KALIDYYYQHNGSFKDSEILKFMTTNLFTVASVDLLMYLSTYFVVGIQYLCKWGVLKWGTTGWIFTSIYEFLFVIFY MYLTENILKLHWLSKIFLFLHSLVLLMKMHSFAFYNGYLWGIKEELQFSKSALAKYKDSINDPKVIGALEKSCEFCS FELSSQSLSDQTQKFPNNISAKSFFWFTMFPTLIYQIEYPRTKEIRWSYVLEKICAIFGTIFLMMIDAQILMYPVAM RALAVRNSEWTGILDRLLKWVGLLVDIVPGFIVMYILDFYLIWDAILNCVAELTRFGDRYFYGDWWNCVSWADFSRI WNIPVHKFLLRHVYHSSMSSFKLNKSQATLMTFFLSSVVHELAMYVIFKKLRFYLFFFQMLQMPLVALTNTKFMRNR TIIGNVIFWLGICMGPSVMCTLYLTF
Ca2	MGRTNTSDQLNAISDKNTKRKSLALDNEYHNNSSSEDDSSKIELSYTIPDNNNIISQETTTSVEDVLSVSSAPQNEL RLRKQKSNNQDSPVDLNGVIVDVSKREKIFLKRKRQIDNKHGSDKSKYLSRFNDITFKAKSSTIFESDEFYKTDFFG MYVLFWLATAFAMVNNLIHTYFENSTPILQWTVVKVFKRDLFKVGLVDLAMYLSTYFAFFVQYACKNGYLSWKKVGW WLQAAFDGLFLFFWLWIASEYCLDFPWIAKVFLVLHSLVFIMKMHSYAFYNGYLWSIYKEGLYSEKYLDKLTNGKVT LPKGHTKNETEKVLQESIAFTKYELEYQSHATTENPDDHHVFDIDQTDKSIAKLQQEGLIKFPQNITLFNYFEYSMF PTLVYTLNFPRTKRIRWSYVFGKTFGIFGLIFLMILIAENNLYPIVLRCEIARKLPVSERIPQYFFLLMDMIPPFLM VYLFTFFLIWDAILNAIAELSKFADRDFYGPWWSCTDFSEFANQWNRCVHKFLLRHVYHSSISAFDVNKQSAAIITF LLSSLVHELVMYVIFGTLRGYLLLFQMSQIPLIIMSRSKFMKDKKVLGNIICWFGFISGPSIICTLYLVF
Rn1	MVGEEMSLRNRLSRSAENPEQDEAQKNLLDTHRNGHITMKQLIAKKRQLAAEAEELKPLFLKEVGCHFDDFVTNLID KSASLDNGGCALTTFSILEEMKNNHRAKDLRAPPEQGKIFISRRSLLDELFEVDHIRTIYHMFIALLIIFILSTLVV DYIDEGRLVLEFSLLAYAFGQFPIVIWTWWAMFLSTLAIPYFLFQRWAHGYSKSSHPLIYSLIHGAFFLVFQLGILG FIPTYVVLAYTLPPASRFILILEQIRLVMKAHSYVRENVPRVLSAAKEKSSTVPVPTVNQYLYFLFAPTLIYRDSYP RTPTVRWGYVAMQFLQVFGCLFYVYYIFERLCAPLFRNIKQEPFSARVLVLCVFNSILPGVLMLFLSFFAFLHCWLN AFAEMLRFGDRMFYKDWWNSTSYSNYYRTWNVVVHDWLYYYVYKDLLWFFSKRFRPAAMLAVFALSAVVHEYALAVC LSYFYPVLFVLFMFFGMAFNFIVNDSRKRPVWNIMVWASLFLGHGVILCFYSQEWYARQHCPLKNPTFLDYVRPRTW TCRYVF
Rn2	MEPKAPQLRRRERQGEEQENGACGEGNTRTHRAPDLVQWTRHMEAVKTQCLEQAQRELAELMDRAIWEAVQAYPKQD RPLPSTASDSTRKTQELHPGKRKVFITRKSLLDELMEVQHFRTIYHMFIAGLCVLIISTLAIDFIDEGRLMLEFDLL LFSFGQLPLALMMWVPMFLSTLLLPYQTLRLWARPRSGGAWTLGASLGCVLLAAHAAVLCVLPVHVSVKHELPPASR CVLVFEQVRFLMKSYSFLRETVPGIFCVRGGKGICTPSFSSYLYFLFCPTLIYRETYPRTPSIRWNYVAKNFAQALG CLLYACFILGRLCVPVFANMSREPFSTRALLLSILHATGPGIFMLLLIFFAFLHCWLNAFAEMLRFGDRMFYRDWWN STSFSNYYRTWNVVVHDWLYSYVYQDGLWLLGRQGRGAAMLGVFLVSALVHEYIFCFVLGFFYPVMLILFLVVGGLL NFTMNDRHTGPAWNILMWTFLFLGQGIQVSLYCQEWYARRHCPLPQPTFWELVTPRSWSCHP
Pt1	MVGEEKMSLRNRLSKSRENPEEDEDQRNPAKESLETPSNGRIDIKQLIAKKIKLTAEAEELKPFFMKEVGSHFDDFV TNLIEKSASLDNGGCALTTFSVLEGEKNNHRAKDLRAPPEQGKIFIARRSLLDELLEVDHIRTIYHMFIALLILFIL STLVVDYIDEGRLVLEFSLLSYAFGKFPTVVWTWWIMFLSTFSVPYFLFQHWATGYSKSSHPLIRSLFHGFLFMIFQ IGVLGFGPTYVVLAYTLPPASRFIIIFEQIRFVMKAHSFVRENVPRVLNSAKEKSSTVPIPTVNQYLYFLFAPTLIY RDSYPRNPTVRWGYVAMKFAQVFGCFFYVYYIFERLCAPLFRNIKQEPFSARVLVLCVFNSILPGVLILFLTFFAFL HCWLNAFAEMLRFGDRMFYKDWWNSTSYSNYYRTWNVVVHDWLYYYAYKDFLWFFSKRFKSAAMLAVFAVSAVVHEY ALAVCLSFFYPVLFVLFMFFGMAFNFIVNDSRKKPIWNVLMWTSLFLGNGVLLCFYSQEWYARQHCPLKNPTFLDYV RPRSWTCRYVF
Tg1	MLDDPLSKTRNSALATNSPRPLPSSLPRNPDLLFLSMTTITDQSSLPAALSPSSSSPSSSSPPSSSPSSSSPSSSSP FSSVCFSSVSPSSSLPSSSVSSASLSSLASGGKLPGSETSEESLPHQQGAEPRVSLEATMCSPSPEKTGPPCSPCPE SCGKQEGNNTDPCTVSSPCESRGSRRTMETARAGASSGKAEDEHARAEGGEPAQGTHEARDKEKSGDRRPASGPGGS ELDKMEKEDGKTFPSKLDFFDANSDLARSDFRGVAVLLFIAAIFYLVANPILRWYDSKEFVDPSLARAMFDDFFFLM FMWAKLFAWSFTAYHLHLLYLRGRISRRALLFLQHLTQSAAIGYAVCSCLYNAWPIIPAAFVQMIAVVQFMKMHSYS STNMNFCDDMRQGKQTLGYPENVTLRNFCDYLFCPVLVYEPMYRRGGGFRPTYFVFKLFSMVGAMVVMYLACTSYLI PTMMRSPSMSITEAIFSLVFPFLFLDILIFYILFECICNLAAEITNFANRNFYDDWWNSTNWDEYSRKWNKPVHRFL LRHVYMETQQRYKWSHQTAAFATFLFSALLHEMILAVCFRFVRLYLFGLMLLQLPLIALGRFYRHKKMVANAIFWAC LMLGPPLLGLAYGREWAQIHFYNAHADHQPLRLF

Table 7 Primers and gBlocks used for construction of disruption cassettes. Melting temperature (Tm) was calculated with the tool OligoAnalyzer 3.1 from Integrated DNA Technologies (IDT).

Name	(bp)	Tm (°C)	Template	Sequence 5'-3'
CYC1t-HR-RV	73	68.1	p426_DHCR7	TAATGAAGTAAATATGATTTATTGTCTGGACAAAGTTC TGTTTTTCCCCAGGCCGCAAATTAAAGCCTTCGAG
CYC1t-lHR-RV	500		pUG6 (loxP+kanMX)	TAAATTTGAAGGTAAGAAGATCAAATTTGATTGAACAT AACGTCTTCATCTCCTAACTTCATGTATAATAAAAACT ATTAGCACATCTATTTTATATATGTACGCGTATATCTT ACATCGTACCGTTATAGCATTTGAATTATTGAGCTTTT GTATCATCTACCGCTGTCATGCTCGCCTTCACGGAACT TAGTTATGCGAAAAAGAATTCAGGAAACCAAAGCTGGC AGGGTGAGTATTTGTTTGTAAAGTCGCACCTTTAGCAG ATCATTAGCTGTAGCGTATGGAAGAAAACTAAATGAAA TTGTTTATAAAACCTGAATATGATAAAAGAAATCTAAA TAATAAATATGATTGCTATATAATAGTTATATTTGAAA TGAAGAGAAAGGGAAGAAAATAAAAGTATTCAAAACGC CAACCCTTAATGAAGTAAATATGATTTATTGTCTGGAC AAAGTTCTGTTTTTCCCCAGGCCGCAAATTAAAGCCTT CGAGCG
DHCR7-FW	47	62.9	056662pScript_ DHCR7	GTTGTTGGATCCAAAAATGATGGCTTCAGATAGAGTTA GAAAAAGAC
DHCR7-RV	44	58.4	056662pScript_ DHCR7	CAACAAGAATTCTCATCAGAAAATATTTGGCAATAATC TATAAG
DSM_TEFt-TDH3-RV	50	65.3	pHyD-0361 (DSM)	TGAAATGGCGAGTATTGATAATGATAAACTtctgggca gatgatgtcgag
HR-1-FW	30	54.9		AAAACATCACATTTTGCTATTCCAATAGAC
HR-1-RV	35	54.7		TAATGAAGTAAATATGATTTATTGTCTGGACAAAG
HR-435-FW	22	56.1		TATTTGTTCCGCAATTTCCGGG
HR-475-RV	36	55.7		TAAATTTGAAGGTAAGAAGATCAAATTTGATTGAAC
HR-DSM_TEFp-FW	73	66.7	pHyD-0361 (DSM)	AAAACATCACATTTTGCTATTCCAATAGACAATAAATA CCTTTTAACAAAGTGACTGTCGCCCGTACATTTAG
HR-TDH3p-FW	89	66.9		AAAACATCACATTTTGCTATTCCAATAGACAATAAATA CCTTTTAACAAAAGTTTATCATTATCAATACTCGCCAT TTCAAAGAATACG
lHR-X-TEFp-FW	500		pUG6 (loxP+kanMX)	TATTTGTTCCGCAATTTCCGGGGCGGGTAATATTTGTT ACCATAGTTCTCGAGAAGGTTTCCCTCGTTTAAGTCTG CGAAGTCTCGTACCTTTTATCGCTGCTGACAAAACATA GCCCAAACCTGCGTCTATATGCTGCCGGTGTTTATATC GCTATTGAAGAGAGCTCATGTTTCGGTTTTGAAAAGAT TTTTTATCGAATCGGTTGTAAAAGATCGTCCTTATTGT CTTCAGGCAAAGGGACTGATTGGTTTATATACGCAAGC AGGGAATCTTGTTGGAAGAAAAAAATTATATATAAGCT AATTGTCTATTGTTCCAAATATCTTATTCTTACTCATT TCTTTCTTGTTATATTGTTTCCTTAATTTTTATCACAA TAAACAAAACATCACATTTTGCTATTCCAATAGACAAT AAATACCTTTTAACAAAAACCCTTAATATAACTTCGTA TAATGTATGCTATACGAAGTTATTAGGTCTAGAGATCT GTTTAG
TDH3-FW	33	56.2	p426_DHCR7	AGTTTATCATTATCAATACTCGCCATTTCAAAG
URA3-HR-FW	29	66.8	p426GPD_ARE2	AAAACATCACATTTTGCTATTCCAATAGACAATAAATA CCTTTTAACAAAATGTCGAAAGCTACATATAAGGAACG TGC
URA3-RV	32	53.1		GGGTAATAACTGATATAATTAAATTGAAGCTC
URA3-TDH3-RV	62	63.4	p426GPD_ARE2	TGAAATGGCGAGTATTGATAATGATAAACTGGGTAATA ACTGATATAATTAAATTGAAGCTC
X-TEFp-FW	65	63.2	pUG6 (loxP+kanMX)	AACCCTTAATATAACTTCGTATAATGTATGCTATACGA AGTTATTAGGTCTAGAGATCTGTTTAG
X-TEFt-RV	83	66.4	pUG6 (loxP+kanMX)	TGAAATGGCGAGTATTGATAATGATAAACTATAACTTC GTATAGCATACATTATACGAAGTTATATTAAGGGTTCT CGAGAGC

Table 8: Primers for SOAT1/2 mutagenesis study and sequencing. *Both primers were desiged by Holly Stolterfoht.

Name		(bp)	Tm (°C)	Sequence 5'-3'
1B_fw	Rn1_916-FW	27	57.3	TATCCTAGAACTCCAACAGTCAGATGG
1C_fw	Rn1_1122-FW	27	57.5	CTTTTTCGCATTTCTGCATTGTTGGTT
1D_fw	Rn1_1242-FW	28	57.8	GAATGTGGTTGTCCACGATTGGTTATAC
1D-mfw	Rn1_K420Q_1272-FW	25	54.9	CTATGTTTACCAAGACCTACTGTGG
1A_rv	Rn1_942-RV	27	57.3	CCATCTGACTGTTGGAGTTCTAGGATA
1B_rw	Rn1_1148-RV	27	57.5	AACCAACAATGCAGAAATGCGAAAAAG
1C_rw	Rn1_1269-RV	28	57.8	GTATAACCAATCGTGGACAACCACATTC
1C-mrv	Rn1_K420Q_1296-RV	25	54.9	CCACAGTAGGTCTTGGTAAACATAG
2B_fw	Rn2_859-FW	27	55.1	TATCCTAGAACACCTTCTATCAGATGG
2C_fw	Rn2_1065-FW	27	55.1	CTTTTTCGCTTTTCTACATTGTTGGTT
2D_fw	Rn2_1181-FW	32	56.6	CATGGAATGTTGTTGTACATGATTGGTTATAC
2D-mfw	Rn2_Q410K_1219-FW	21	55.9	GTCTACAAAGACGGCTTGTGG
1A_rv	Rn2_885-RV	27	55.1	CCATCTGATAGAAGGTGTTCTAGGATA
2B_rw	Rn2_1091-RV	27	55.1	AACCAACAATGTAGAAAAGCGAAAAAG
2C_rw	Rn2_1212-RV	32	56.6	GTATAACCAATCATGTACAACAACATTCCATG
2C-mrv	Rn2_Q410K_1239-RV	21	55.9	CCACAAGCCGTCTTTGTAGAC
A-fw	*p426Seq_fw	30	54.5	TTAGTTTTAAAACACCAGAACTTAGTTTCG
D-rv	*p426Seq_rev	22	58.3	TTACATGACTCGAGGTCGACGG

2.2 Methods

2.2.1 Genetic modification tools

Amplification of DNA fragments was performed as shown in Table 9 using Phusion DNA-polymerase or Maxima Hot Start Taq DNA Polymerase.

For genetic analysis of Rn1/Rn2 mutagenesis transformants, a more quickly protocol was applied using three primers instead of a single primer pair in one PCR reaction. Here, 10 µL of yeast cell culture was taken from microtiter plates and mixed with 45 µL of zymolyase [2.5 mg/mL]. After incubation for 20 min at 37°C, mixture was centrifuged for 30 s in a table top centrifuge and supernatant was discarded. DNase deactivation of pellets at 95°C for 5 min was carried out with a thermocycler. Finally, 28 µL of PCR Master Mix was added: 15 µL Hot Start Green Master Mix, 7.6 µL ddH_2O, 3.6 µL forward primers ($^2/_3$ primer A and $^1/_3$ primer B) and 1.8 µL reverse primer.

Table 9: PCR reagents and cycling conditions. a, x, y: 1-10 ng of template; * Enzymatic cell wall digestion of one yeast colony with 50 µL of zymolyase [2.5 mg/mL], 15 min at 37°C, DNase deactivation of pellet at 95°C for 5 min.

Reagents	**PCR-Mix**	**OE-PCR 1st round**	**OE-PCR 2nd round**	**Colony-PCR**	**cycling conditions** T (°C)	t (min', s'')	
HF-buffer 5x	10 µL	10 µL	10 µL	Hot Start	98	30''	
dNTPs 10mM	1 µL	1 µL	1 µL	Green Master	98	10''	
DNA polymerase	0.5 µL	0.3 µL	5 µL	Mix: 25 µL	55-72	30''	15-33 x
fw. primer 10µM	2.5 µL	/	5 µL	2.5 µL	72	30''- 1'/kb	
rv. primer 10µM	2.5 µL	/	0.4 µL	2.5 µL	72	7'	
Template	a µL	x; y µL	/	~ 2 µL *	4	∞	
ddH_2O	33.5 - a	38.7 - x+y	28.6 µL	18 µL			
	total volume: 50 µL						

Digestion of plasmids and PCR products (300 - 500 ng) were digested by restriction endonucleases at 37°C for 30 min with reagents listed in Table 10. For control cuts, loading dye was added to the mix which was separated by gel electrophoresis. For subsequent ligation steps, enzymes where deactivated at 80°C for 5 min, then dephosphorylation of the vector backbone was done using 1 µL of 1 U Thermo Scientific Fast AP (Alkaline Phosphatase) at 37°C for 15 min and inactivated at 75°C for 5 min. Ligation was performed with a vector:insert molar ratio of 4:1, incubated over night at 16°C and inactivated at 65°C for 10 min.

Table 10: Digestion and ligation.

Double Digest Mix	
buffer (10x)	2 µL
*Bam*HI	0.5 µL
*Eco*RI	0.5 µL
Template	a µL
ddH_2O	17-a µL
	20 µL

Ligation Mix	
T4 buffer (10 x)	2 µL
T4 DNA Ligase (2 U/mL)	0,5 µL
vector 100ng	x µL
insert	y µL
ddH_2O	17.5-(x+y) µL
	20 µL

Agarose gel electrophoresis was used for separation and purification of DNA fragments using standard protocols. Gels containing 0.8 - 1.5% of agarose were run in TAE buffer at 120 V for 45 min for analytical purposes, and at 90 V for 1.5 h for preparative gels. Sizes of the DNA fragments were assigned by comparison to the standard Gene Ruler DNA ladder mix of Fermentas (Figure 7). PCR products were purified and isolated from preparative gels according to Promega's Wizard SV Gel and PCR Clean Up system manual.

Plasmids were isolated from clones with the Fermentas Gene Jet Kit and eluted with 50 µL of ddH_2O. Cell material was scraped off from streak-outs on agar plates with a toothpick.

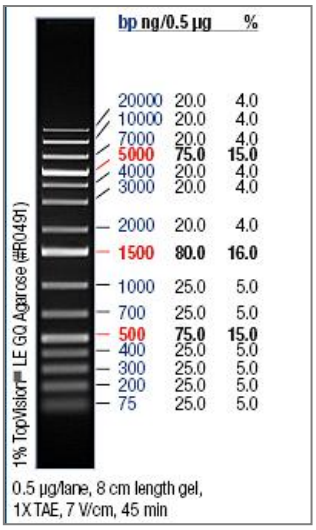

Figure 7: DNA Standard. Thermo Scientific™ GeneRuler™ 1 kb Plus DNA Ladder 75 to 20,000 bp.

2.2.2 Transformation of electrocompetent *E. coli* cells

For transformation of plamids, 50 µL of electrocompetent *E. coli* TOP10 F' cells frozen at -80°C were thawed on ice. Then, about 1 - 5 µL of DNA (desalted ligation mix, purified isolated plasmids or Gibson assembly mix) was added and cells were transferred into pre-cooled electroporation cuvettes. Cells were shocked with 2.5 kV electro pulse and immediately regenerated in 1 mL of SOC medium for 1 h at 37°C and 750 rpm. Finally, cells were plated out onto LB-amp and incubated for 1 day at 37°C.

2.2.3 Transformation of yeast strains

Prior to transformation, all strains were cultivated in YPD at 30°C in 10 mL pre-cultures over night. Then, main cultures were inoculated to an OD_{600} of 0.05 in 50 mL, grown over night until an OD_{600} of 1.5 – 2 units was reached after approximately 18 h incubation of 7DHC- and CLR-strains (ERG-strain was growing faster). Transformation of plasmids was performed according to high efficiency LiAc/SS carrier DNA/PEG protocol described by Gietz and Woods (2002). Briefly, cells were harvested at 3000 x g for 5 min, washed with 25 mL of sterile water at 3000 x g for 5 min, resuspended in 1 mL of sterile water, washed again at 500 x g for 1 min, and filled up to a final volume of one mL with sterile water. Aliquots of 100 µL (≈ 10^8 cells) were centrifuged at 500 x g for 1 min and transformation mix containing 240 µL of PEG 3500 (50%), 36 µL of 1 M LiAc, 50 µL of boiled SS-carrier DNA and 34 µL water containing 1 - 2 µg vector DNA was added to cell pellets, vigorously mixed and incubated at 42°C for 40 min. After the transformation event, samples were regenerated in 1 mL YPD for 3.5 h. The suspension was centrifuged for 5 min at 500 x g to gently spin down the cells. Finally, cells were suspended in approximately 200 µL of the supernatant and plated out on selection plates (YPD agar, 100 µM geneticin).

For the construction of the CLR-strain, transformation of cassette (*d*) *ERG5*::*DHCR7* was performed according to the protocol described above using two strains: (1) *S. cerevisiae* "10A" (7DHC-strain) without any SOAT expression and (2) *S. cerevisiae* "10A-F9" containing p42GPD_Are2. Either 1 or 2 µg of the expression cassette were applied. As negative control, water was used instead. After the transformation event, every sample was regenerated in 1 mL of YPD for 3.5 h and then transferred into 50 mL tubes with 10 mL of YPD (or YPD + geneticin [100 µg/mL]) for 15 h incubations at 28°C and 90 rpm. Then, cell suspension was centrifuged for 5 min at 1000 x g to gently spin down the cells and get rid of the supernatant. Cells were transferred into a 1.5 mL tube for better handling and to adjust the volume (100 - 250 µL) for plating on YPD containing either 40 µM or 60 µM of natamycin.

2.2.4 Gibson assembly for Rn1/Rn2 mutagenesis

One-pot assembly of pre-amplified rat SOAT1 and SOAT2 fragments with cut p42kanGPD expression vector was performed following the instruction manual of Gibson Assembly® Cloning Kit NEB #E5510S from New England Biolabs Inc. (Version 3.2, 3/14). Briefly, 100 ng of vector together with three or four inserts at equimolar amounts was mixed with 15 µL Gibson assembly mix to get a total volume of 20 µL. Then, after incubating 1 h at 50°C, 5 µL of the mix was diluted 1:3 with water and 5 µL of the dilution was used for transformation to *E. coli* TOP10 by electroporation as explained above.

2.2.5 Sequencing

Sequences of expression cassettes and GOI (genes of interest) were confirmed by Sanger sequencing at LGC Genomics (Berlin, Germany). A volume of 40 - 60 µL of samples (plasmids or PCR products) at a concentration of 70 - 100 ng/µL were conveyed together with 50 µL of sequencing primers at a concentration of 10 µM. Redundant sequencing primers were stored for further commissions.

2.2.6 Cultivation of yeast strains

CLR-strain clones were cultivated at 28°C in 250 mL baffled shake flasks for 48 h. Inoculation was done at an OD_{600} of 0.1 in 50 mL of YPD media. Glucose (20 %) was fed: 5 mL after 20 h and 5.5 mL after 41 h of incubation time. Final OD_{600}/mL was measured: BA-C I (24.75), BA-C II (24.05), BA-C III (23.65) and samples were taken according to OD values (10, 20, 200) needed for analyses.

SOAT expression clones (ERG-, 7DHC- and CLR-strain transformants) were cultivated at 28°C in 250 mL baffled shake flasks for 65 h. Inoculation was done at an OD_{600} of 0.1 in 50 mL of YPD media containing 100 µM geneticin. Cell cultures were fed with 5 mL glucose (20 %) after 40 h and after 52 h of incubation time. The final OD_{600}/mL was measured and samples were taken corresponding to 10, 20 and 200 OD units. Suspensions were centrifuged at 1500 x g for 5 min and cell pellets were frozen at -20°C for further analyses.

Rn1/Rn2 mutagenesis study suffered from time limitations. It was not possible to follow the same procedure described for previous SOAT sequences. ERG-strains expressing mutated SOATs Rn1/Rn2 were cultivated in 50 mL of YPD at 30°C and 120 rpm in metal capped 250 mL baffled flasks. Cells were fed with 5 mL of glucose (20 %) after 24 h and 48 h of incubation time. Samples were taken after 70 h. CLR-strains expressing mutated SOATs Rn1/2 were cultivated in 50 mL of YPD at 30°C and 110 rpm in non-capped 250 mL baffled flasks. Cells were fed with 5 mL glucose (20 %) after 31 h and 55 h of incubation time. Samples were taken after 66 h.

2.2.7 Lipid analyses

Gas liquid chromatography/mass spectrometry (GC/MS)

Procedure for sample preparation and extraction of sterols from whole yeast cells was adapted from Quail and Kelly (1996), and Müllner et al. (2005). Frozen samples of 10 OD_{600} units derived from yeast cultivation were transferred to Pyrex tubes and centrifuged for 5 min at 2500 x g subsequently removing the supernatant. Alkaline hydrolysis solution consisting of 0.6 mL methanol, 0.4 mL of 0.5% pyrogallol dissolved in methanol and 0.4 mL of 60% aqueous KOH was added to samples together with 5 µL of cholesterol [2 mg/mL] (or as appropriate ergosterol) dissolved in ethanol as an internal standard. The suspension was mixed by vortexing and incubated for 2 h at 90°C in a sand bath or a water bath. Lipids were extracted three times with 1 mL of *n*-heptane shaking for 3 min on a Vibrax at 1500 rpm followed by spinning for 3 min at 1500 x g. Combined extracts were transferred into a second Pyrex tube and taken to dryness under a stream of nitrogen. (Optional: Dried lipids were stored at -20°C). Lipids were dissolved in 10 µL of pyridine and incubated for 30 min for derivatization after adding 10 µL of *N*,*O*-bis(trimethylsilyl)-trifluoroacetamide. Samples were diluted with 200 µL of ethyl acetate and transferred to crimp-top vials with micro inlay.

GC/MS analysis of silylated sterols was performed with an Agilent 19091S-433 column HP 5-MS (cross-linked 5% phenyl methyl siloxane; dimensions 30 m × 0.25 mm × 0.25 µm film thickness). Aliquots of 1 µL (syringe size = 10 µL) were injected in the splitless mode at 270°C injection temperature with helium as carrier gas at a flow rate of 0.9 mL/min in constant flow mode for a total run time of 38.67 min. The following temperature program was used: 1 min at 100°C, 10°C/min to 250°C, 3°C/min to 300°C, and 10°C/min to 310°C. Mass spectra were acquired in scan mode. Sterols were identified based on their mass fragmentation pattern, their retention time relative to cholesterol and sterol standards.

High-performance liquid chromatography (HPLC) and HPLC/MS

Sample preparation and analysis was done according to ACIB protocol “Sterol and Sterol Ester Analysis by HPLC” (Barbara Petschacher, 2014). Briefly, biomass pellets of 200 OD units stored at -

20°C in 15 mL Greiner tubes were used for extraction process. Samples were thawed at room temperature (RT), resuspended in 1 mL Zymolyase solution (5 mg/mL in 50 mM KP_i with 1 M D-sorbit) and incubated for 15 min at 37°C. After centrifugation at 3000 x g for 5 min, supernatant was discarded and pellet was resuspended in 1 mL of 100% EtOH. Then, 2.8 mL of 100% EtOH and 200 µL of internal standard (e.g. 2 mg/mL cholesteryl acetate dissolved in EtOH) was added and mixed in tightly closed tubes at 70°C and 750 rpm for 1 h. Cooled to RT, tubes were centrifuged at 3000 x g for 5 min and, subsequently, 3 mL of supernatant was transferred to Pyrex glass tubes. Extracts were brought to dryness under N_2 (e.g. VLM Evaporator) and were stored at -20°C or directly taken up in 200 µL of ethyl acetate. Samples were shaken at 40°C for 15 min to dissolve lipids. Then, undissolved particles were spun out at 3000 x g for 5 min and supernatant was transferred to GC vials (with inlay). HPLC analysis was performed with a mobile phase containing 80% EtOH 20% MeOH and 0.1% trifluoracetic acid at a flow of 0.6 mL/min. Ten µL samples were injected at 40°C. Compounds were separated in a YMC-Pack Pro C18 RS column at 20°C and were detected by UV at 210 nm for aromatic structures/sterols in general, or at 280 nm for sterols with conjugated double bonds such as 7-DHC and ergosterol. Alternatively, an MS detector in scan mode and positive SIM at sterol-specific masses minus the OH-group (-17) was employed. Analysis of HPLC data was done by integrating sterol peaks and normalizing against internal cholesteryl acetate (CLR-Ac) standard to account for any losses during extraction. If necessary, data was normalized to an external CLR-Ac standard to adjust the results for comparing data of different runs. Then, data was evaluated by calculating sterol concentrations using trend lines of sterol specific standard dilutions.

Thin layer chromatography (TLC)

Sample preparation and lipid extraction was conducted according to Folch et al. (1957). Lipids were dissolved in 100 µL chloroform - methanol (2:1 by volume); then, 15 µL or 30 µL were spotted onto TLC Silica gel 60 F_{254} plates. The first solvent consisting of petrolether - diethylether - acetic acid (25:25:1, v/v) was applied until a migration distance of 3 cm. Then a second solvent consisting of petrolether - diethylether (50:1, v/v) was applied for the total migration distance of 9 cm. TLC analysis was done according to ACIB protocol “TLC based Screening of Sterol O-Acyltransferases” by Holly Stolterfoht (2014). Images were taken with G:Box HR16 (Syngene, Bio Imager) under UV light for 80 ms exposure time (conjugated double bonds (like 7-DHC) quench the fluorescence of coated plates) and under white light for 15 ms. Then, TLC plate was dipped into charring solution (600 mL of H_2O, 600 mL of CH_3OH, 40 mL of H_2SO_4 conc., 4 g $MnCl_2$ or 6.3 g $MnCl2.4H_2O$) and heated for 20 min at 100°C so that all carbons get charred. Again images were taken under 15 ms exposure to white light.

2.2.8 Protein expression analysis

Western blot

Cells cultivated for 24 h in 10 mL of YPD media with 100 µM geneticin were collected to 10 OD_{600} units and frozen until Western blot preparation. Sample preparation for total protein extracts was performed using a modified protocol derived from Volland et al. (1994). Frozen cell pellets were dissolved in 200 µL of cold aq. protease inhibitor and kept on ice after mixing with 50 µL of 1.85 M NaOH to break up cells. After incubation for 15 min, 50 µL of 50% TCA were added, vortexed rigorously and incubated for 20 min. Samples were centrifuged for 10 min at 4°C and full speed (16,000 x g) and the supernatant was discarded. Pellets were resuspended in 70 µL of sample buffer mix containing 45.5 µL of ddH_2O, 17.5 µL of NuPAGE sample buffer (4x) and 7 µL of NuPAGE reducing agent (10x). Finally, preparation was stored at -20°C. Prior to loading onto gels, samples were incubated for 30 min at 37°C.

Proteins were separated and blotted to a nitrocellulose membrane pursuing the NuPage protocol for SDS-PAGE and Western blotting. Gels were run in cold MES-Buffer at 200 V for 1 h 30 min. Blotting conditions were set to a current of 230 mA for a running time of 1 h 10 min. Successful blotting was checked by staining with PonceauS and destained with TBST. Blocking of the membrane was carried out over night/the weekend at 4°C or for 1 h at RT in 50 mL of 5 % TBST-milk. FLAG-tagged proteins were detected using polyclonal mouse anti-FLAG AB (1:20,000 in 40 mL of 5%TBST-milk) as primary antibody (AB) and HRP-conjugated goat anti-mouse AB (1:10,000 in 50 mL of 5% TBST-milk) as secondary antibody. Additionally, a polyclonal AB against human SOAT1 was used as primary AB together with a HRP-conjugated goat anti-rabbit AB (1:10,000 in 50 mL of 5% TBST-milk) as secondary AB. Primary ABs were incubated for 1.5-2 days at 4°C while shaking moderately. Secondary AB were incubated 2 h at room temperature. Washing of membranes was done before and after applying secondary AB three times for 5 min with TBST. Detection was performed using Thermo Scientific Chemiluminescence Super Signal Kit following the supplier's manual and the signal was visualized by G:Box HR16 bioimager using appropriate software.

2.3 CLR-strain development

To generate a new *S. cerevisiae* strain which stably produces cholesterol instead of ergosterol, the yeast sterol biosynthesis pathway has to be manipulated. We followed a strategy described by Souza et al. (2011). First, knockout of the sterol C-22 desaturase encoded by *ERG5* and the sterol C-24 methyl transferase encoded by *ERG6* disrupts formation of ergosterol from its precursor zymosterol leading to the accumulation of mainly cholesta-5,7,24-trienol. Then, knock-in of two codon-optimized heterologous dehydrocholesterol reductases *DHCR24* and *DHCR7* originating from *Danio rerio* (Zebrafish) saturate cholesta-5,7,24-trienol at its double bond position C-24 giving 7-DHC and at C-7 resulting in the final product cholesterol. Since our group already had established a strain "10A" efficiently producing 7-DHC, only one further manipulation step was necessary for achieving formation of cholesterol, namely the integration of a *DHCR7* expression cassette into the *ERG5* locus (Figure 8). For detailed sequences see digital appendix.

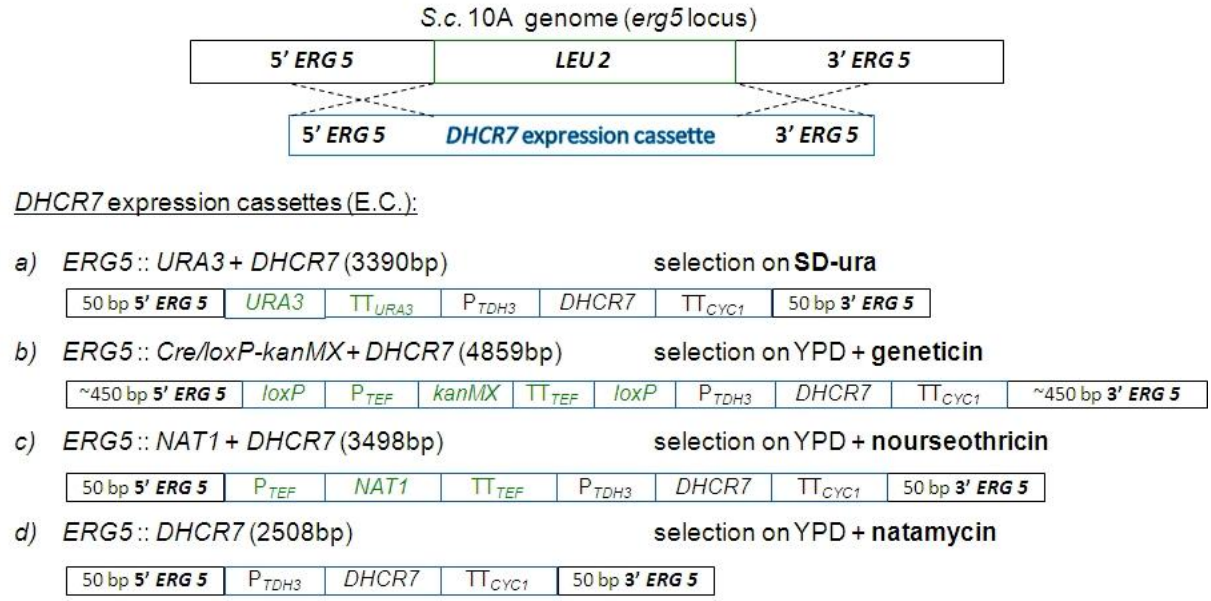

Figure 8: Expression cassettes designed for genomic integration of *DHCR7* at the *ERG5* locus.

2.3.1 Preliminary work

As depicted in Figure 9, the *DHCR7* gene was amplified by PCR from vector 056662pScript (Figure 35) along with *Bam*HI and *Eco*RI restriction sites and an additional 5' Kozak consensus sequence "AAAA" for *S. cerevisiae* using primers DHCR7-FW and DHCR7-RV (Table 16) giving a fragment of 1456 bp. This PCR-product was then used as an insert for *Bam*HI and *Eco*RI sticky-end ligation into the vector backbone of p426GPD_ARE2 (Figure 36). The created vector p426GPD_DHCR7 (Figure 37) contained our gene of interest flanked by the strong *S. c.* GAPDH/GPD promoter "P_{TDH3}" and the terminator of iso-1-cytochrome c "TT_{CYC1}". This part capable of introducing *DHCR7* overexpression was ultimately amplified by PCR, simultaneously adding the 3' homologous *ERG5* region, and later is referred to as "*7R-fragment*".

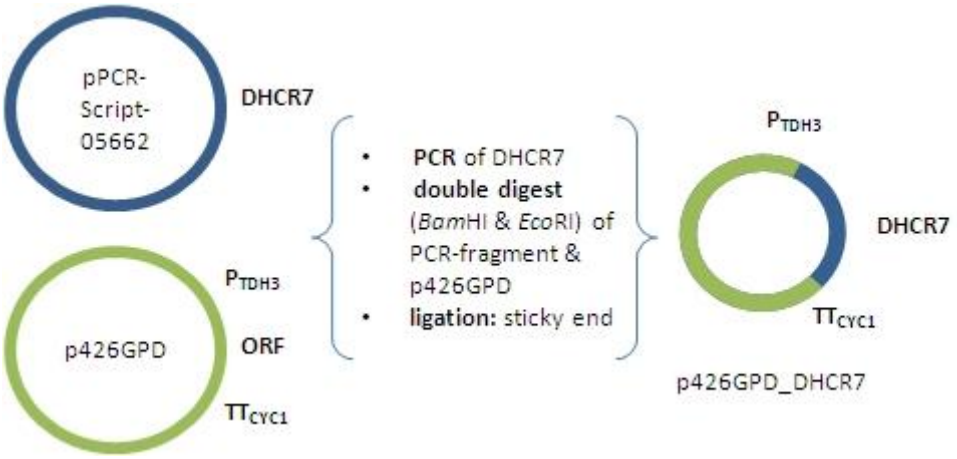

Figure 9: Schematic view of preliminary cloning.

2.3.2 Construction of expression cassettes

Expression cassette (*a*) was constructed by overlap extension (OE) PCR from two afore-generated PCR products (1) uracil marker and (2) *7R-fragment*. After the overlap at region P_{TDH3}, this construct was then amplified using primers URA3-HR-FW and CYC1t-HR-RV.

(1) Primer: URA3-HR-FW, URA3-TDH3-RV; template: p426GPD_ARE2

(2) Primer: TDH3-FW, CYC1t-HR-RV; template: p426GPD_DHCR7

Cassette (*b*) construction:

(1) PCR of selection marker
Primer: X-TEFp-FW, X-TEFt-RV; template: pUG6 (Figure 38)

(2) OE-PCR of 5' region
Primer: HR-435-FW, X-TEFt-RV; templates: gBlock (lHR-X-TEFp-FW); marker (1)

(3) OE-PCR of 3' region
Primer: TDH3-FW, HR-475-RV; templates: gBlock (CYC1t-lHR-RV), *7R-fragment*

(4) OE-PCR of total cassette overlapping at region P_{TDH3}
Primer: HR-435-FW, HR-475-RV; templates: (2) and (3)

Cassette (*c*) construction:

(1) PCR of selection marker
Primer: HR-DSM_TEFp-FW, DSM_TEFt-TDH3-RV; template: pHyD-0361
(Plasmid pHyD-0361 was provided by DSM)

(2) OE-PCR of total cassette overlapping at region P_{TDH3}
Primer: HR-DSM_TEFp-FW, CYC1t-HR-RV; templates: (1); *7R-fragment*

Cassette (*d*) construction by PCR:

Primer: HR-TDH3-FW, CYC1t-HR-RV; template: p426GPD_DHCR7

2.3.3 Expression cassette (*a*) failed

The idea behind cassette (*a*) *ERG5*::*URA3* + *DHCR7* (Figure 8) was to integrate the *7R-fragment* together with the *URA3* marker gene into our 7-DHC producing host strain, placing *URA3* expression under control of the native P_{ERG5} and, thus, screening for transformants harboring the ability to grow on minimal media lacking uracil. Despite the effort of several transformation attempts with varying concentrations of the expression cassette, no transformants could be detected on SD-ura plates even after a long incubation period of up to 14 days. There are at least three possible reasons for this outcome: 1) No recombination event happened, so that the *URA3* selection marker was not integrated and, thus, none of the clones were able to synthesize uracil. 2) Recombination at the *ERG5* locus was the case, however, P_{ERG5} was not able to promote expression of *URA3* sufficiently. 3) Expression of selection marker and sterol C-7 reductase was working properly. In spite of all that, the yeast cell could not tolerate high amounts of cholesterol while struggling with the growth on minimal media.

Expression cassettes (*b*), (*c*) and (*d*)

The experience with cassette (*a*) led us to develop three new strategies: Promoting *in vivo* recombination, the *ERG5* homologous regions of cassette (*b*) were extended by around 400 bp. Selection marker was changed to kanMX controlled by TEF promoter and terminator sequences, so that transformants can grow in full media and can be selected for resistance towards geneticin (G418). Also, the selection marker was flanked by *LoxP* sites enabling excision from the genome using the Cre-Lox system. Cassette (*c*) offered another selection marker, thus transformants could be selected in full media for resistance to Nourseothricin. Transformation with cassettes (*b*) and (*c*) was finally not performed because of the results gained with cassette (*d*). With cassette (*d*) we pursued the elegant attempt to screen directly for cholesterol production without using any additional marker gene. As previously reported by te Welscher et al. (2008), the polyene antibiotic natamycin blocks fungal growth by binding rather specifically to ergosterol, whereas a cholesterol-producing strain was shown to be 16-fold less sensitive toward natamycin compared with the corresponding wild type strain. Interactions of natamycin with sterols seem to depend strongly on the *sp*2 hybridization of C-7 in the B-ring present in ergosterol and 7-DHC, but not in cholesterol. Therefore, this drug is useful for screening clones expressing a functional sterol C-7 reductase and converting 7-DHC into cholesterol.

A negligible drawback of this strategy is an additional expenditure of time necessary for replacement of 7-DHC that already existed in the cell membranes prior to transformation. Otherwise, if cells would be plated out on selective media immediately or after insufficient regeneration time, natamycin would still be able to efficiently act on the native sterols present, particularly 7-DHC in the "10A" strain. Taking a wild guess, three to five doublings were considered sufficient for sterol

replacement, and to make sure of that, we decided to incubate for at least 18 h. Even taking this procedure into account, advantages over the other design strategies prevail. The burden to express another protein is reduced, because no additional selection marker was necessary for selection of transformants. The remaining selection marker instead could be used for a further gene knock-out or knock-in. Also, time is saved compared to reusable marker approaches like we pursued with cassette (*b*), not having to excise the marker via Cre recombinase. Perhaps transformation efficacy could be improved as well, because shorter expression cassettes might find their way more easily into the cell than longer DNA fragments. Also, construction of the expression cassettes was fast and simple, without the necessity to use overlap extension PCR. Finally, if the saying holds true, that you get what you screen for, then variants found inevitably have to produce cholesterol, because only higher cholesterol content would lead to natamycin resistance.

2.3.4 Success with cassette (*d*) *ERG5*::*DHCR7*

LiAc-transformation of cassette (*d*) *ERG5*::*DHCR7* was performed using two strains. First, *S. cerevisiae* "10A" not having a functional ACAT and, secondly, *S. cerevisiae* "10A-F9" containing p42GPD_Are2 hence over-expressing a wild-type Are2p and being capable of sequestering sterols in lipid particles in the form of sterol esters. Assuming a start OD_{600} of 10, which was used for each transformation mix, and comparing this amount with OD_{600} values measured after 18.5 h of incubation (Table 11), we would get only 2-3 doublings for the "10A" strain and around 1 cell division for the "10A-F9" strain. This unexpected long lag-phase resulting in a reduced number of doublings could have affected our selection procedure. Using 1 µg of cassette (*d*) for *S. cerevisiae* "10A" transformation resulted in only two clones, one on the 40 µM and another one on the 60 µM natamycin plate. However, 2 µg yielded in a total of 13 colonies. Distribution of "10A" transformants was approximately according to the plated volume ratios (listed in Table 11). No colonies were able to grow on control plates with a concentration of 60 µM, proving the growth inhibiting effect of natamycin on cells producing mainly 7-DHC. At a concentration of only 40 µM, many small colonies were observed on the control plate of "10A-F9" strain. One colony of the control plate, termed "F9_C", was chosen together with potential cholesterol strain candidates (10A_1-12 and F9_1) for simple streak out tests (Figure 10) and colony PCR (Figure 11). Results are summarized in Table 12.

Table 11: Transformation results of expression cassette (*d*) *ERG5*::*DHCR7* into strains *S. c.* "10A" and *S. c.* "10A-F9".

		40 µM natamycin		60 µM natamycin	
	OD_{600}	plated vol.	colonies	plated vol.	colonies
"10A" 1 µg DNA	69	2 plates, 1/3	1	1/3	1
"10A" 2 µg DNA	65	2 plates, 1/3	10	1/3	3
"10A" control	57	1/2	-	1/2	-
"10A-F9" 1 µg DNA	19	1/2	1	1/2	-
"10A-F9" control	24	1/2	many	1/2	-

Streak outs on YPD + natamycin plates suggested that ten of twelve chosen "10A" transformants were producing cholesterol instead of 7-DHC. Differences in growth intensities might be caused by using unequal amounts of cell material, as colony size was bigger on original YPD transformation plates with 40 µM natamycin compared to the colony size on 60 µM natamycin. Furthermore, these ten clones grew on SD-his and not on SD-leu plates, suggesting that recombination of the expression cassette eliminated the *LEU2*-disruption cassette from the *ERG5* locus as anticipated. On the other hand, streak outs of the only "F9_1" colony, exhibited significant sensitivity towards natamycin. Although growth on SD-leu indicated no recombination event at the *ERG5* locus, the expression cassette could have been integrated somewhere else into the chromosome that could be accompanied by lower expression of *DHCR7*. An explanation for reduced tolerance towards natamycin could be the functional Are2p strongly acting on free cholesterol and reducing its amount relative to CLR precursors.

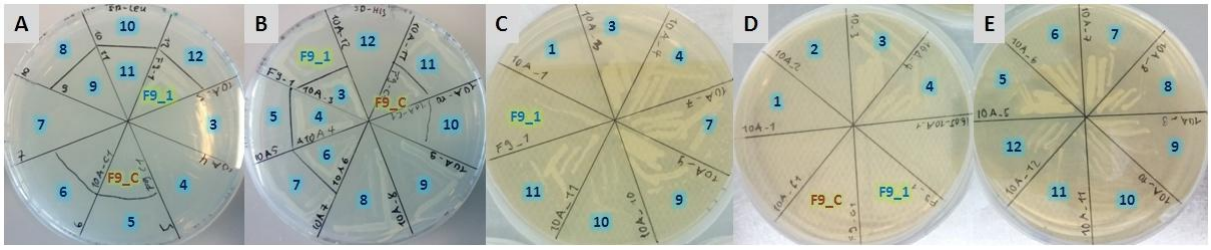

Figure 10: Streak-out plates of potential BA-C transformants on selective media plates. A SD-leu; **B** SD-his; **C** YPD + 40 µM natamycin; **D, E** YPD + 60 µM natamycin; **# 1-10** colonies derived from strain 10A transformation; **F9_1** single colony derived from strain 10A-F9 transformation; **F9_C** colony derived from negative control plate of strain 10A-F9 transformation.

Table 12: Test results of potential BA-C transformants. Colony streak out on selective media (Figure 10) to test for cholesterol production (growth on natamycin), correct expression cassette integration into *ERG5* locus (no growth on SD-ura) and control for strain background (growth on SD-his): **+++** strong, **++** medium, **+** weak growth; **-** no visible growth. Also indicated are 6 colonies which were further checked by colony PCR. Three verified transformants (**BA-C** I, II, III) chosen for further analyses.

Original plate	Short name	YPD + natamycin		Minimal media		Colony PCR	BA-C
		40 µM	60 µM	SD-leu	SD-his		
10A 1 µg, 40 µM	10A_01	-	-				
	10A_02		-				
	10A_03	+++	+++	-	+	#2	
	10A_04	+++	+++	-	+	#3	I
10A 2 µg, 40 µM	10A_05		++	-	+		
	10A_06		++	-	+		
	10A_07	+++	++	-	+	#4	II
	10A_08		++	-	+		
10A 1 µg, 60 µM	10A_09	+++	++	-	+	#5	III
	10A_10	+	+	-	+		
10A 2 µg, 60 µM	10A_11	+++	+	-	+	#6	
	10A_12		+	-	+		
F9 1 µg, 40 µM	F9_1	+	-	+	+		
F9 control, 40 µM	F9_C		-	-	+	#1	

The colony PCR results shown in Figure 11 finally confirmed correct integration of cassette (*d*) into at least four transformants. Primers of reaction mix A should bind 5' and 3' to the cassette (*d*) within the *ERG5* locus giving a PCR product of around 1.5 kb if the *LEU2* was still present at the disrupted gene (lane 1, N). However, if cassette (*d*) replaced *LEU2* at the *ERG5* locus, this would give a PCR product of around 2.8 kb as shown in lines 3-6. Interestingly, no band was visible in lane 2 because of unknown reason. Primers of reaction mix B bind within cassette (*d*) and 5', so that a band at 1.8 kb also indicated correct recombination. Here, lane 2 also exhibited a band with the expected size. Both primer sets of C and D bind within cassette (*d*) and, thus, only confirm its presence in the genome. If only C and D gave the expected band, but not B or only the 1.5 kb band in mix A, then this would be an indication of ectopic integration. With respect to all previous test results, three clones were chosen out of many possible candidates for further analyses regarding their sterol composition.

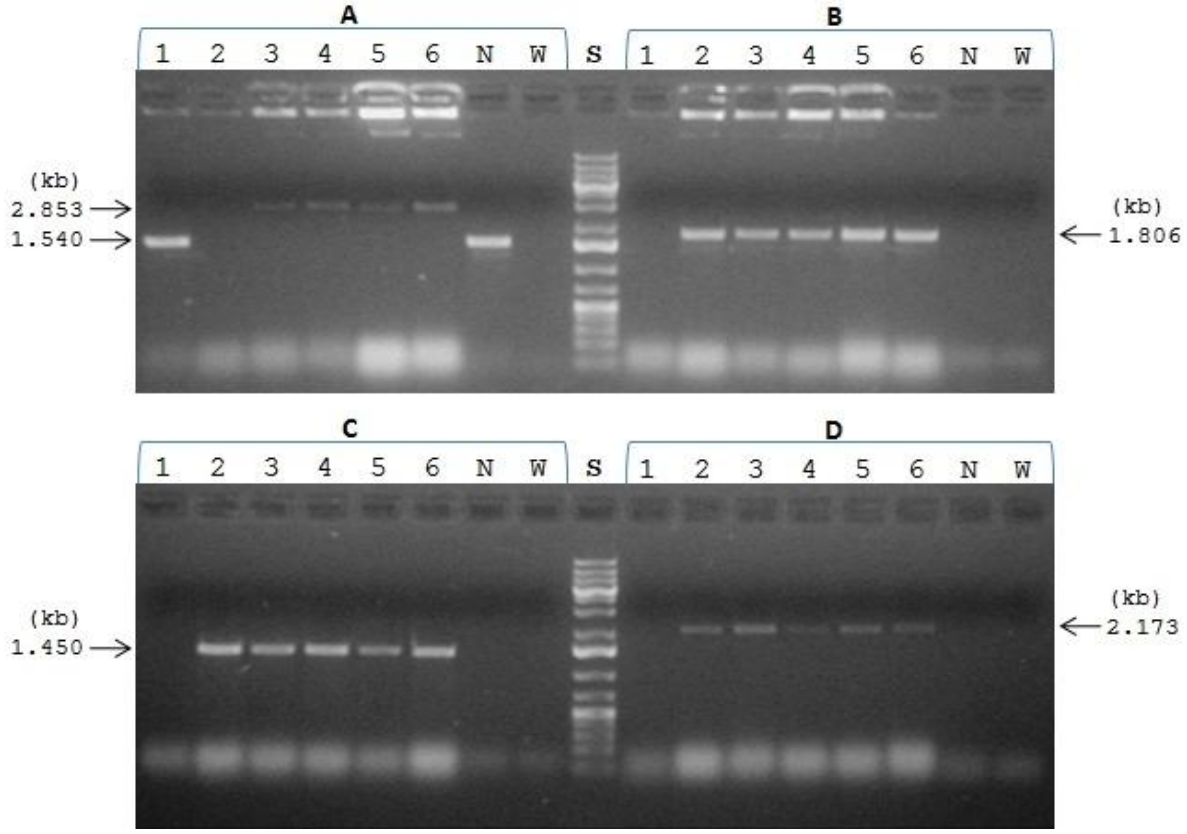

Figure 11: Colony PCR confirms correct genome integration of *ERG5*::*DHCR7* in at least four BA-C transformants. Gel-electrophoresis with 1% agarose. Primer pairs used for colony PCR reaction: **A** K1E5 + K2exE5; **B** DHCR7-FW + K2exE5; **C** DHCR7-FW + DHCR7-RV; **D** HR-1-FW + DHCR7-RV. Colony templates as noted in Table 12: **1** "F9_C"; **2** "10A_03"; **3** "10A_04"; **4** "10A_07"; **5** "10A_09"; **6** "10A_11"; **N**: WT 10A colony used as negative control, **W**: water used instead of colony template. **S** Thermo Scientific™ GeneRuler™ 1 kb Plus DNA Ladder.

Compared to plasmid transformations in general, the efficiency of the newly developed transformation and screening procedure was rather low, but sufficient for our objective. Considering the long incubation time of around 18.5 h after the transformation event, one cannot rule out the possibility that all BA-C clones gained from one transformation mix, actually derived from one successful recombination event in only one single cell. If that were the case, one could argue that

more than one colony producing sufficient cholesterol should have appeared from the “10A 1 µg” transformation mix (compare Table 11 with Table 12). Therefore, it remains unclear how often cell divisions actually took place during this extraordinarily long incubation period.

When looking at the two different natamycin concentrations for selecting cholesterol producers, it is obviously more likely to find positive clones at 60 µM compared to 40 µM. Based on these results we recommend to use 60 µM natamycin plates to be sure of cholesterol production and to make further streak out tests obsolete. Though, higher efficacies might be obtained when using a lower concentration. Interplay between incubation time and antibiotic concentration is conceivable, thus reducing incubation time would go along with reduced natamycin concentration. This, of course, harbors the risk of contamination. Also, we can conclude that at least 2 µg of expression cassette should be used for transformation.

2.4 SOAT expression in sterol engineered strains

Overexpression of heterologous membrane proteins can be a delicate process. Sometimes slow translation and lower expression levels are beneficial for correct folding and cell growth, whereas too high expression often ends up in bottlenecks (Ashe and Bill 2011). Overproduction of ER-resident membrane proteins in yeast can lead to enhanced proliferation of ER membranes, but there are various tools and strains available to overcome the obstacles as recently reviewed by Emmerstorfer et al. (2014). In our study, we decided to use straightforward GPD promoter for constitutive and strong expression, hoping for similar expression conditions in all sterol-engineered strains. Also, the influence of native and codon-optimized sequences on activity of mammalian SOATs was tested (GC-MS results). Cloning of SOAT sequences into p42kanGPD vector (Figure 12) was performed by Holly Stolterfoht and Clemens Farnleitner. Plasmids were constructed by double digestion of plasmid backbone and FLAG-tagged SOAT inserts using restriction enzymes *Bam*HI and *Eco*RI, ligation and cloning into *E. coli*. Then, plasmids were transformed into yeast strains and cultivated for SOAT expression and lipid analyses including empty vector controls not containing any SOAT.

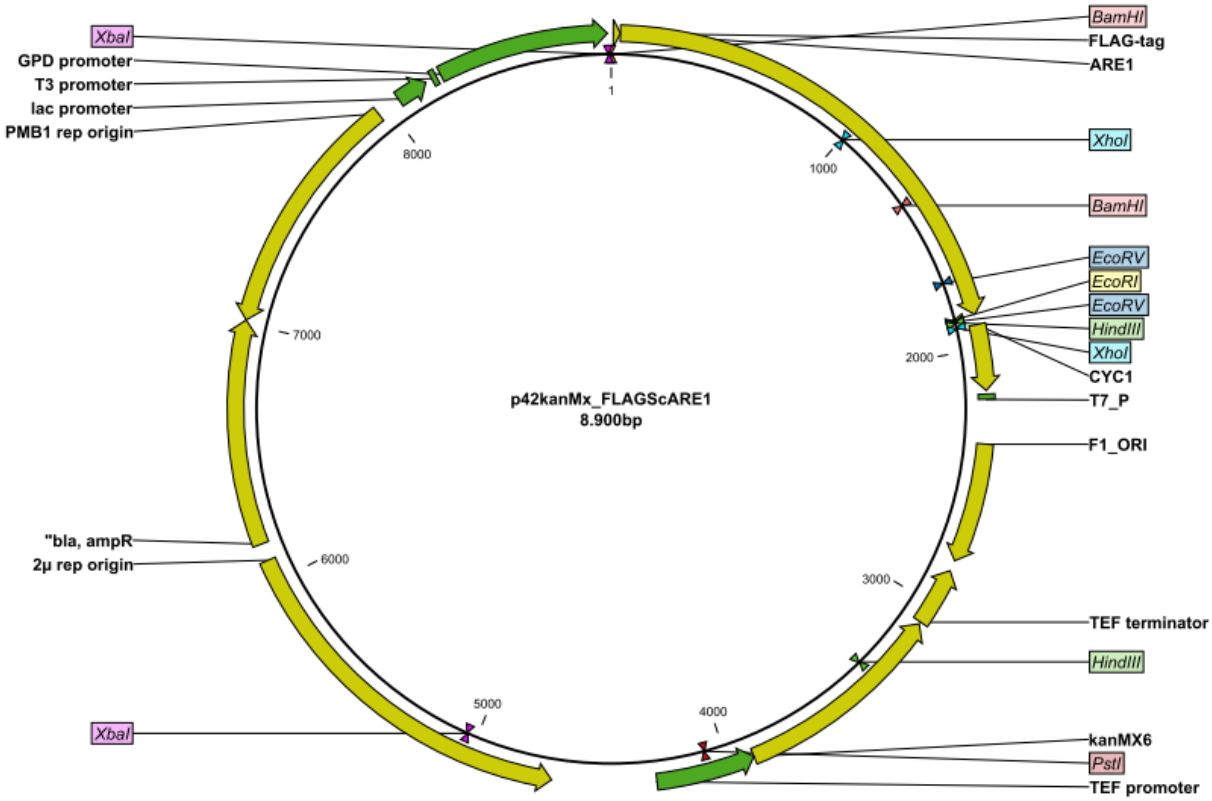

Figure 12: Gene map p42kanGPD SOAT expression vector. Multicopy 2µ based plasmid for replication in *S. cerevisiae* and cloning in *E. coli*. Genetic elements are ampicilin and geneticin resistance cassettes, GPD promoter and *CYC1* terminator. Gene of interest Sc1 (*ARE1*) is presented as an example.

2.5 Rn1/Rn2 mutagenesis

Here, an unconventional strategy was tested on rat SOAT1 (Rn1) and SOAT2 (Rn2) in order to locate substrate specificity determining regions. Our results indicated that both enzymes share highly conserved regions. However, enzyme activity was inversely regulated by sterol background. Rn1 prefered ergosterol whereas Rn2 acylated 7-DHC and cholesterol, but not ergosterol. Previous mutagenesis studies focused on single amino acid exchanges and N- or C-terminal truncations. Screening for point mutations is time consuming and expensive. In this study, we wanted to approximate important locations by exchanging large regions of both isoenzymes from rat. As a desirable outcome, an important location from Rn1 would restore activity towards ergosterol in a variant of Rn2. Exchanging only four regions in all possible combinations result in at least 16 experiments for expression in only one strain. The fractional factorial design (Table 13) further reduced the number of experiments and still allowed for the analysis of all exchanged regions within a few weeks. Furthermore, we could simultaneously examine possible interactions between two exchanged regions. The basic strategy was to amplify four fragments from Rn1 and Rn2 expression vectors by PCR and combine them as shown in Figure 13 and Table 13. In case that Gibson assembly failed, fragments could be fused alternatively by overlap extension PCR, followed by digestion with restriction enzymes and ligation into expression vector.

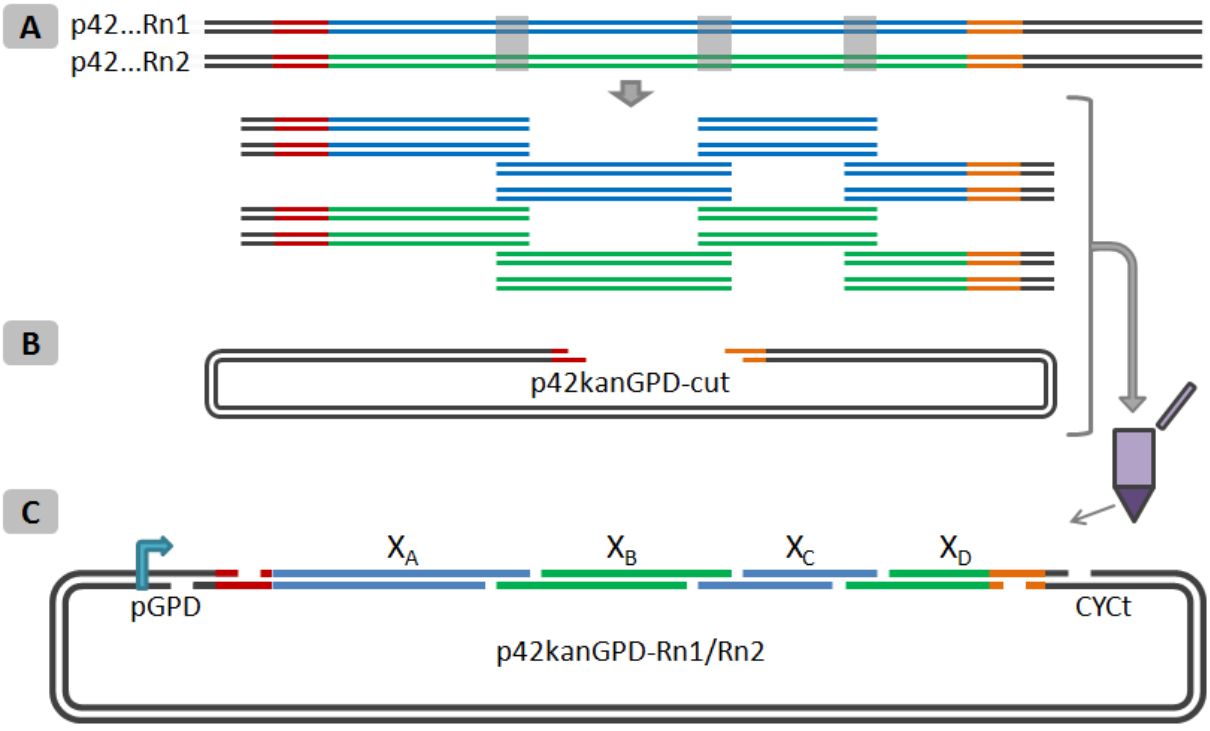

Figure 13: Rn1/Rn2 mutagenesis strategy. A: PCR-amplification of Rn1 and Rn2 fragments flanking internal conserved regions (grey boxes) and plasmid regions within promoter and terminator including FLAG-tag and restriction sites. **B:** Linearization of vector backbone at restriction sites *Bam*HI (red) and *Eco*RI (orange). **C:** Gibson assembly of pre-selected Rn1 and Rn2 fragments into expression vector.

Gibson cloning products were transformed into *E. coli* and clones were verified by colony PCR, double digestion pattern on agarose gels and sequencing of isolated plasmids. Three constructs ($1_A1_B1_C2_D$, $2_A1_B1_C2_D$ and $2_A2_B2_C1_D$) and additional controls were transformed into yeast and confirmed by colony PCR. An example for mutants in CLR-strains is shown in Figure 14. Fragment combinations beginning with 1_A ($1_AX_BX_CX_D$) have double band patterns, whereas only one intense band at 1.7 kb is amplified from combinations beginning with 2_A.

Table 13: Rn1/Rn2 mutagenesis design table. Light grey squares represent fragments from Rn1, dark squares from Rn2.

combination		X_A	X_B	X_C	X_D
1	(Rn1)				
2	ad				
3	bd				
4	ab				
5	cd				
6	ac				
7	bc				
8	abcd (Rn2)				

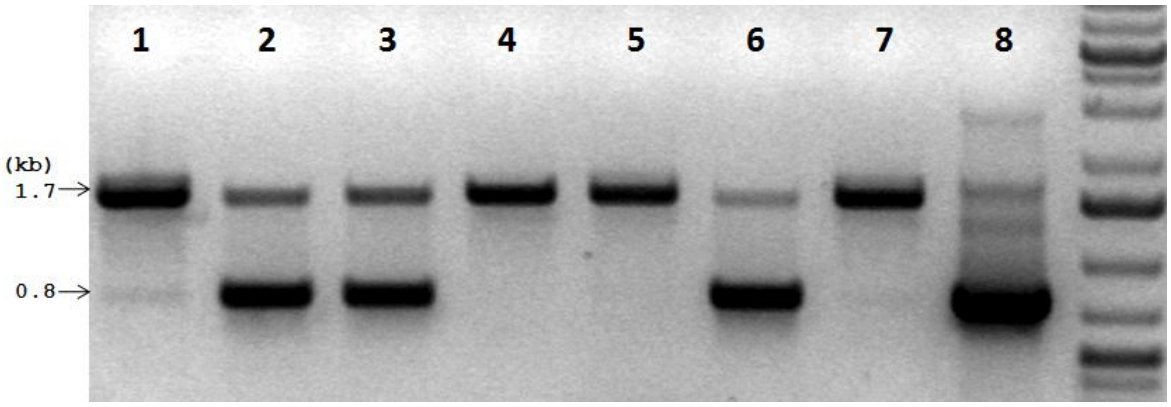

Figure 14: Confirmed CLR-strain transformation of Rn1/2 mutants. Excerpt from colony PCR results of following fragment combinations: (1) 2112; (2) 1112a; (3) 1112b; (4) 2221a; (5) 2221b; (6) 1111; (7) 2222 (8) p42kanGPD-Rn1 control. Primer: A-fw, 1B-fw and D-rv.

3 RESULTS AND DISCUSSION

3.1 Lipid composition of *S. cerevisiae* producing cholesterol

3.1.1 Total sterol analysis reveals high cholesterol production

Upon silylation of total sterols extracted from duplicates of BA-C I, BA-C II and BA-C III culture, quantification of these components was performed by gas liquid chromatography/mass spectrometry (GC-MS) to calculate the cells' sterol composition. The chromatogram example shown in Figure 15 from a BA-C I sample is very similar to the data obtained from other BA-C samples (listed in Table 16). Two major peaks within the section between 25 to 30 minutes (min) of expected sterol retention times (ret.) correspond to cholesterol at a ret. 26.1 min (mass spectrum: 458, 443, 368, 353 and 329) and the internal standard ergosterol [10 µg] at ret. 27.4 min (MS: 468, 378, 363 and 337). Mass spectra of minor peaks in-between indicate the presence of cholesta-5,8-dienol at 26.21 min and cholesta-7-enol at 26.927 min, whereas MS of the peak at ret. of 26.329 min does not account for a sterol compound. Also, ergosta-5,8,14,22-tetraenol at ret. 26.692 min and other ergosta-compounds with ret. greater than the internal standard were detected. All ergosta-compounds might be a result of impure IS and, thus, are not included into further calculations for the cells' sterol composition.

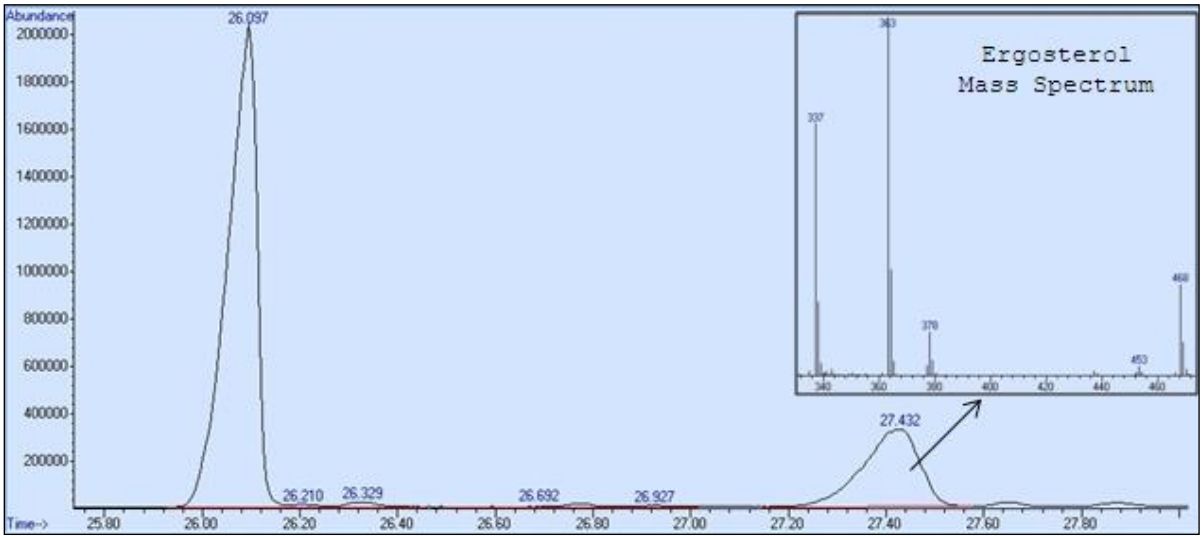

Figure 15: Total sterol analysis of BA-C I measured by GC-MS reveals high cholesterol production. Selected chromatogram section of sample BA-C I and associated mass spectrum of ergosterol as internal standard (retention time: 27.432 min); cholesterol (ret. t.: 26.097 min).

As depicted in Figure 16-A, cholesterol levels of all three BA-C transformants ranged between 99.12 ± 0.04 % - 99.31 ± 0.14 %. First of all, these values confirmed that cholesterol was clearly the major sterol present in these cells, also proving that our transformation approach was successful. Second, all three transformants can be considered as equal because of their highly similar intracellular sterol composition. Yet, total cholesterol amounts varied around 14 % between transformants in a range of 28.3 µg and 32.8 µg per 10 OD_{600} (Figure 16-B). Here, these values were calculated by relating the

integrated areas of cholesterol peaks to corresponding areas of 10 µg of internal standard ergosterol, assuming similar detection properties. Mistakes during pipetting of a small volume of 10 µL IS to the samples could account for an explanation. Extrapolated mean cholesterol production of all three cholesterol strains would give a value of 73 ± 7 mg/L culture, not accounting for any losses during extraction procedure. With the focus on the cells' sterol composition, we could freely choose any of these clones for further transformation and analysis of heterologous SOATs.

With the data gained in this study, we can announce a strain producing more than 99 % cholesterol, which is even higher than the latest described stable strain by Souza, et al. (2011) comprising more than 96 % cholesterol of total sterols. In contrast to our BA-C strain, the published strain RH6829 (*MATa ura3 leu2 his3 trp1 can1 bar1 erg5D::HIS5-TDH3-DHCR24 erg6D::TRP1-TDH3-DHCR7*) still contained functional SOATs (Are1 and Are2) which might be the decisive factor here. Since the smaller percentage of sterols was not identified in RH6829, we can only presume that SOATs act on cholesterol and its precursors, so that they are stored as sterol esters in lipid particles.

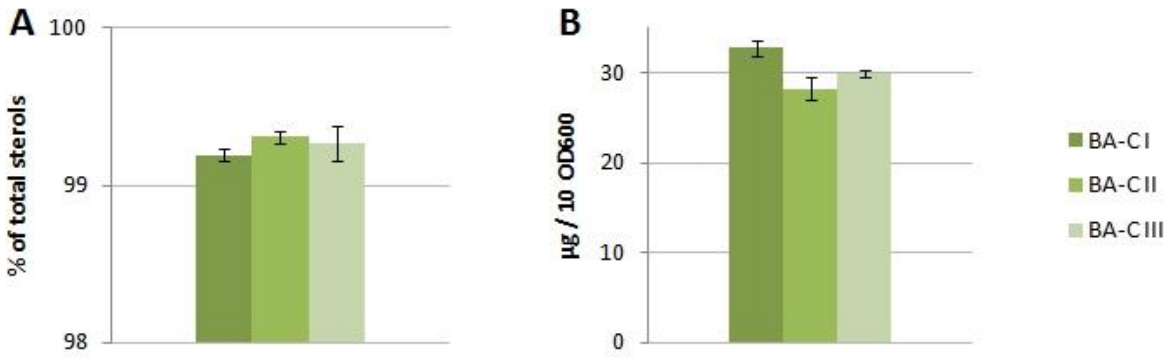

Figure 16: Comparison of cholesterol production in three BA-C transformants measured by GC/MS. Mean values were calculated from duplicate samples. **A** reflects the intracellular percentage of cholesterol of all cellular sterols. **B** shows the amount of cholesterol produced in 10 OD_{600} units of "BA-C" transformants, which was calculated by relating the integrated areas of cholesterol to those of internal standard ergosterol.

3.1.2 Detection of cholesterol and steryl esters

With high pressure/high-performance liquid chromatography (HPLC) we have the possibility to measure sterols without the need for modification during sample preparation, thus one can also distinguish between free sterols and sterol ester present in the cell. This fact became crucial for the ongoing study of SOATs, but since SOATs were knocked out in our cholesterol strain, it was unlikely that any sterol ester would be measured. The chromatogram of sample BA-C I (Figure 17) can be taken as an example for the other two samples. In all samples, either cholesterol or the IS are the only peaks identified as free sterols present in the cell. While cholesteryl acetate was used as an IS for BA-C I, ergosterol was used for BA-C II and BA-C III. Retention times of cholesterol and internal standards were verified by separate runs of standards (not shown). Interestingly, separate runs of the standards did show lower area values than those integrated from internal standard areas of the

sample runs. It is therefore not possible to estimate efficiency of lipid extraction. Several peaks elute after cholesteryl acetate. HPLC-MS analysis of these peaks suggested that none of these can be related to any sterols or sterol esters (data not shown). We concluded from HPLC measurements that free cholesterol was the only sterol present in our CLR-strain.

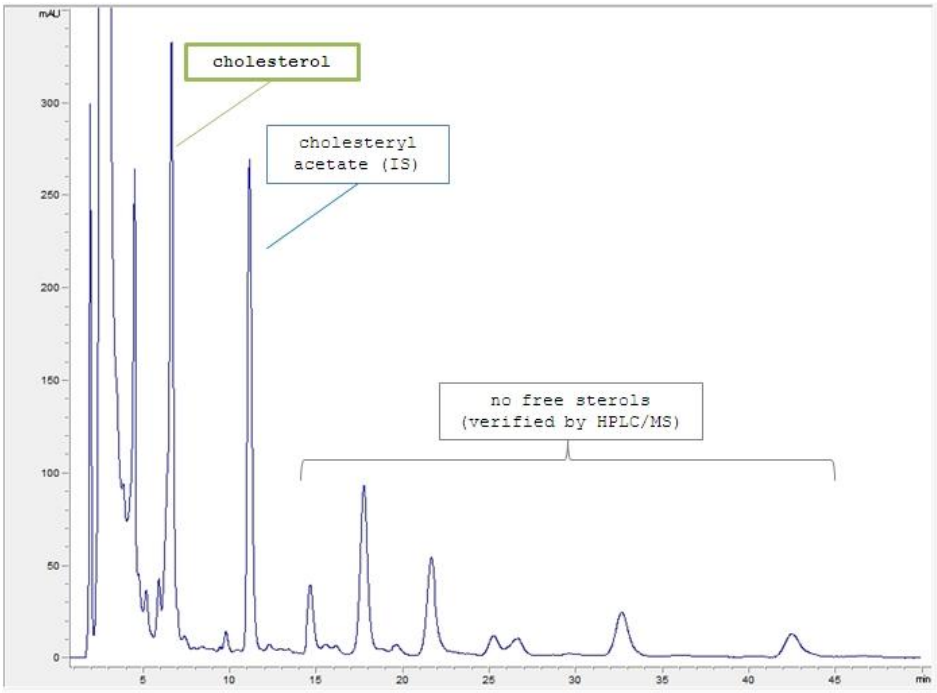

Figure 17: Detection of Cholesterol in BA-C I by HPLC measurement. UV detection at 210 nm. Cholesteryl acetate [1 mg/mL] was used as internal standard. Retention time of cholesterol and IS was verified using measurements of standard solutions (not shown).

3.1.3 Lipid fractionation

Triplicates of 100 OD_{600} unit samples were used for thin layer chromatography (TLC) after lipid extraction according to Folch et al. (1957). This method once again supported the results already described above, given that cholesterol appeared to be a major compound of the cells' lipid composition. Prior to charring, the TLC plate was observed under UV light (Figure 18-A), where molecules comprising conjugated double bonds appear as dark spots, as they quench out fluorescence of the coated TLC plate. The first, minor band belongs to cholesterol, which has only one double bond, but is still slightly visible under UV. The second band is very intense, located between the cholesterol band and the band #3 on the char picture (Figure 18-B). It remains unclear what sort of molecule this band might represent, as it must be highly conjugated and not sensitive towards charring. Considering the polarity of the band/smear #5 on the char picture, it possibly belongs to diglycerides and fatty acids. Triglycerids are to be found at the next band, which is also present in the standard (triolein). The two faint upper bands (#6, #7) seem to be sterol ester, because of a similar migration distance like cholesteryl oleate. This observation of possible sterol ester is in conflict with GC-MS and HPLC-MS results and the theoretical background of our strain genotype.

Nevertheless, there is always the chance that unknown mechanisms exist within the cell to esterify at least small amounts of sterols.

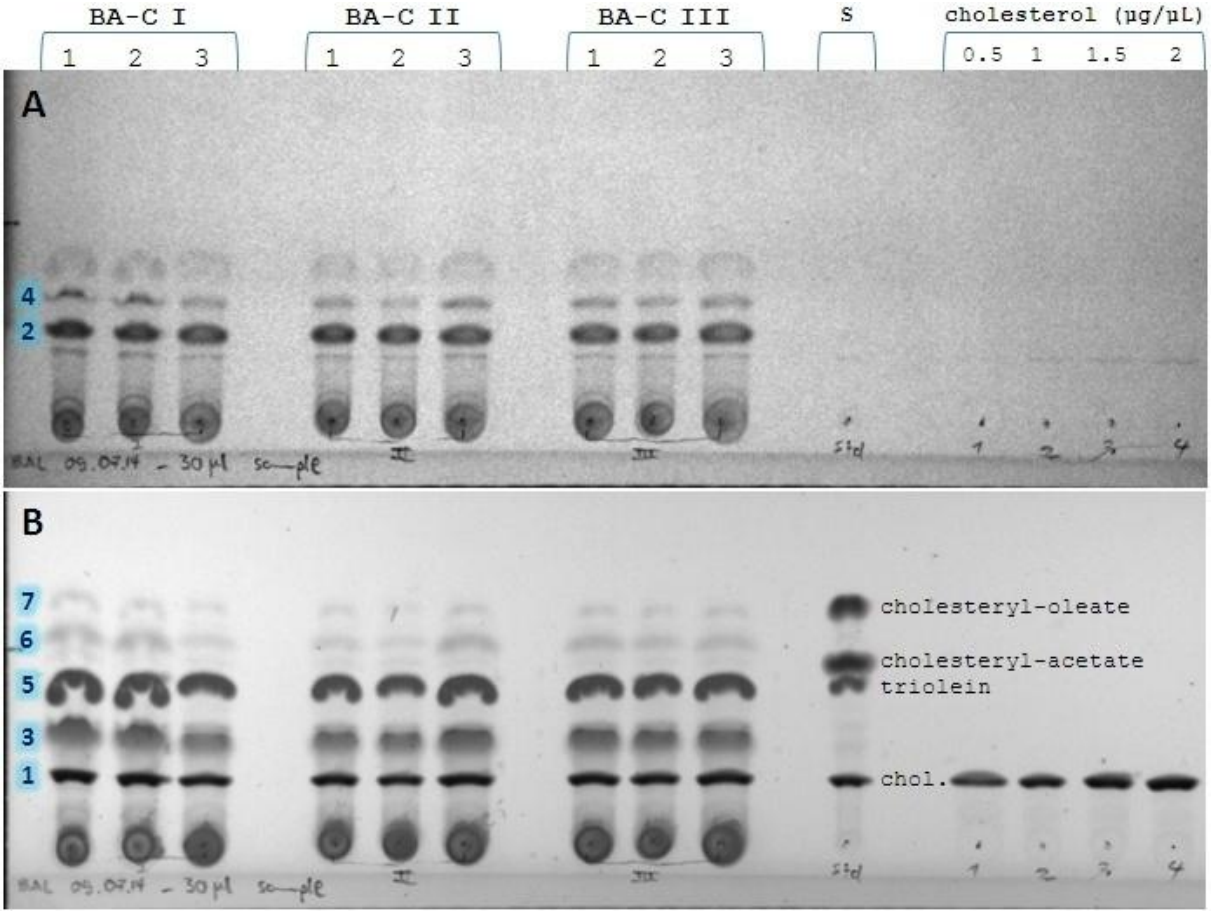

Figure 18: Lipid composition of three selected BA-C transformants. Thin layer chromatography (TLC) results after lipid extraction from 100 OD_{600} sample triplets of BA-C I, II and III dissolved in 100 µL $CHCl_3$/MeOH using the Folch method. Because of no visible bands at a higher migration distance, only 5 of 9 cm migration lengths are shown. Volumes of 30 µL samples and 15 µL of standards were topically applied on a TLC Silica gel 60 F_{254} plate. In addition to four different concentrations of cholesterol, also one multiple standard (S) containing 1 µg/µL cholesterol, triolein, cholesteryl-acetate and cholesterol oleate were applied. **A** Conjugated double bonds quench out fluorescence of the coated TLC plate under UV light (Epi short wave UV, short wave band pass filter, 80 ms exposure time), picture taken before charring. **B** Char picture (upper white, no filter, 15 ms exposure time). **# 1-7** Numbering of bands is according to migration distance.

Clone BA-C III was used for further experiments on sterol acyltransferases and is referred to as the CLR-strain.

3.2 Overexpression of SOATs in sterol engineered yeast strains

3.2.1 Relationship of SOATs in this study

In this study we focus on published Sterol-O-Acyltransferases that have been successfully expressed in *Saccharomyces cerevisiae*. They were chosen by Regina Leber also because of their potential to acylate 7-DHC. The selection reflected a great diversity that comprises three yeast SOATs including both endogenous isoenzymes from *S. cerevisiae* ARE1/Sc1 and ARE2/Sc2 (Yang et al. 1996) and one from *Candida albicans* ARE2/Ca2 (Kim et al. 2004), and three mammalian enzymes from *Rattus norvegicus* SOAT1/Rn1 and SOAT2/Rn2 (Matsuda et al. 1998), *Pan troglodytes* SOAT1/Pt1 (human SOAT: Chang et al. 1993) and one from a parasitic protozoan *Toxoplasma gondii* SOAT1/Tg1 (Nishikawa et al. 2005). The diversity of enzymes chosen for this study is visualized by a phylogenetic tree of total SOAT sequences, where Tg1 seems to be distant to all other SOATs (Figure 19). Close up view on conserved sequences like putative binding sites also suggest Tg1 to be an outlier (Figure 20), although Nishikawa et al. (2005) argued that Tg1 was more closely related to yeast than to mammals. Also Rn1 is more similar to Pt1, than to Rn2, suggesting an early gene duplication event.

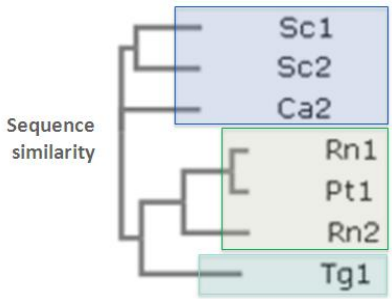

Figure 19: Protein sequence similarity of selected SOATs. Sc (*Saccharomyces cerevisiae*); **Ca** (*Candida albicans*); **Rn** (*Rattus norvegicus*); **Pt** (*Pan troglodytes*); **Tg** (*Toxoplasma gondii*). SOAT numbering is according to literature (uniprot). Sc1: P25628, Sc2: P53629, Ca2: P84285, Rn1: O70536, Rn2: Q7TQM4, Pt1: H2Q0P3, Tg1: B9QNV5. Tree generated with Clustal Omega.

A

```
Pt1   ASRFIIIFEQIRFVMKAHSFV
Rn1   ASRFILILEQIRLVMKAHSYV
Rn2   ASRCVLVFEQVRFLMKSYSFL
Sc1   VTRIFLFLHSVVFVMKSHSFA
Sc2   LSKIFLFLHSLVLLMKMHSFA
Ca2   IAKVFLVLHSLVFIMKMHSYA
Tg1   IPAAFVQMIAVVQFMKMHSYS
       :: .:.:.: ::** :*:
```

B

```
Pt1   FLHCWLNAFAEMLRFGDRMFYKDWWNSTSYSNYYRTWNVVVHDWLYYYAYKDFLWFFSKRFKSAAM
Rn1   FLHCWLNAFAEMLRFGDRMFYKDWWNSTSYSNYYRTWNVVVHDWLYYYVYKDLLWFFSKRFRPAAM
Rn2   FLHCWLNAFAEMLRFGDRMFYRDWWNSTSFSNYYRTWNVVVHDWLYSYVYQDGLWLLGRQGRGAAM
Sc1   IWDALLNCVAELTRFADRYFYGDWWNCVSFEEFSRIWNVPVHKFLLRHVYHSSMGALHLS-KSQAT
Sc2   IWDAILNCVAELTRFGDRYFYGDWWNCVSWADFSRIWNIPVHKFLLRHVYHSSMSSFKLN-KSQAT
Ca2   IWDAILNAIAELSKFADRDFYGPWWSCTDFSEFANQWNRCVHKFLLRHVYHSSISAFDVN-KQSAA
Tg1   LFECICNLAAEITNFANRNFYDDWWNSTNWDEYSRKWNKPVHRFLLRHVYMETQQRYKWS-HQTAA
      : .. :*..**: :*.:* **  **....: :: . **  **.:*  :.*:. :  :    :  *
```

Figure 20: Alignment of potential substrate binding sites (Oelkers et al. 1998). (**A**) Putative sterol binding site H/Y-S-F/Y (green/blue) of which serine was invariant, on the left site in between lysine and arginine (grey) are potential CRAC/CARC pattern located. (**B**) Highly conserved region with putative acyl-CoA binding site FYxDWWN (green/blue). Generated with T-COFFEE, Version_11.00.8cbe486.

3.2.2 SOAT expression

Protein expression and folding influence activity and could account for some of the effects we observed on sterol and sterol ester content. Likely, enzymes derived from yeast (Sc1, Sc2 and Ca2) are better expressed and folded in our yeast host strains than the other selected enzymes. Therefore, we want to find out if mammlian SOATs are better expressed in a CLR-strain compared to ERG-strain. Possibly, sterol structure specific interactions with SOAT transmembrane domains influence protein stability. Protein samples from main cultures used for sterol analysis after 65 h or 42 h resulted in low and unreliable detection of SOATs (not shown). For this reason, all strains were independently cultivated for a period of 24 h to get comparable expression results. Western blottinhg (WB) of SOATs expressed in CLR-strain (Figure 22) demonstrated differences in detection efficiency of yeast and mammalian SOATs. Also, expression levels were strongly influenced by strain background (Figure 23). Sc2 showed by far the best expression results.

All SOATs form monomer and multimer patterns. This pattern was observed in previous studies (for example: Kyung-Hyun Cho et al., 2003). It is speculation, if SOATs necessarily form dimer and tetramer *in vivo* or if this is an artifact resulting from sample preparation. Calculated molecular weight of mammalian SOATs differs from the observed band pattern. Monomer bands are located about 15 kDa below calculated apparent mass, which is consensual with literature results (Matsuda et al., 1998 and Kyung-Hyun Cho et al., 2003). In most cases, the monomer bands had the highest intensity; an exception was Sc1 in the 7DHC-strain. Detection of the FLAG-tag located at the N-terminal domain (NTD) gave much stronger bands for SOATs from yeast than for mammalian SOATs expressed in the CLR-strain (Figure 22-A). Anti-FLAG Western blot detection of mammalian SOATs was inconclusive, because individual clones did not show monomer bands and multimer bands were too faint to distinguish expression levels. An alternative antibody against the human SOAT1, which is identical to Pt1, also binds to Rn1 with lower efficiency (Figure 22-B). Interestingly, strong monomer bands were observed also for the same protein samples for which anti-FLAG detection failed. Comparing Figures 22 and 23), two unspecific bands were visible between 100 kDa and 130 kDa as a result of using an additional antibody against GAPDH (approximately 37 kDa). Loading control antibody against GAPDH resulted in extreme signal intensities under these conditions and is not appropriate to distinguish small differences in protein loading (Figure 23). As shown in Figure 21, band intensities were equally strong in almost all samples.

Comparing the influence of strain background, ERG-strain samples had the lowest expression of SOATs, whereas CLR-strain expressed best in most cases (Figure 23). CLR-strain expression of Tg1 was not shown in these figures, yet the signal was already stronger in the 7DHC-strain than in the ERG-strain. Also, band intensities of Sc1, Sc2 and Pt1 were equal or slightly improved in the 7DHC-strain

compared to CLR-strain. Sterol-engineering towards 7-DHC and CLR seems to have a positive impact on SOAT expression in yeast, no matter from which species it originally derived.

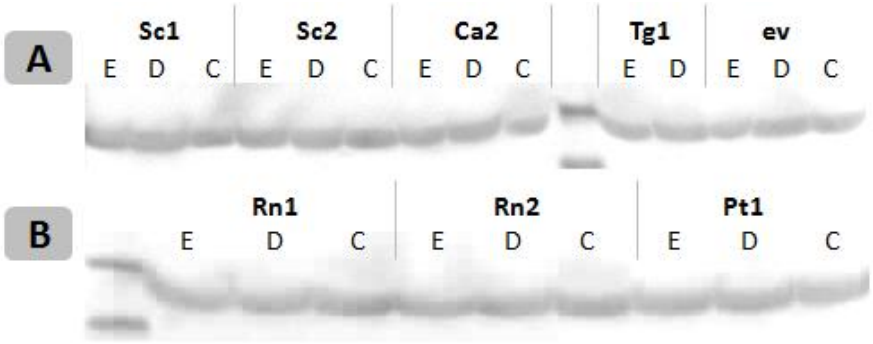

Figure 21: GAPDH loading controls. Brown staining of nitrocellulose membranes from Figure 23 as a result of strong signal intensity upon addition of high sensitivity substrate: SuperSignal West Femto Chemiluminescent Kit.

It is wise to evaluate these Western blot results with care, especially when comparing expression of various heterologous SOATs with each other. The N-terminally fused FLAG-tag of mammalian SOATs could be masked as a result of not completely unfolded proteins. Sample preparation of membrane proteins is tricky because hydrophobic regions tend to aggregate. Thus, bigger protein tags like a GST-tag would possibly improve detection of mammalian SOATs in WB studies. The C-teminal part (CTD) of SOATs is probably located inside the ER lumen. In yeast SOATs, the CTD ends shortly after the last predicted transmembrane domain and in mammalian SOATs is only a bit longer. Thus, a fusion to the short CTD instead of the long and highly variable NTD of SOATs could also improve detection. On the contrary, the NTD was chosen because fusion of tags at the long, N-terminal cytoplasmic tail would possibly have only little impact on protein folding. What about the impact concerning the three expression strains? A simple explanation for dinstict expression of SOATs is the observation that 7DHC- and CLR-strains have a much longer lag-phase compared to ERG-strains. Maybe a slower metabolism actually favours folding and integration of all TMDs of these complex proteins. Also, expression levels cannot directly be related to high or low sterol ester production, as later discussed for activity results. Sc2 was most expressed in the CLR-strain for example, although Ca2 produced similar or even more cholesteryl esters. Reversely, Rn1 was better expressed in the CLR-strain but its activity was lower than in the ERG-strain.

It is a necessity to prove protein expression, especially when low enzyme activity is observed. But we find many discrepancies between Western blot and HPLC results with the latter considered to be less prone to errors than the detection of complex membrane proteins. Also, it is difficult to rule out the folding problem from our list of possible influences on activity, because structural integrity would be hard to analyze. Nevertheless, we can assume that folding is much less of concern in our *in vivo* approach compared to any so far performed *in vitro* study.

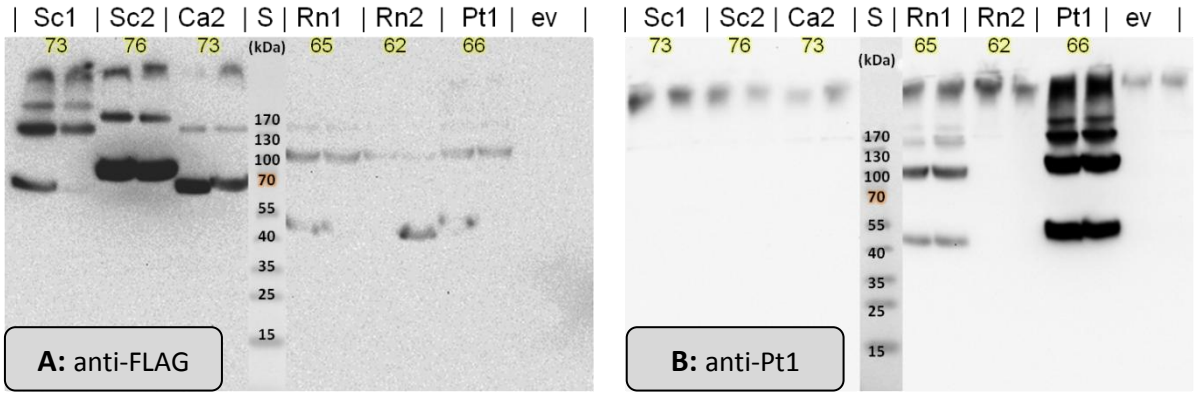

Figure 22: SOAT expression in the cholesterol strain after 24 h. Western blot using primary antibody against FLAG-tag (**A**) or antibody against human or chimpanzee SOAT1 (**B**). Exposure time 25 min. Numbers highlighted in yellow indicate predicted molecular weight. Two biological replicates for each enzyme (except for Tg1) or empty vector control (ev) protein samples derived from 2 OD units were applied. Substrate for detection: SuperSignal West Pico Chemiluminescent Kit.

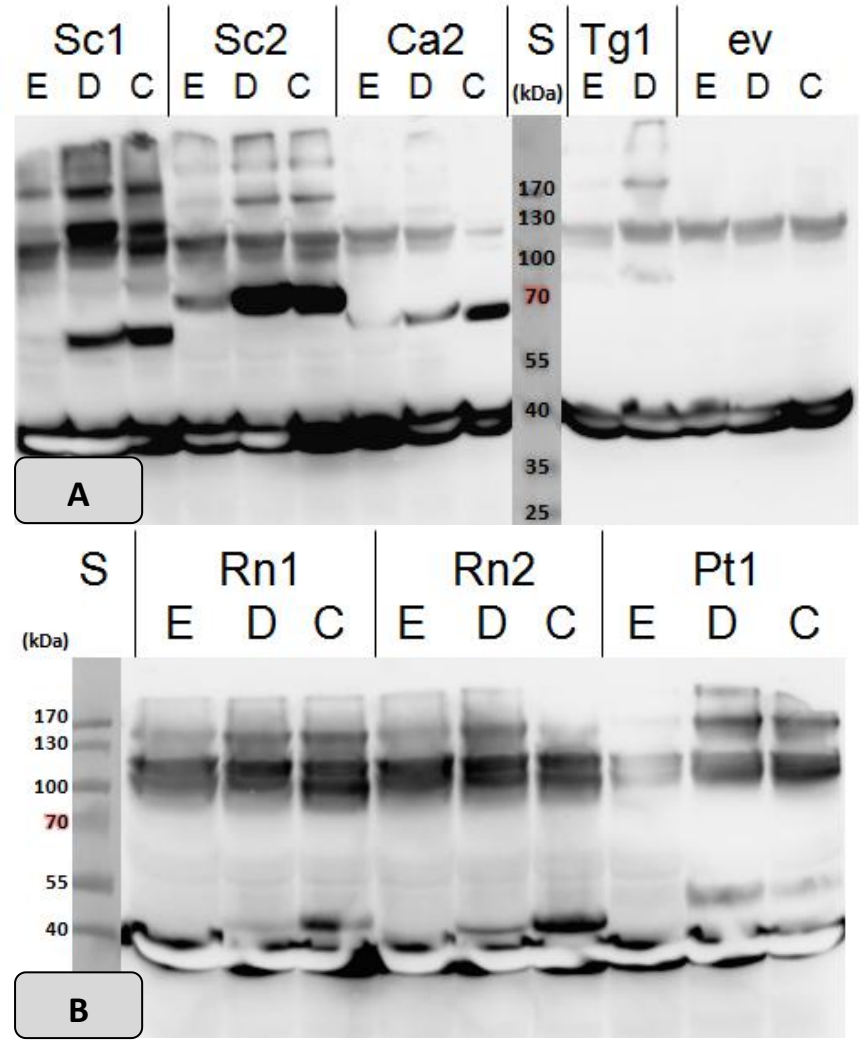

Figure 23: SOAT expression in all strains after 24 h. Western blot with primary antibody against FLAG-tag, primary antibody against GAPDH and secondary antibody-HRP conjugate against mouse IgG. Exposure time 1 min. Protein samples of 2 OD units applied for strains expressing yeast Sc1, Sc2, Ca2 and protozoan Tg1 and empty vector controls (**A**); samples of 4 OD units were applied for strains expressing mammalian Rn1, Rn2 or Pt1 (**B**). Expression strains: **E**, ERG-strain; **D**, 7DHC-strain; **C**, CLR-strain. Loading control antibody against GAPDH resulted in extreme signal intensities approximately 37 kDa. Substrate for detection: SuperSignal West Femto Chemiluminescent Kit.

3.2.3 Sterol composition of SOAT expression strains

One of our three expression strains ("BA-C" or CLR-strain) has already been described above. At this point, we continued with the characterization of our strains also with respect to possible changes accompanying SOAT expression. SOATs combine two types of substrates: Sterols and fatty acyl-CoAs. In our *in vivo* approach, we can test the impact of SOAT activities from various species in different substrate environments upon manipulating the sterol pathway. The question is, if these SOATs differ in their activity and substrate specificity so that this leads to a change in total cellular sterol composition. Here, we analyzed the total cellular amount of several sterol species detected by GC-MS (Table 14).

Table 14: Sterols detected in SOAT expression strains. Numbers and ranking is according to retention time in GC-MS between 21 and 30 min, converted into relative retention to cholesterol. *Detected in an unstable 7DHC-strain that produced high amounts of 7-DHC precursors. Question marks denote uncertainty of the exact identity of a sterol.

#	Compound name	Mass	Major MS peaks upon silylation	Strain	Rel. RT
1	Squalene	410	149_137_81_69	ERG, 7DHC	0.817
2	**Cholesterol [Cholesta-5-enol]**	**386**	**458_443_368_353_329_129**	**CLR**	**1.000**
3	? Cholesta-5,8-dienol	384	456_441_366_351_325	7DHC	1.005
4	? similar to cholesterol	386	458_443_368_353	CLR	1.010
5	Cholesta-8-enol	382	458_443_353_255_229	7DHC	1.012
6	?Ergosta-5,8,14,22-tetraenol	394	466_376_251_207	CLR	1.025
7	**7-Dehydrocholesterol [Cholesta-5,7-dienol]**	**384**	**456_441_366_351_325**	**7DHC**	**1.025**
8	Lathosterol [Cholesta-7-enol]	386	458_443_353_255	7DHC	1.035
9	Zymosterol [Cholesta-8,24-dienol]	384	456_441_351_229_213_107	ERG	1.037
10	7-dehydrodesmosterol [Cholesta-5,7,24(25)-trienol]	382	454_439_364_349_323	*7DHC	1.050
11	**Ergosterol [Ergosta-5,7,22-trienol]**	**396**	**468_378_363_337_253_211**	**ERG**	**1.053**
12	Cholesta-7,24(25)-dienol	384	456_441_343	*7DHC	1.058
13	Ergosta-7,22-dienol	398	470_455_343_255_229_213	ERG	1.061
14	Fecosterol [Ergosta-8,24(28)-dienol]	398	470_455_413_380_365_343	ERG	1.073
15	Ergosta-5,7-dienol	398	470_455_380_365_339	ERG	1.089
16	Episterol [Ergosta-7,24(28)-dienol]	398	470_455_386_343_255_213	ERG	1.095
17	Ergosta-7-enol	400	472_457_367_255_213	ERG	1.098
18	Lanosterol [Lanosta-8,24-dienol]	426	498_483_393	ERG	1.109
19	4,4-Dimethyl-cholesta-8,24(25)-dienol	412	484_469_394_379	ERG	1.126

The sterol biosynthetic pathway comprises a greater number of intermediates than those detected in our strains. For example, published ergosterol precursors ergosta-5,7,24(28)-trienol and ergosta-5,7,22,24(28)-tetraenol were not found in the ERG-strain. Probably, both precursors are quickly transformed into ergosterol and/or are not substrate for SOATs in our strain background. For that reason, the pathway model built up from GC-MS results shown in Figure 24 serves only as to illustration of possible reactions. As depicted, the first part of the pathway is identical for all three strains, beginning with the conversion from sterol precursor molecule squalene (SQL) to cholesta-8,24-dienol (ZYM). Then, ZYM can further be modified in a non-linear path through alternative intermediates. The sterol modified yeast strains produce ergosterol, 7-dehydrocholesterol or cholesterol as their major cellular sterol. Analysis of all SOAT expression strains (ERG-, 7DHC- and CLR-strain) revealed varying quantities of squalene and several intermediate sterol components (Figures 25 – 28, Tables 14 and 15).

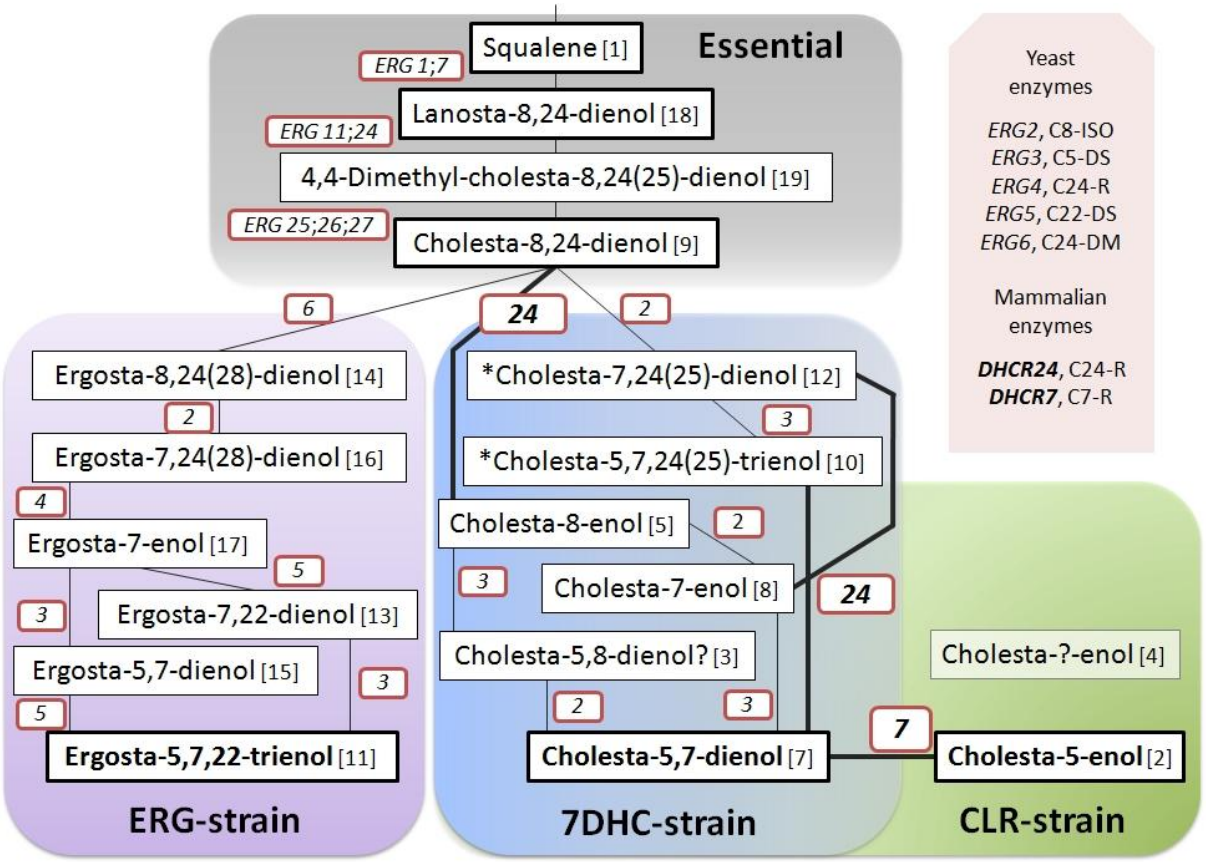

Figure 24: Sterol pathway model. Metabolites (black boxes) were arranged based on GC-MS data: Essential part of sterol biosynthetic pathway (grey background); specific part for ERG-strain (violet); 7DHC- and CLR-strains (blue and green). Metabolite numbers are according to GC-MS retention time, end products in bold; *only found in unstable clones of 7DHC-strain. Enzymes (red boxes) and potential reactions (black lines) represent possible pathways towards sterol end products, introduced reactions in bold. Enzymes: ISO, isomerase; DS, desaturase; R, reductase; DM, demethylase.

Genetic modification of the 7DHC-strain (deletion of *ERG5* and *ERG6* and integration of *DHCR24*) changed the sterol pathway and resulted in decreased amounts of intermediates compared to ERG-strain, although amounts of total sterols were consistent in both empty vector controls (≈ 2

µg/OD_{600}). Integration of *DHCR7* not only further decreased intermediates in favor of the end product cholesterol (CLR-strain), but also doubled the total sterol amount in the control strain (4 µg/OD_{600}). By contrast, the increase in total sterols was not observed with HPLC measurements (Figure 31). For that reason, we put the main focus on analyzing the sterol distribution within each strain using percentage values calculated from GC-MS data (Table 15).

Before getting into details, it is important to mention major issues with some clones of the 7DHC-strain with anomalous sterol compositions. All of them produced high amounts of a 7-DHC precursor identified as cholesta-5,7,24-trienol. This type of sterol is typically produced in *erg5/6* deletion strains (Souza et al. 2011; Petschacher et al., in prep). So, we can assume that malfunction of *DHCR24* is likely the cause for the anomaly and is not connected to expression of specific SOATs. The problem seems to be based on the production of 7-DHC. Because it is less similar to ergosterol than cholesta-5,7,24-trienol, perhaps 7-DHC is not recognized by regulatory mechanisms or disturbs accustomed interactions between lipids or lipids and proteins. This is also reflected by an extended lag-phase of sterol modified strains. Anyway, 7-DHC production might cause more trouble for the cell, so that some clones with lower C24 reductase activity become prevalent due to selection pressure. This phenomenon has not been observed for the CLR-strain. Of course it is a matter of chance that two enzymes become damaged at the same time. But also the production of cholesterol does not seem to have additional negative effects compared to 7-DHC production.

GC-MS data proves that SOAT expression leads to an increase of cellular sterols. As discussed in the introduction section, sterols have individual structural characteristics such as length and flexibility of the side chain or conformation and polarity of the four ring structures. All these differences can play a role for the interaction between SOATs and substrates. Then, what exactly makes some sterols a better substrate for SOATs than others? The search for important characteristics is complicated by the fact that each SOAT seems to have unique substrate preferences. Also, each strain provides different conditions to which SOATs behave unexpectedly. So we should be rather asking: Which enzyme acts better on certain substrate characteristics? We can answer this question for the sterols investigated in this study. But we are dealing with a competing system of multiple potential substrates that provides some interesting insights on SOAT substrate specificity.

3.2.4 Varying activities of microbial and mammalian SOATs *in vivo*

Overexpression of N-terminal FLAG-tagged SOATs in three modified strains (listed in Table 4) was under control of P_{TDH3} using a multicopy, 2µ-based plasmid. Thus, SOATs should be generated abundantly as discussed above. Mammalian SOATs were expressed from codon-optimized sequences, although their native sequences were also tested as shown in Figure 28. This data showed that the amounts of total sterols differed in some strains, but similarities in sterol

composition prevailed and it was not clear whether expression of native or optimized sequences generally improved the activity of mammalian SOATs.

Upon SOAT expression, an increase of intermediate sterols can be observed in all stable strains (Table 15, Figure 27). Intermediates were present to a great extent in the ERG-strain (28% ev; 36% Sc1). However, contribution of intermediates to total sterols decreased in the 7DHC-strain (6% ev; 13% Sc1) and reached a minimum in the CLR-strain (1% ev; 4.6% Tg1). Squalene is the obligatory precursor for all sterols and therefore, its abundance might be an indicator for pathway flux regulation. SOATs act on the hydroxy moiety of sterols to form esters with fatty acyl-CoA. Because squalene consists only of hydrocarbons, it is not a substrate of SOATs until squalene is oxidized and converted into lanosterol (LAN). Based on elevated lanosterol levels in ERG-strain expressing Sc1, LAN is presumably taken as a preferred substrate by this enzyme. LAN levels are generally low in the 7DHC-strain and can only be detected upon Sc1, Ca2 and Tg1 expression. Besides, Sc1 promoted increased amounts of cholesta-5-enol, ergosta-5,7-dienol, ERG (ergosta-5,7,22-trienol), ergosta-7,24-dienol, ZYM (cholesta-8,24-dienol) and it gives outstanding results for 7-DHC (cholesta-5,7-dienol). Other yeast enzymes Sc2 and Ca2 have similar sterol substrate preferences. Sc2 worked best on ERG, whereas Ca2 was the most active on CLR. Mammalian SOATs did not seem to have preferences for any of the intermediates although Tg1 expression led to high levels of ergosta-7,24-dienol. Rn1 worked best on ERG, whereas Rn2 showed no increase in ERG but gave high amounts of CLR. Parasite SOAT Tg1 was rather substrate tolerant.

Beside the end products ERG, 7-DHC and CLR, our data indicate that yeast SOATs act preferably on sterols with desaturated C8 position, whereas mammalian SOATs do not. As discussed previously, double bonds at this positions give the ring structure a more planar form. Ergosta-8,24(28)-dienol, cholesta-8-enol and zymosterol (cholesta-8,24-dienol) levels were strongly elevated upon expression of yeast SOATs. However, early sterol compound 4,4-dimethyl-cholesta-8,24(25)-dienol levels stayed relatively constant in all ERG-strains and this compound could not be detected in any other strains. Likely, this dimethylated sterol was not a good substrate of SOATs and its abundance depended only on the variable pathway flux. It is odd that Sc1 probably accepts LAN as a substrate which is highly similar with one additional methyl group at C14.

A

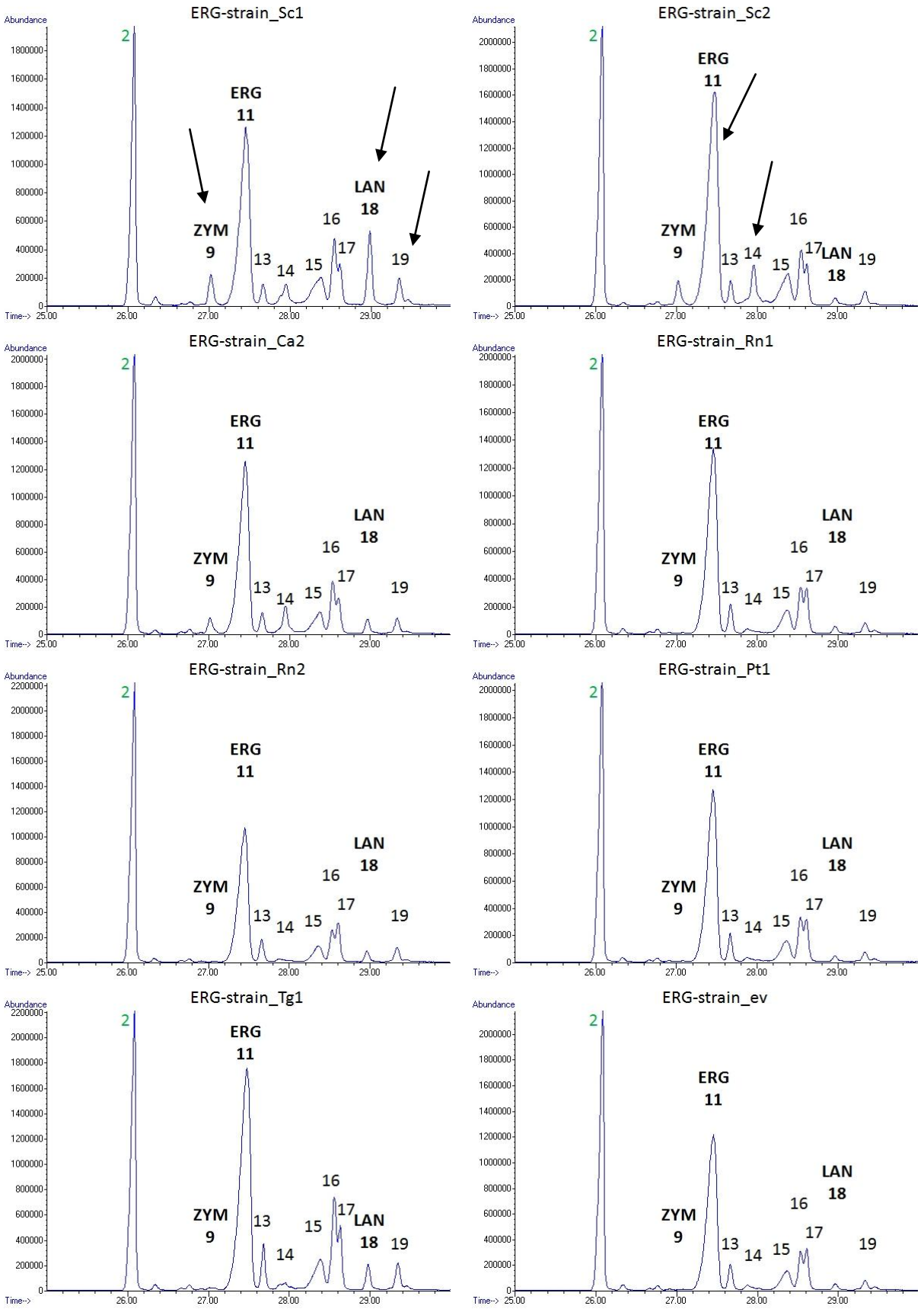

Legend: **1** Squalene (not shown) **2** Cholesterol; **3** ?; **4** ?; **5** Cholesta-8-enol; **6** ?; **7** 7DHC [Cholesta-5,7-dienol]; **8** Cholesta-7-enol; **9** Zymosterol [Cholesta-8,24-dienol]; **10** Cholesta-5,7,24(25)-trienol; **11** Ergosterol [Ergosta-5,7,22-trienol]; **12** Cholesta-7,24(25)-dienol; **13** Ergosta-7,22-dienol; **14** Ergosta-8,24(28)-dienol; **15** Ergosta-5,7-dienol; **16** Ergosta-7,24(28)-dienol; **17** Ergosta-7-enol; **18** Lanosterol [Lanosta-8,24-dienol]; **19** 4,4-Dimethyl cholesta-8,24(25)-dienol

B

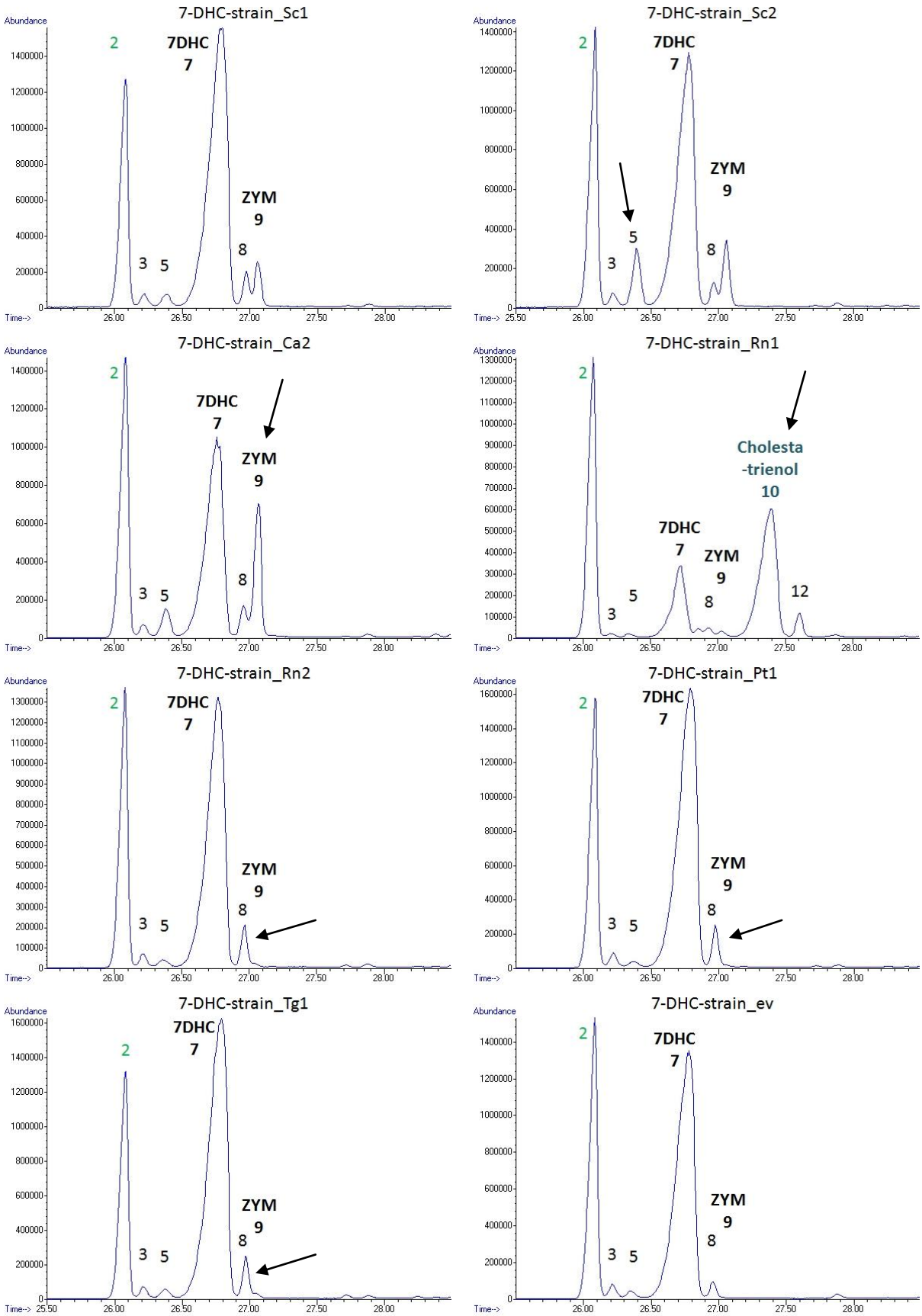

Legend: **1** Squalene (not shown) **2** Cholesterol; **3** ?; **4** ?; **5** Cholesta-8-enol; **6** ?; **7** 7DHC [Cholesta-5,7-dienol]; **8** Cholesta-7-enol; **9** Zymosterol [Cholesta-8,24-dienol]; **10** Cholesta-5,7,24(25)-trienol; **11** Ergosterol [Ergosta-5,7,22-trienol]; **12** Cholesta-7,24(25)-dienol; **13** Ergosta-7,22-dienol; **14** Ergosta-8,24(28)-dienol; **15** Ergosta-5,7-dienol; **16** Ergosta-7,24(28)-dienol; **17** Ergosta-7-enol; **18** Lanosterol [Lanosta-8,24-dienol]; **19** 4,4-Dimethyl cholesta-8,24(25)-dienol

C

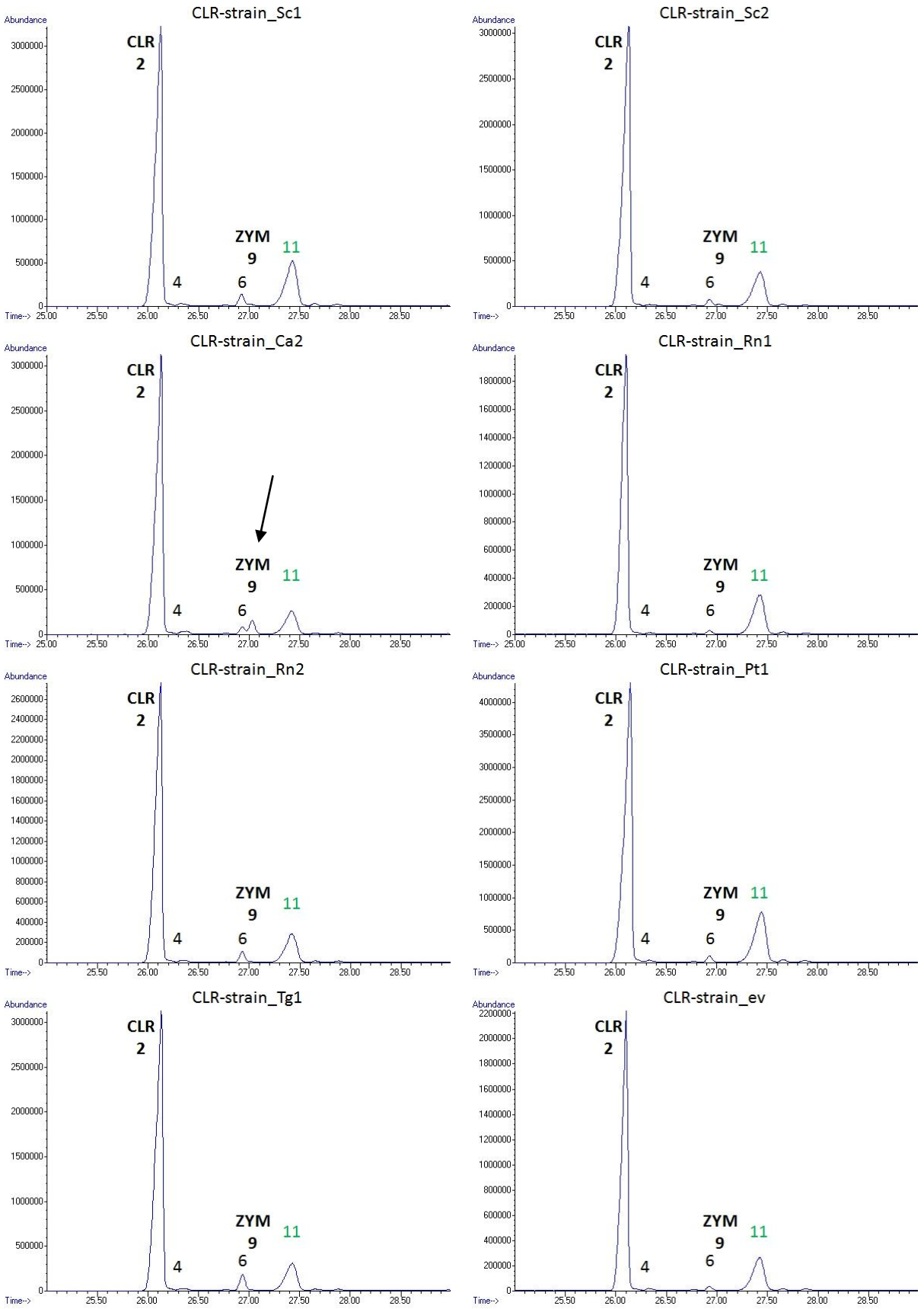

Figure 25: Sterols detected in SOAT expression strains. Standard in green. Legend:**1** Squalene (not shown) **2** Cholesterol; **3** ?; **4** ?; **5** Cholesta-8-enol; **6** ?; **7** 7DHC [Cholesta-5,7-dienol]; **8** Cholesta-7-enol; **9** Zymosterol [Cholesta-8,24-dienol]; **10** Cholesta-5,7,24(25)-trienol; **11** Ergosterol [Ergosta-5,7,22-trienol]; **12** Cholesta-7,24(25)-dienol; **13** Ergosta-7,22-dienol; **14** Ergosta-8,24(28)-dienol; **15** Ergosta-5,7-dienol; **16** Ergosta-7,24(28)-dienol; **17** Ergosta-7-enol; **18** Lanosterol [Lanosta-8,24-dienol]; **19** 4,4-Dimethyl cholesta-8,24(25)-dienol

Table 15 Cellular sterol composition of SOAT expression strains. Quantitation of the total cellular sterols identified by GC-MS detection upon silylation of lipid extracts. Summarized sterol amounts (TOTAL) include precursor molecule squalene (SQL). Values are calculated in µg/OD_{600} relative to cholesterol (ERG- and 7DHC-strains) or ergosterol (CLR-strain) as an internal standard. Percentage values of sterols are relative to TOTAL sterols. Mean values of duplicate measurement (*single). °Instable 7DHC-strain expressing Rn1, likely caused by defective C24 sterol reductase (DHCR24).

	Sc1	Sc2	Ca2	Rn1	Rn2	Pt1	Tg1	ev
ERG-strain								
TOTAL (µg/OD_{600})	2.6 ± 0.2	2.9 ± 0.1	2.2 ± 0.1	2.3 ± 0.1	1.7 ± 0.0	2.1 ± 0.1	3.2 ± 0.2	2.0 ± 0.1
ERG (%)	50.5 ± 2.6	58.0 ± 2.7	57.8 ± 0.3	61.1 ± 0.9	60.9 ± 1.3	60.9 ± 0.6	54.0 ± 0.7	59.5 ± 1.4
ZYM (%)	4.3 ± 0.1	3.4 ± 0.0	3.0 ± 0.1					
LAN (%)	7.6 ± 3.0	1.3 ± 1.8	2.4 ± 0.1	1.0 ± 1.4	1.1 ± 1.6	0.7 ± 1.0	3.8 ± 1.4	4.6 ± 3.1
SQL (%)	5.6 ± 0.0	6.0 ± 0.2	6.2 ± 0.1	11.3 ± 0.2	9.1 ± 0.3	11.3 ± 0.3	11.8 ± 0.2	12.5 ± 0.4
Other (%)	32.0 ± 0.3	31.3 ± 1.2	30.5 ± 0.2	26.6 ± 0.3	28.9 ± 0.6	27.0 ± 0.0	30.5 ± 0.9	23.4 ± 4.9
7DHC-strain								
TOTAL (µg/OD_{600})	3.2 ± 0.0	2.7 ± 0.1	2.2 ± 0.1	°1.7 ± 0.3	2.3 ± 0.1	2.4 ± 0.3	2.9 ± 0.2	2.0 ± 0.2
7DHC (%)	85.5 ± 1.2	75.9 ± 0.8	74.1 ± 9.3	°26.9 ± 3.1	90.0 ± 0.4	90.1 ± 0.3	90.5 ± 0.1	91.5 ± 0.6
ZYM (%)	5.1 ± 0.1	8.2 ± 0.1	14.1 ± 6.3	°1.3 ± 0.2				
LAN (%)	0.4 ± 0.6		0.6 ± 0.9				0.4 ± 0.0	
SQL (%)	1.2 ± 0.3	2.7 ± 0.5	1.3 ± 0.4	°1.1 ± 0.4	1.2 ± 0.2	0.9 ± 1.2	0.7 ± 0.0	2.4 ± 0.7
Other (%)	7.8 ± 0.2	13.2 ± 0.2	9.9 ± 1.7	°70.7 ± 3.7	8.7 ± 0.2	9.0 ± 1.6	8.4 ± 0.1	6.1 ± 0.1
CLR-strain								
TOTAL (µg/OD_{600})	4.7 ± 1.1	5.3 ± 0.3	6.4 ± 1.7	3.8 ± 0.2	6.0 ± 0.1	3.6*	6.3 ± 0.7	4.2 ± 0.5
CLR (%)	96.4 ± 0.0	98.5 ± 0.0	94.2 ± 0.4	99.4 ± 0.8	96.9 ± 0.3	98.3*	95.4 ± 0.1	99.4 ± 0.9
ZYM (%)			3.7 ± 0.5					
LAN (%)								
SQL (%)								
Other (%)	3.6 ± 0.0	1.5 ± 0.0	2.1 ± 0.1	0.6 ± 0.8	3.1 ± 0.3	1.7*	4.6 ± 0.1	0.6 ± 0.9

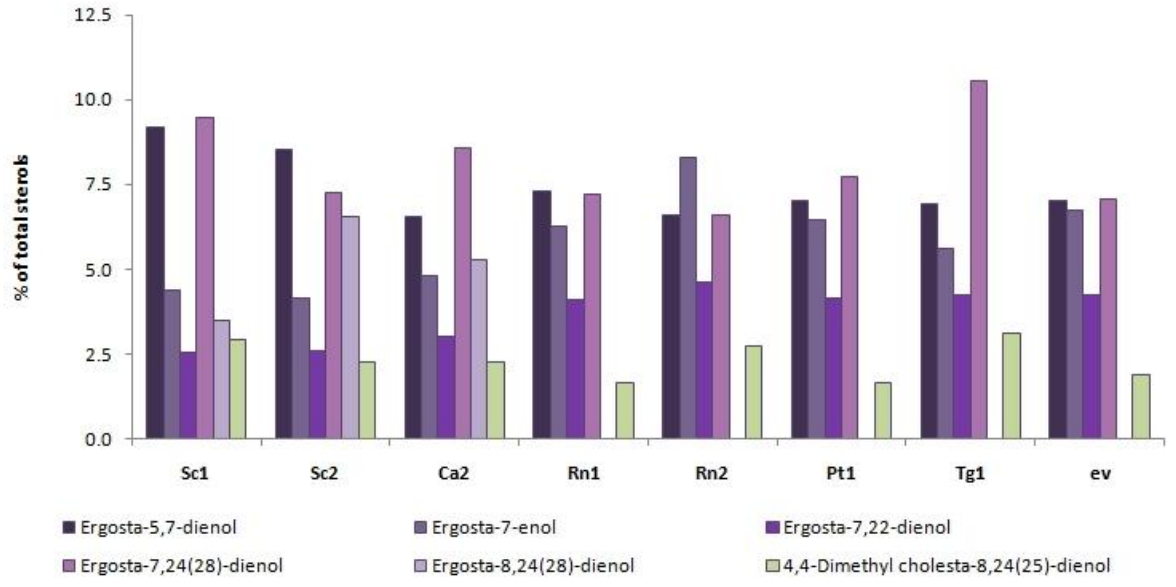

Figure 26: Distribution of other sterols in the ERG-strain. Detailed GC-MS data of some ergosterol pathway intermediates.

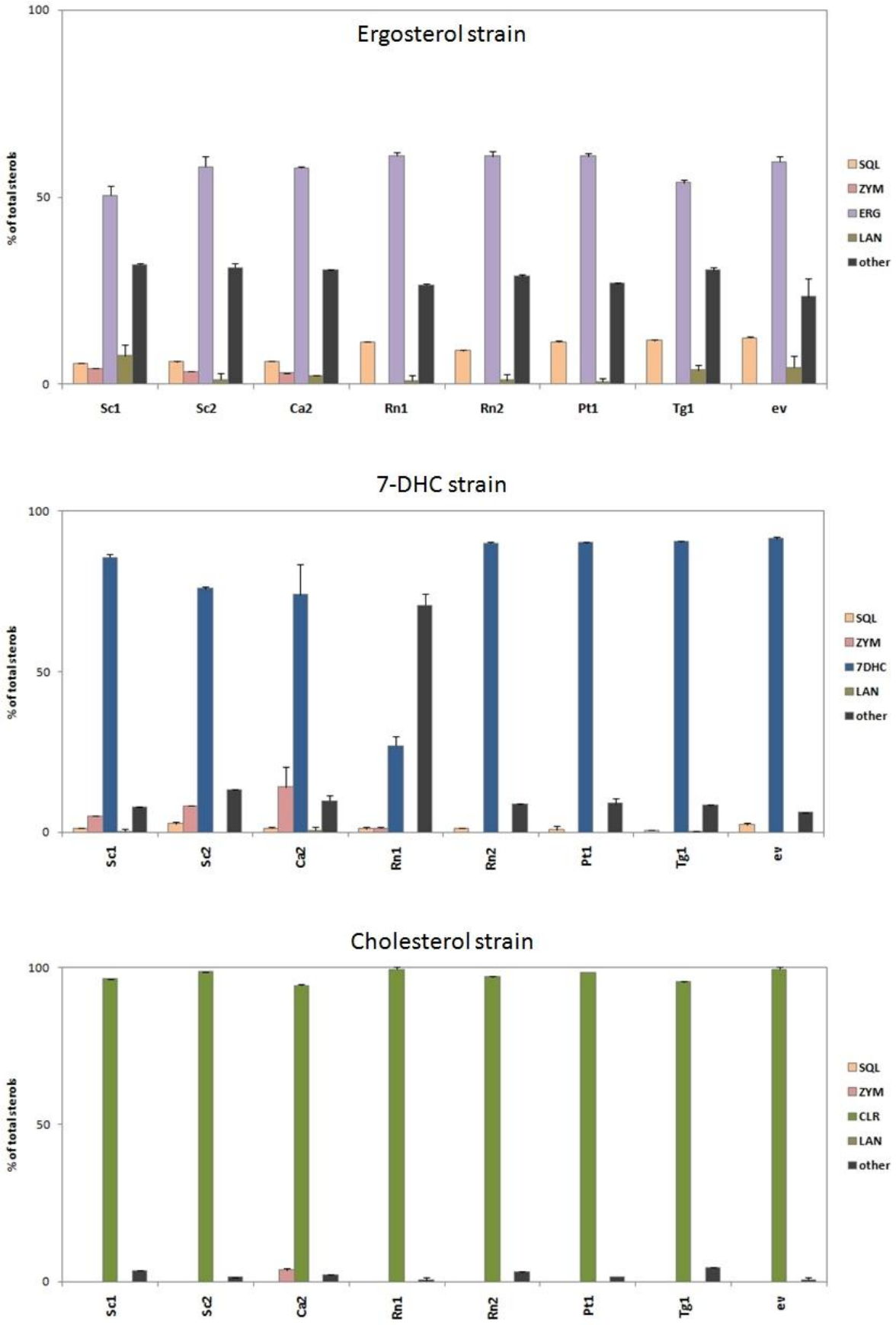

Figure 27: Cellular sterol composition of SOAT expression strains. Cellular sterols identified by GC-MS detection. Percentage values of sterols are relative to TOTAL sterols including precursor molecule squalene (SQL). Mean values and range of duplicate measurements (single measurement only for Pt1 Cholesterol-strain).

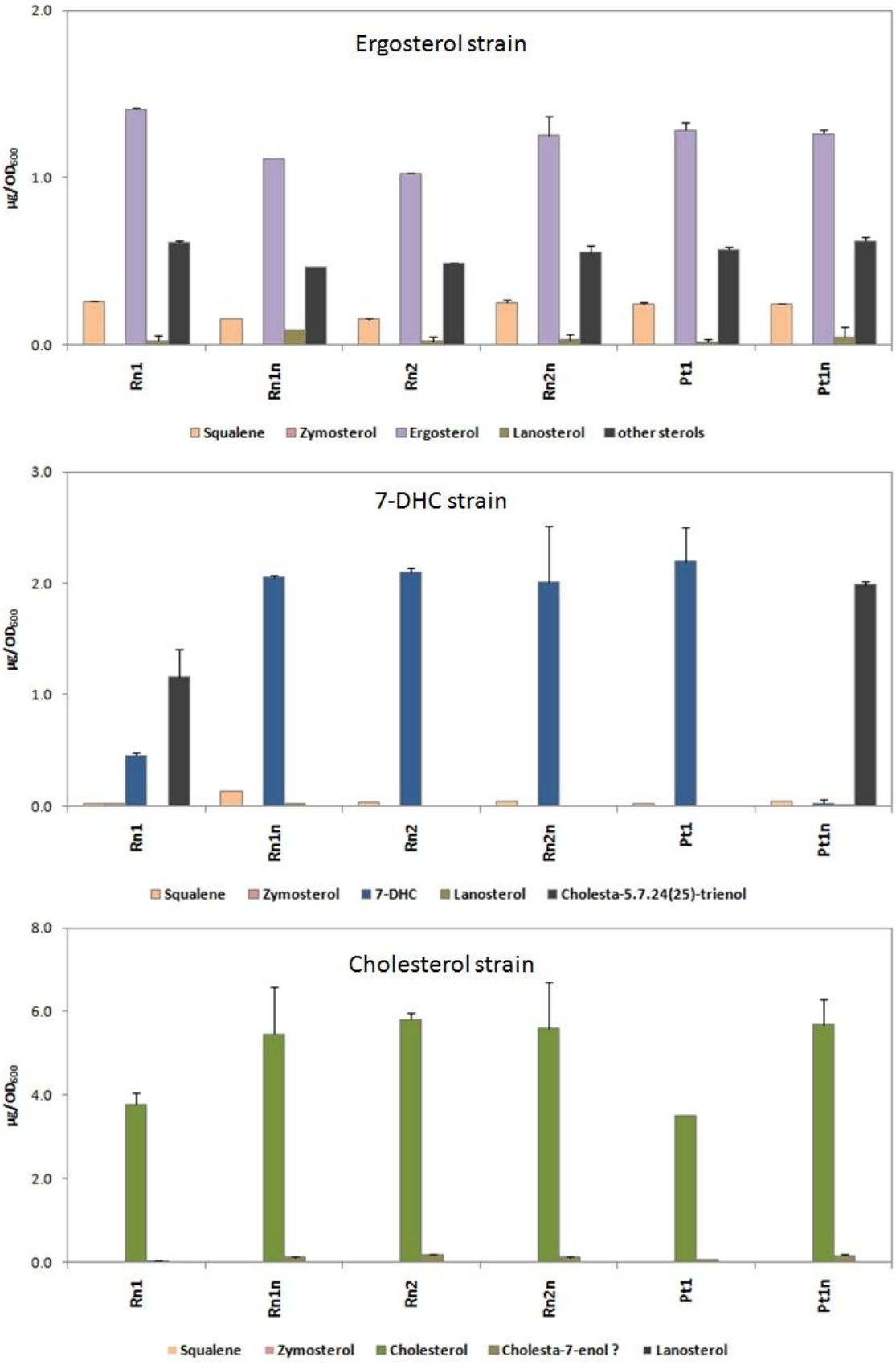

Figure 28: Influence of SOAT codon sequence on sterol formation. Comparing codon-optimized with native (n) sequences regarding sterol formation upon expressing mammalian SOATs. Two clones (Rn1 and Pt1n) were instable in their 7-DHC production.

In addition to GC-MS data, detection of major sterols and steryl esters was also performed with HPLC-MS, integrating the measured peaks and normalizing the data to cholesteryl-acetate (Ch-Ac) as an internal standard. Normalized data was then recalculated for each sterol type to specific standard curves (Figure 29). With the HPLC method, it is possible to distinguish between non-acylated sterols or free sterols within a retention time range of five to eight minutes and steryl esters (SE) within 20 to 50 minutes. Two main types of SE were detected in the 7DHC- and CLR-strains. SOATs probably use either 16:1 or 18:1 acyl-CoA as a co-substrate as reported by Zweytick et al. (2000). Additionally, 16:0 and 18:0 acyl-CoA appear to be used to greater extent in the ERG-strain, likely due to different fatty acid composition in each strain background.

Over-expression of SOATs increased the amount of steryl esters, although levels of free sterols were relatively constant compared to empty vector controls (ev) (Figure 30). All SOATs expressed in our modified host strains were active, even though SOAT Rn2 produced only traces of SE in the ERG-strain. The fact that the amounts of free sterols stayed constant independent of steryl ester production indicated that indeed sterol homeostasis is precious and sophisticated in yeast. If SOAT activity is high, a surplus of sterols must be synthesized *de novo*. In terms of activity, there were strong distinctions between yeast and mammalian derived SOATs. Strains expressing yeast SOATs Sc1, Sc2 and Ca2 produced much higher amounts of total SE and also more zymosterol (ZYM) esters compared to mammalian SOATs. Only Rn2 showed activity similar to Sc1 in the CLR-strain. Interestingly, ZYM can only be detected in the form of zymosteryl esters and its quantity is strongly influenced by strain background.

Zymosterol is of major interest for various reasons. ZYM appears to be the final essential sterol produced in the biosynthetic pathway (as reviewed by Lees et al 1999; Parks et al 1999). From biotechnological point of view, production and accumulation of specific sterol compounds is impaired when ZYM-esters are generated by SOATs as side products. To reach higher purity of desired products, accumulation of ZYM could be avoided either by improving pathway design or enzyme engineering of SOATs. Our results indicate that expression of yeast SOATs produces much more ZYM esters compared to expression of mammalian SOATs. The question is whether yeast SOATs have higher specificity for ZYM as a substrate or if we observe side effects of an overall higher activity. With a focus on strain background, the maximal amount of ZYM was clearly produced in the 7DHC-strain; ZYM was relatively high in the ERG-strain and was barely present in the CLR-strain except if expressing Ca2. In other words, ZYM ester formation was not only caused by activity of specific SOATs alone but rather was determined by the major sterol present in the cell.

There are a few possible explanations for the shift in ZYM acylation observed in different SOAT expression strains. We cannot assume identical conditions for all expression strains. With respect to

strain modifications, ZYM could be simply less accessible in the strain producing cholesterol compared to the strain producing ergosterol or 7-DHC. Disruption of the *erg5* and *erg6* genes and replacing them with heterologous enzymes *DHCR24* and *DHCR7* for sterol pathway modification might have caused an increase in metabolic flux from ZYM towards CLR. If this was true, then why was acylation of ZYM even stronger in the 7DHC-strain? The heterologously expressed C24 reductase might not be as active as the C7 reductase. Then, metabolic flux towards 7-DHC was lower compared to cholesterol and thus ZYM was more accessible.

Thinking further, we need to take a look at more details. First of all, the ERG-strain provides the native sterol biosynthetic pathway, including many intermediates until ergosterol is formed. Results from GC-MS measurements tell that about 23% of total sterols were intermediates without ZYM accumulation. Upon SOAT expression (Sc2), the amount of intermediates increased up to 2.5-fold of which only 10% consisted of ZYM, indicating that also other intermediates were used as substrates by SOATs. In particular, ergosta-8,24(28)-dienol (fecosterol or FEC) was presumably only a substrate for yeast SOATs but not for mammalian SOATs (Figure 26). We cannot distinguish free sterols from steryl esters by GC-MS, so that we do not know whether FEC-esters are formed. In contrast, accumulation of FEC could be as well an afflux effect caused by saturation of steryl esters in lipid particles. Assuming that accumulation of sterols may be a result of their conversion into esters, then SOATs Sc1, Sc2 and Ca2 seem to have a preference for desaturated C8 and C24 positions no matter if it was an ergosta- (FEC) or cholesta- (ZYM) species. Yeast SOAT expression led to similar ZYM-ester levels (7DHC-strain) and FEC levels (ERG-strain). The pathway of the 7DHC-strain is probably shortened. Hence, fewer intermediates accumulated in the cell (6%). Because of *erg6* deletion, FEC was no longer produced by the 7DHC-strain and ZYM had an increased chance to be taken on as a substrate. As a result, SOAT expression (Sc2) increased the amount of intermediates up to 4.7-fold including 40% ZYM.

Another explanation is the influence of some lipids acting as enzyme activators. It has been reported for many membrane protein that their function is influenced by structural interaction with sterols (Opekarova and Tanner 2003; Levitan et al. 2014). SOATs possibly sense small changes in membrane constitution due to their direct contact through multiple transmembrane domains. Sterols may somehow interact structurally with SOATs and allosterically introduce a change in characteristics of the substrate cavity. Following this idea, it would imply for 7-DHC to be a much better activator for ZYM acylation than cholesterol. Other studies by Chang and co-workers investigated in that direction and came to the following conclusions about human SOATs (reviewed in Rogers et al. 2014). When assayed in reconstituted liposomes or in mixed micelles, the enzymes respond to cholesterol and derivates in a sigmoidal manner. In contrast, when 7-ketocholesterol was the substrate, the addition

of cholesterol changed the shape of the substrate saturation curve from sigmoidal to hyperbolic. All in all, cholesterol was the best substrate and the best activator compared to oxysterols (Zhang et al. 2003). Furthermore, SOAT1 from *T. gondii* (Tg1) was highly active on 25-hydroxycholesterol (Nishikawa et al. 2005). Pregnenolone (3β-hydroxypregn-5-en-20-one) or PREG is a precursor for all steroid hormones and looks structurally similar to cholesterol, but with a truncated tail. Interestingly, PREG was efficiently esterified only in the presence of other sterols. This suggests that SOATs have distinct sterol binding sites; one catalytic binding site that accepts also substrates without the *iso*-octyl side chain and another activating binding site that is dependent on the presence of the side chain (Rogers et al. 2012). As shown in our SOAT1 topology model from rat (Figure 34), we found various possible cholesterol binding sites all over the enzyme when scanning through the peptide with so called CRAC or CARC patterns. Some of these sites are more conserved among SOATs than others, but many are distinct for each individual SOAT (not shown). It seems even possible that several different sterols interact with SOATs at the same time while only one specific site binds to the actual substrate. We have not specifically tested for activators in our study. Nevertheless, in the case of zymosterol acylation shifts in different strains, we may speculate on the possibility of allosteric activation by 7-DHC for some SOATs.

We found plenty of explanations for the big variances in ZYM acylation. But that was easy compared to explaining all the other interesting phenomena we observed. Strains expressing yeast SOAT Sc2 contained up to 80% sterol esters of total major sterols (ERG, CLR or 7-DHC) not showing any substrate preference (Figure 31-A). But Sc2 was by far the most active SOAT for ergosterol. Sc1 on the other hand produced similar cellular ERG and CLR ester levels of around 60% of total sterols, whereas 7-DHC was preferred. Interestingly, Ca2 was less active on 7-DHC but worked even better on CLR. Ca2 produced around 60-70% SE of ERG and 7-DHC and around 80% of CLR. In the 7DHC-strain, Sc1 with a total 7-DHC amount of 4.4 µg per OD_{600} seemed to have the highest capacity to form 7-DHC esters (3.2 µg, ~60%) and the lowest level of cellular zymosterol accumulation (23%) within the group of yeast SOATs (Figure 30, Figure 31). After all, mammalian Pt1 produced 2.3 µg of total sterols containing around 50% cellular SE further divided into 93% 7-DHC and 7% zymosteryl esters (3% total cellular ZYM).

Comparing Sc1 and Sc2 expressed in the ERG-strain, Sc2 was more active and selective producing 3.5 µg per OD_{600} ERG and a SE purity of 86% ERG, compared to Sc1 (2.1 µg and 75%). Sc1 had the highest capacity for cellular zymosterol accumulation (21%) compared to Sc2 (17%), although the total ZYM amounts were about the same. Thus, for the ERG-strain and in terms of zymosterol and ergosterol acylation, our observation matched previous studies (Zweytick et al., 2000) claiming that Are1p (Sc1) has a preference for ERG precursors and Are2p (Sc2) is more active on ERG. Yeast SOATs were

surprisingly active on 7-DHC although it is not a natural substrate. These enzymes also preferred desaturated positions C5 and C7 in the ERG-strain and thus might explain their extra potential to convert 7-DHC (cholesta-5,7-dienol) into esters. It is remarkable that Ca2 worked even better with CLR than with ERG or 7-DHC.

To comment on the matter of human SOAT1 which is identical to *P. troglodytes* SOAT1 (Pt1), early heterologous expression studies from Yang et al. (1997) demonstrated that SOAT1 was well expressed in yeast and active on cholesterol but not able to use 7-DHC or ERG as substrates. Yeast endogenous SOATs (Sc1 and Sc2) however were active on all three substrates, whereas rat liver microsomes were active on CLR and 7-DHC but not on ERG. With respect to our findings, we can agree with the results for Sc1 and Sc2 only. Based on reports from Oelkers et al. (1998), SOAT2 is only expressed in liver and small intestines, although human SOAT1 accounts for most of the activity in human adult liver but SOAT1 from other mammals not (Buhman et al. 2000). Also Chang et al. (2010) reported that SOAT1 is ubiquitously expressed in essentially all tissues, while SOAT2 is mainly expressed in the hepatocytes and intestines providing SE for lipoprotein assemblies. If it holds true for rat, that Rn2 but not Rn1 is expressed in liver, we see an interesting link to the huge differences we found for substrate specificity of Rn1 and Rn2, the latter not accepting ERG. Our results for Pt1 activity albeit proved its ability to use also ERG, and even more so 7-DHC as substrates. So in this case, there must be something with our system that improved Pt1 or human SOAT1 activity, which could be the presence of other sterol intermediates.

Mammalian SOATs and Tg1 typically use CLR or 7-DHC as natural substrates. It is intriguing that heterologous expression of Rn1 and Tg1 led to similar or higher ERG ester formation without a clear preference for its native substrates. In contrast, Rn2 expression in CLR- and 7DHC-strains resulted in notably higher formation of SE compared to expression in the ERG-strain. Characteristics of Rn1 and Rn2 are similar to Sc1 and Sc2, although more pronounced, having one highly active and selective isoenzyme (Sc2 or Rn2) and one, that is less active with a broad substrate tolerance (Sc1 or Rn1). Based on sequence similarity (Figure 19), Rn1 is more similar to Pt1 than to Rn2. As mentioned above, SOAT1 and SOAT2 are differentially expressed in mammalian tissues. Our results on expression levels cannot directly be related to high or low sterol esters production. Sc2 was most expressed in the CLR-strain for example, although Ca2 produced similar or even more cholesteryl esters and at the same time much more zymosteryl esters compared to Sc2. One might conclude that either Ca2 is less substrate specific than Sc2, or CLR formation simply reached saturation levels upon Ca2 expression and zymosterol was used instead as an alternative substrate because of unknown feedback regulation mechanisms. The same holds true for the ERG-strain having low SOAT expression, but strong activities.

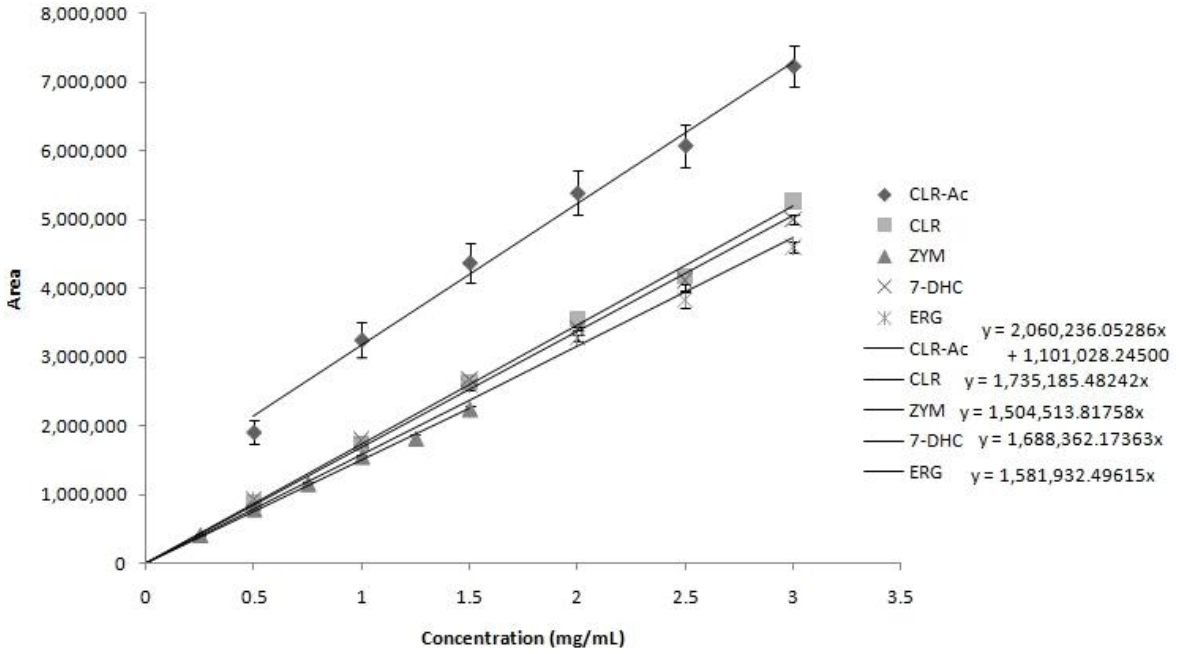

Figure 29: Standards for HPLC analysis. Sterols standards were dissolved in ethyl acetate. All six dilutions of standard solutions were measured in quadruplicates during one extensive sample analysis run. Trend line point of intersection was set (0,0) except for CLR-Ac (cholesteryl acetate).

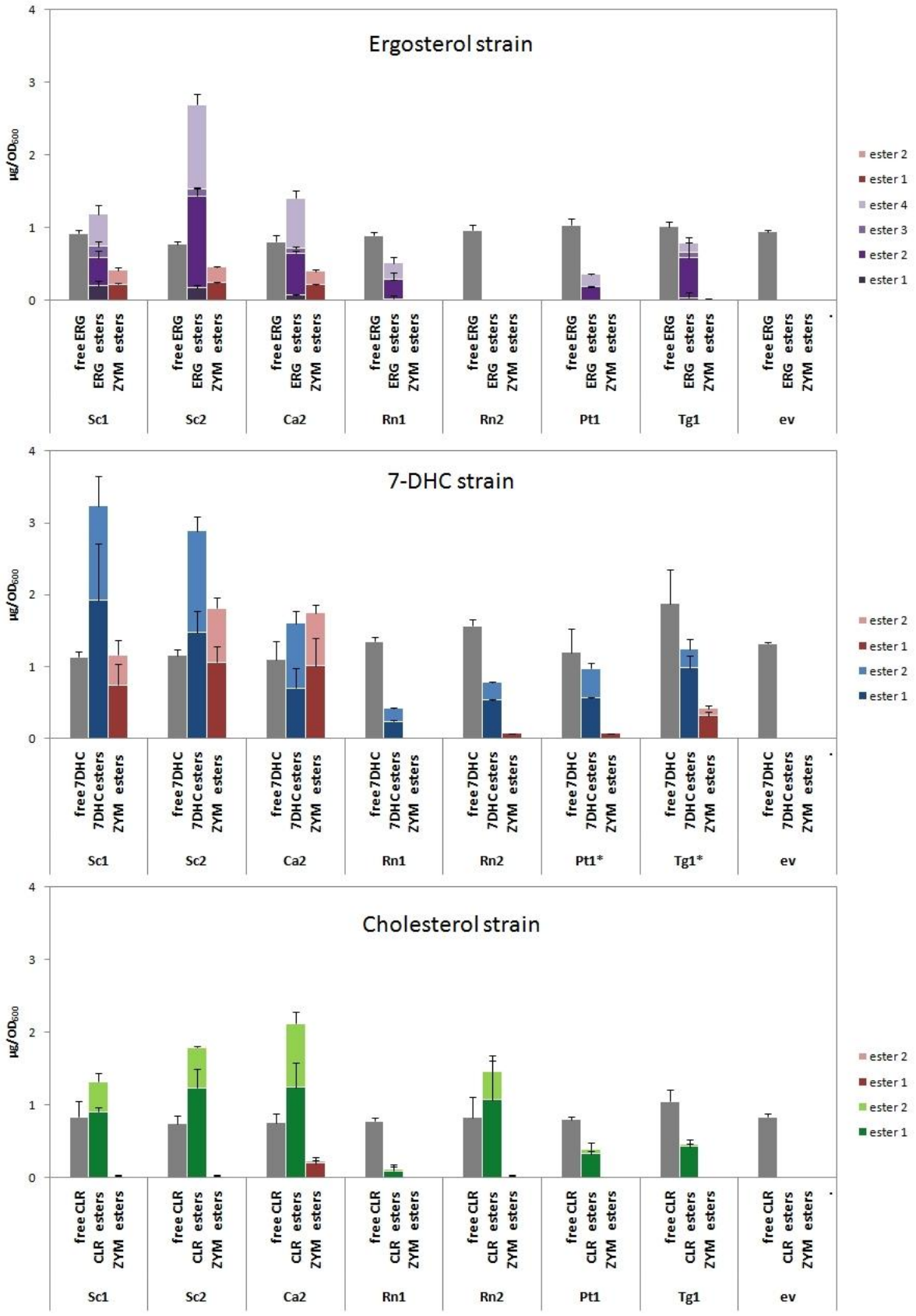

Figure 30: Free sterol and sterol esters composition in SOAT expression strains. HPLC-MS analyses of ergosterol (ERG), 7-Dehydrocholesterol (7DHC), cholesterol (CLR) and zymosterol (ZYM). Samples of 200 OD_{600} units were taken after 65 h of SOAT expression. Mean values and standard deviations for ERG- and CLR-strains calculated from biological triplicates; for 7DHC-strain from biological duplicates cultivated in parallel (except for Pt1*, Tg1*: independent cultivation).

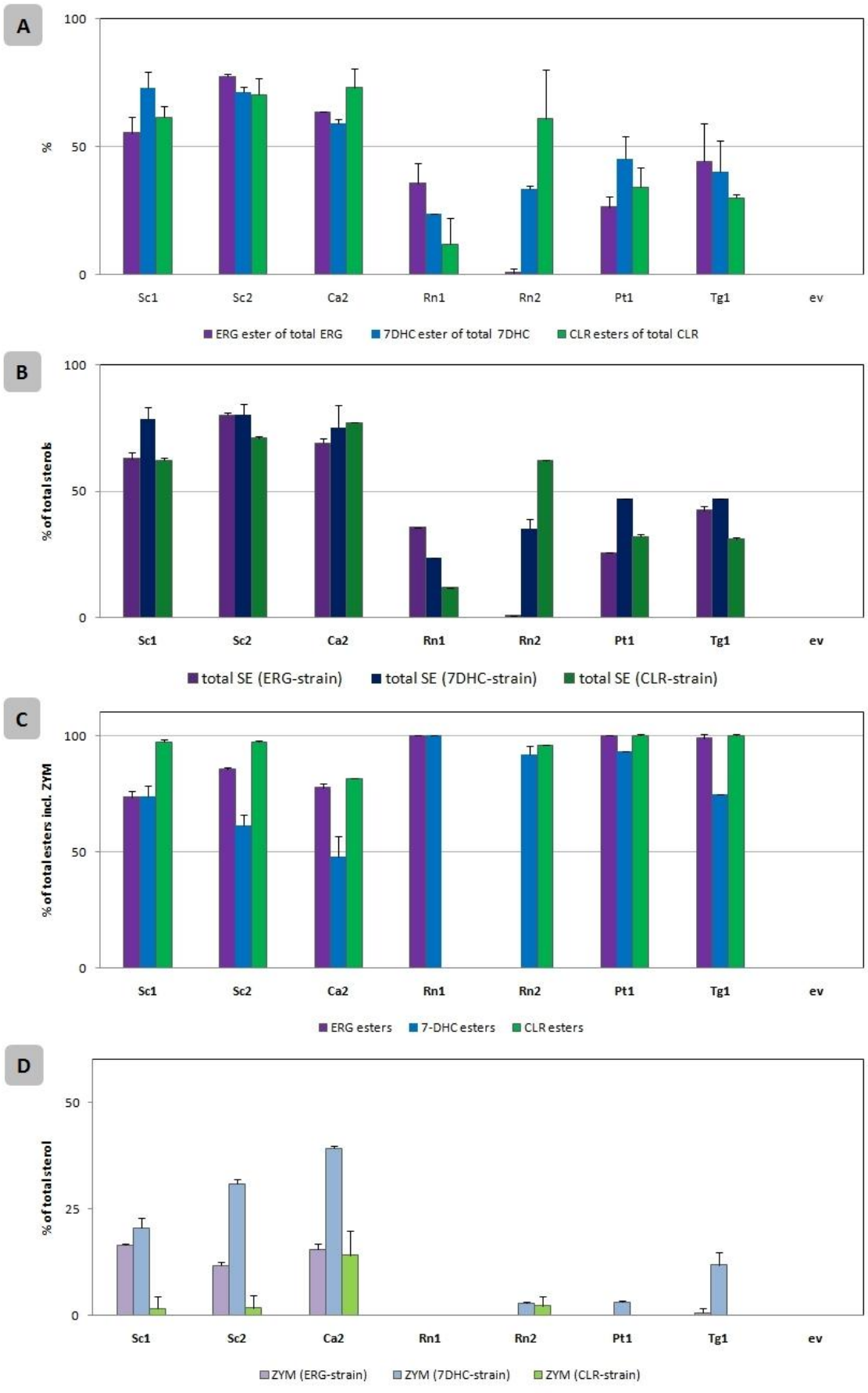

Figure 31: Strain specific relative sterol ester (SE) distribution. Calculations with data from Figure 30. Chart **(A)** shows how much of the major sterol (ERG, 7DHC or CLR) was converted into SE. **(B)** Percentage of SE (major steryl and zymosteryl esters) among total sterols. **(C)** Percentage share of main sterol on SE. **(D)** Percentage share of zymosterol on total sterols.

3.3 Mutation of rat SOAT1 and SOAT2

With an Rn1 and Rn2 shuffling attempt, we tried to reverse the sterol specificity of these SOATs by exchanging large protein regions. Unfortunately, time limitations restricted our analysis to only three combinations. For simplicity reasons, the two central fragments from the original annotation $X_AX_BX_CX_D$ will be combined and shortened to $X_AX_BX_C$ here. Sequencing results verified the combinations 111, 222, 212, 112 and 221 shown in Figure 32. In this first try, none of the generated shuffling products showed an increase in activity when expressed in ERG-and CLR-strains (Figure 33). Contrarily, most of them produced only traces of steryl esters compared to amounts from vector controls. Cultivation conditions differed from previous HPLC data and so did control results. We can give a hunch, that exchanging the C-terminal X_C or middle part X_B for the more active SOAT part retained some of the activity, whereas permutation of the N-terminal part had no effect. But, we should not jump to any conclusions here without completing this study.

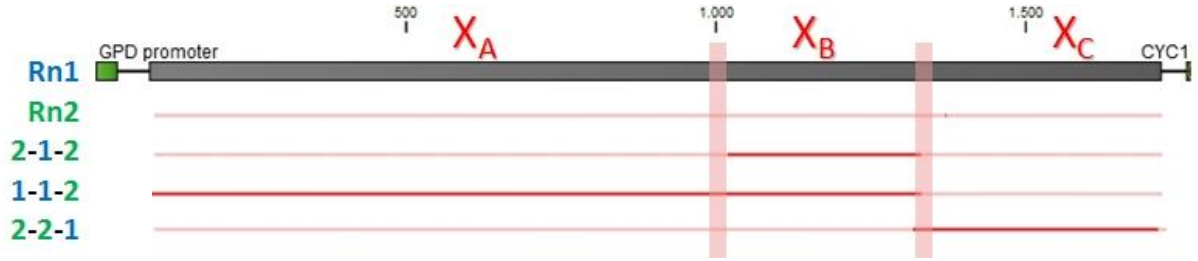

Figure 32: Rn1 and Rn2 shuffling. Schematic view on sequencing results of mutant SOAT isoenzymes from *R. norvegicus*.

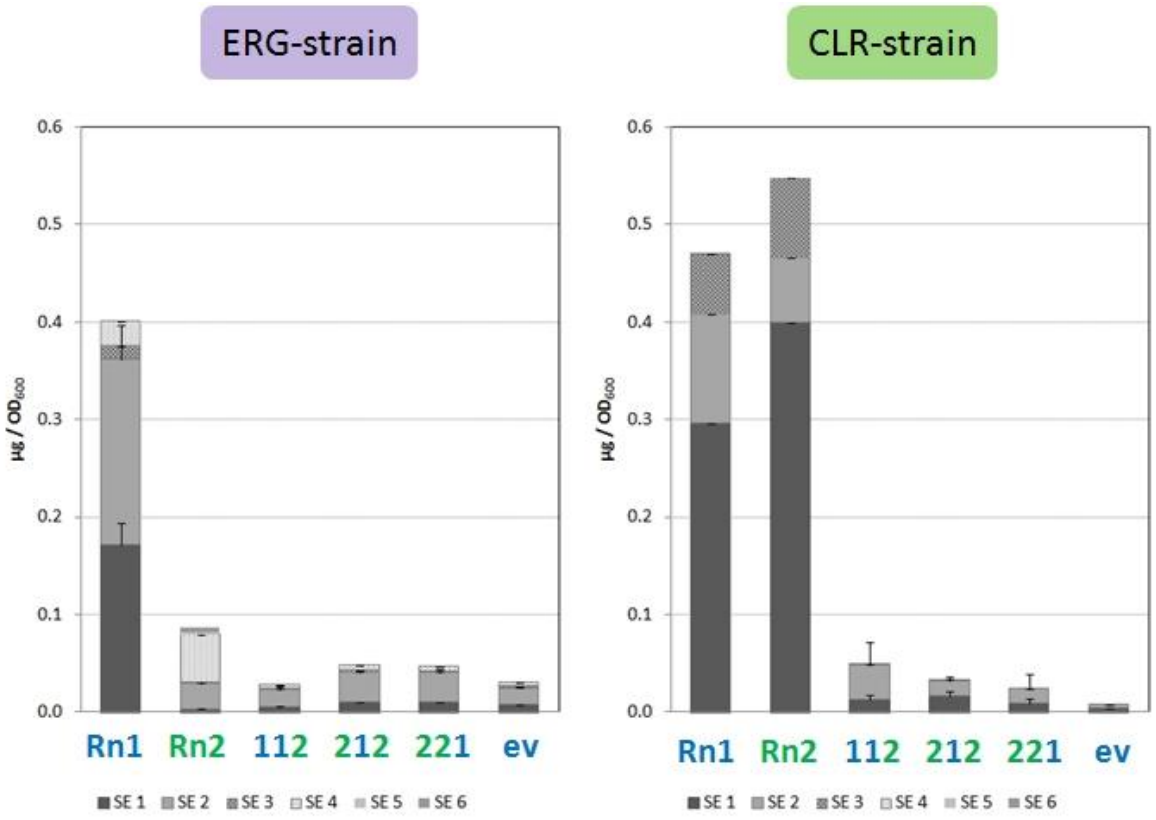

Figure 33: Activity of generated mutants. Sterol esters produced by Rn1, Rn2 and shuffling products in the ERG- or CLR-strain.

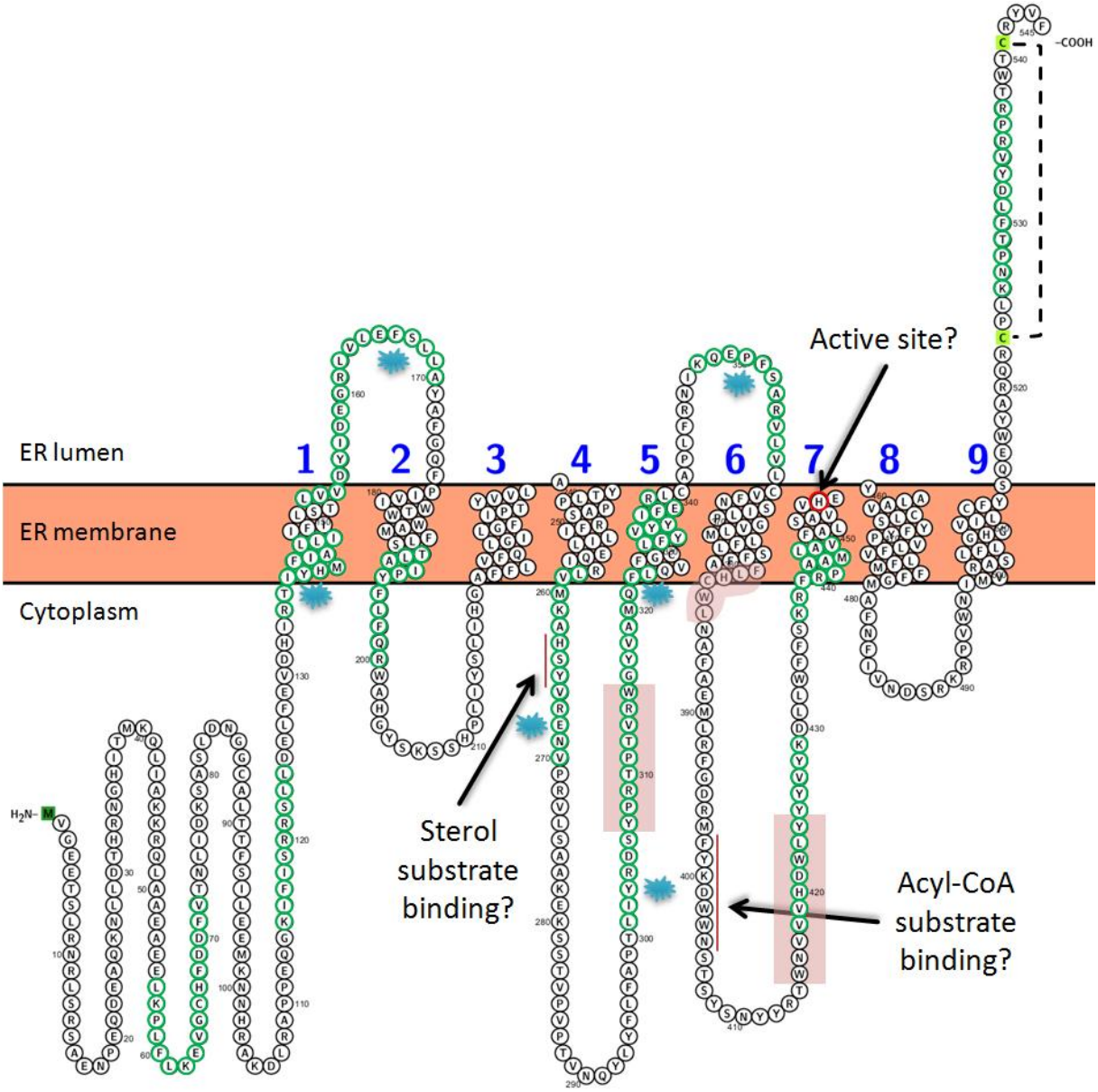

Figure 34: Rat SOAT1 topology model. Topology was generated with Protter (Omasits et al. 2014) using TMD annotation from UniProt (O70536). Potential CLR binding sites (green circles) detected by Prosite scan using patterns: (L/V)-X_{1-5}-(Y)-X_{1-5}-(K/R) and (K/R)-X_{1-5}-(Y/F)-X_{1-5}-(L/V), conserved within SOAT2 (blue stars). Potential binding sites described in literature (red bars) and putative active site (red circle). Conserved regions used for Rn1/Rn2 mutagenesis study (red boxes). Dashed line indicates possible disulfide bridge.

4 CONCLUSION AND OUTLOOK

In the course of this thesis, samples from over hundred multi-day yeast cultivations were analyzed with different methods for lipid and protein detection and thus generated an enormous amount of data. The evaluation of gas chromatography-mass spectrometry results led to a deeper understanding about the effects on total sterol distribution in sterol-pathway modified yeast. First of all, we observed a decrease in sterol diversity, possibly due to boosted pathway flux towards the end products ergosterol, 7-dehydrocholesterol or cholesterol. Many sterol-O-acyltransferases are capable of further increasing the amount of total sterols up to 1.6-fold, furthermore elevating the levels of some intermediates according to their substrate tolerance. With the benefit of high performance liquid chromatography we easily and consistently quantified esters and free sterols in our SOAT expression strains. Summing up our findings about the diverse sets of selected microbial and mammalian enzymes, SOAT activities dramatically changed in different strain backgrounds. In the group of yeast derived enzymes, *S. cerevisae* SOAT2 was the most active on ergosterol, SOAT1 the most active on 7-DHC and *C. albicans* SOAT2 the most active on cholesterol. Enzymes from the other species showed generally lower activities, which could be a result of lower expression levels. *T. gondii* and *P. troglodytes* SOAT1 were relatively substrate tolerant. On the other hand, SOAT1 and SOAT2 from *R. norvegicus* showed opposite substrate specificities, which could be associated with mammalian tissue specific expression pattern of both isoenzymes and different physiological roles. Therefore, it would be interesting to target Pt2 and other isoenzyme pairs in future studies. Possibly, an extreme difference in sterol specificity of SOATs is a typical mammalian trait and has evolved due to specialized tissue functions. Furthermore, results from protein analysis indicate that expression alone can only account for little impact on SOAT activity, so there must be other regulatory mechanisms involved like, for example, the formation of homo- or hetero-multimers.

More broadly speaking, the results indicate that sterols have strong influence on SOAT function in the role as substrates and likely as activator through interaction at several binding sites. Our approach contributes to a more complete picture about sterol and steroid homeostasis and complements preliminary *in vivo* and *in vitro* assay findings. Taking advantage of differences in enzyme substrate utilization, directed mutagenesis of the rat isoenzymes might provide insight into the molecular mechanisms behind sterol substrate specificity of SOATs. Although incomplete, exchanging some of the protein domains was worth the try and is an approach in the right direction. Yet shorter fragment and site directed exchanges would be the best strategy to follow in further studies. Future work should build on that by incorporating other SOATs and further sterol-modified strains into the assay. For instance, it would be interesting to test oxysterols like 25-hydroxycholesterol. By modulating or fine tuning of sterol levels such as 50% cholesterol, 50% 7-DHC or other intermediates, one could take this assay to the next level. Also modulating the pool of fatty

acyl-CoAs might expose unexpected specificities for the second substrate of SOATs. Nevertheless, all the information will be difficult to inteprete without a good working model. Therefore, it is inevitable to promote the work for crystal structure analysis to get insights into catalytic and regulatory mechanisms or performing topology studies to verify predicted transmembrane domains as it was accomplished for the Ghrelin O-Acyltransferase (Taylor et al. 2013). Our results may support engineering of an advanced sterol acyltransferase for improved production of industrially relevant sterols. Ultimately, the generated data will inevitably raise our understanding of the molecular interactions governing acyltransferase function.

5 REFERENCES

Acimovic J and Rozman D (2013) Steroidal triterpenes of cholesterol synthesis. Molecules 18:4002–4017.

Alegret M, Llaverias G and Silvestre JS (2004) Acyl coenzyme A:cholesterol acyltransferase inhibitors as hypolipidemic and antiatherosclerotic drugs. Methods Find Exp Clin Pharmacol, 26:563-586.

Ashe MP and Bill RM (2011) Mapping the yeast host cell response to recombinant membrane protein production: relieving the biological bottlenecks. Biotechnol J. 6:707-714.

Buhman KF, Accad M and Farese RV (2000) Mammalian acyl-CoA:cholesterol acyltransferases. Biochim Biophys Acta. 1529:142-154.

Chang CC, Huh HY, Cadigan KM and Chang TY (1993) Molecular cloning and functional expression of human acyl-coenzyme A:cholesterol acyltransferase cDNA in mutant Chinese hamster ovary cells. J Biol Chem. 268:20747-20755.

Chang CC, Miyazaki A, Dong R, Kheirollah A, Yu C, Geng Y, Higgs HN and Chang TY (2010) Purification of Recombinant Acyl-Coenzyme A:Cholesterol Acyltransferase 1 (ACAT1) from H293 Cells and Binding Studies Between the Enzyme and Substrates Using Difference Intrinsic Fluorescence Spectroscopy. Biochemistry, 49:9957–9963.

Chang TY, Chang CC and Cheng D (1997) Acyl-coenzyme A:cholesterol acyltransferase. Annu Rev Biochem. 66:613-638.

Chang TY, Chang CC, Ohgami N and Yamauchi Y (2006) Cholesterol sensing, trafficking, and esterification. Annu Rev Cell Dev Biol. 22:129–157.

Chang TY, Li BL, Chang CC, Urano Y (2009) Acyl-coenzyme A:cholesterol acyltransferases. Am J Physiol Endocrinol Metab. 297:E1-9.

Cherezov V, Rosenbaum DM, Hanson MA, Rasmussen SG, Thian FS, Kobilka TS, Choi HJ, Kuhn P, Weis WI, Kobilka BK and Stevens RC (2007) High-resolution crystal structure of an engineered human beta2-adrenergic G protein-coupled receptor. Science 318(5854):1258–1265.

Daum G, Wagner A, Czabany T and Athenstaedt K (2007) Dynamics of neutral lipid storage and mobilization in yeast. Biochimie. 89:243–248.

Emmerstorfer A, Wriessnegger T, Hirz M and Pichler H (2014) Overexpression of membrane proteins from higher eukaryotes in yeasts. Appl Microbiol Biotechnol. 98(18):7671-7698.

Fahy E, Subramaniam S, Brown HA, Glass CK, Merrill AH Jr, Murphy RC, Raetz CR, Russell DW, Seyama Y, Shaw W, Shimizu T, Spener F, van Meer G, VanNieuwenhze MS, White SH, Witztum JL and Dennis EA (2005) A comprehensive classification system for lipids. J Lipid Res. 46(5): 839–861.

Fantini J and Barrantes FJ (2013) How cholesterol interacts with membrane proteins: an exploration of cholesterol-binding sites including CRAC, CARC, and tilted domains. Front Physiol. 4:31.

Farese RV Jr. (2006) The nine lives of ACAT inhibitors. Arterioscler Thromb Vasc Biol. 26(8):1684-1886.

Fazio S, Dove DE and Linton MF (2005) ACAT inhibition: bad for macrophages, good for smooth muscle cells? Arterioscler Thromb Vasc Biol. 25(1):7-9.

Folch J, Lees M and Stanley GHS (1957) A simple method for the isolation and purification of total lipids from animal tissues. Journal of Biological Chemistry. 226:497-506.

Gimpl G and Fahrenholz F (2002) Cholesterol as stabilizer of the oxytocin receptor. Biochim Biophys Acta 1564:384–392.

Gimpl G, Burger K and Fahrenholz F (1997) Cholesterol as modulator of receptor function. Biochemistry. 36:10959–10974.

Head BP, Patel HH and Insel PA (2014) Interaction of membrane/lipid rafts with the cytoskeleton: impact on signaling and function: Membrane/Lipid Rafts, Mediators of Cytoskeletal Arrangement and Cell Signaling. Biochimica et Biophysica Acta. 1838(2):532-45.

Hirz M, Richter G, Leitner E, Wriessnegger T and Pichler H (2013) A novel cholesterol-producing Pichia pastoris strain is an ideal host for functional expression of human Na, K-ATPase α3β1 isoform. Appl Microbiol Biotechnol. 97:9465–9478.

Kanungo S, Soares N, He M and Steiner RD (2013) Sterol metabolism disorders and neurodevelopment—an update. Dev Disabil Res Revs. 17:197–210.

Kim KY, Shin YK, Park JC, Kim JH, Yang H, Han DM, and Paik YK (2004) Molecular cloning and biochemical characterization of Candida albicans acyl-CoA:sterol acyltransferase, a potential target of antifungal agents. Biochemical and biophysical research communications. 319(3):911–919.

Kristan K and Rižner TL (2012) Steroid-transforming enzymes in fungi. J Steroid Biochem Mol Biol. 129:79–91.

Lee SS, Li J, Tai JN, Ratliff TL, Park K and Cheng JX (2015) Avasimibe Encapsulated in Human Serum Albumin Blocks Cholesterol Esterification for Selective Cancer Treatment. ACS Nano. 9(3), 2420-2432.

Levitan I, Singh DK and Rosenhouse-Dantsker A (2014). Cholesterol binding to ion channels. Frontiers in Physiology. 5:65.

Li H, and Papadopoulos V (1998) Peripheral-type benzodiazepine receptor function in cholesterol transport. Identification of a putative cholesterol recognition/interaction amino acid sequence and consensus pattern. Endocrinology 139:4991–4997.

Lucero HA and Robbins PW (2004) Lipid rafts-protein association and the regulation of protein activity. Arch Biochem Biophys. 426:208–224.

M. Opekarova, W. Tanner (2003). Specific lipid requirements of membrane proteins - a putative bottleneck in heterologous expression. Biochimica et Biophysica Acta. 1610:11–22.

Masumoto N, Lanyon-Hogg T, Rodgers UR, Konitsiotis AD, Magee AI and Tate EW (2015) Membrane bound O-acyltransferases and their inhibitors. Biochem Soc Trans. 43(2):246-52.

Matsuda H, Hakamata H, Kawasaki T, Sakashita N, Miyazaki A, Takahashi K, Shichiri M and Horiuchi S (1998). Molecular cloning, functional expression and tissue distribution of rat acyl-coenzyme A:cholesterol acyltransferase. Biochim Biophys Acta. 1391(2):193-203.

Müllner H and Daum G (2004) Dynamics of neutral lipid storage in yeast. Acta Biochim Pol. 51(2):323-347.

Müllner H, Deutsch G, Leitner E, Ingolic E and Daum G (2005) YEH2/YLR020c Encodes a Novel Steryl Ester Hydrolase of the Yeast Saccharomyces cerevisiae. J Biol Chem. 280:13321-13328.

Murphy SR, Chang CC, Dogbevia G, Bryleva EY, Bowen Z, Hasan MT and Chang TY (2013) Acat1 Knockdown Gene Therapy Decreases Amyloid-β in a Mouse Model of Alzheimer's Disease. Molecular Therapy. 21(8):1497–1506.

Nishikawa Y, Quittnat F, Stedman TT, Voelker DR, Choi JY, Zahn M, Yang M, Pypaert M, Joiner KA and Coppens I (2005) Host cell lipids control cholesteryl ester synthesis and storage in intracellular Toxoplasma. Cell Microbiol. 7(6):849-867.

Oelkers P, Behari A, Cromley D, Billheimer JT and Sturley SL (1998) Characterization of two human genes encoding acyl coenzyme A:cholesterol acyltransferase-related enzymes. J Biol Chem. 273(41):26765-26771.

Omasits U, Ahrens CH, Müller S and Wollscheid B (2014) Protter: interactive protein feature visualization and integration with experimental proteomic data. Bioinformatics. 30:884–886.

Opekarova M (2003) Specific lipid requirements of membrane proteins? A putative bottleneck in heterologous expression. Biochim Biophys Acta. 1610:11–22.

Pagac M, de la Mora HV, Duperrex C, Roubaty C, Vionnet C and Conzelmann A (2011) Topology of 1-Acyl-sn-glycerol-3-phosphate Acyltransferases SLC1 and ALE1 and Related Membrane-bound O-Acyltransferases (MBOATs) of Saccharomyces cerevisiae. The Journal of Biological Chemistry. 286(42):36438–36447.

Petschacher B (2014) Sterol and Sterol Ester Analysis by HPLC. ACIB protocol.

Porter FD and Herman GE (2011) Malformation syndromes caused by disorders of cholesterol synthesis. Journal of Lipid Research. 52(1):6–34.

Quail MA and Kelly SL (1996) The extraction and analysis of sterols from yeast. Methods Mol Biol. 53:123–131

Rogers MA, Liu J, Kushnir MM, Bryleva E, Rockwood AL, Meikle AW, Shapiro D, Vaisman BL, Remaley AT, Chang CC and Chang TY (2012) Cellular pregnenolone esterification by acyl-CoA:cholesterol acyltransferase. J Biol Chem. 287(21):17483-17492.

Rogers MA, Liu J, Song BL, Li BL, Chang CC and Chang TY (2014) Acyl-CoA:cholesterol acyltransferases (ACATs/SOATs): Enzymes with multiple sterols as substrates and as activators. J Steroid Biochem Mol Biol. in press.

Rong JX, Kusunoki J, Oelkers P, Sturley SL and Fisher EA (2005) Acyl-coenzymea (coa):Cholesterol acyltransferase inhibition in rat and human aortic smooth muscle cells is nontoxic and retards foam cell formation. Arterioscler Thromb Vasc Biol. 25:122–127.

Santa Cruz Biotechnology, Inc., List of ACAT/SOAT inhibitors (http://www.scbio.de/chemicals-table-acat_inhibitors.html) online 04.2015.

Seo T, Oelkers PM, Giattina MR, Worgall TS, Sturley SL and Deckelbaum RJ (2001) Differential modulation of ACAT1 and ACAT2 transcription and activity by long chain free fatty acids in cultured cells. Biochemistry. 2001 Apr 17;40(15):4756-62.

Souza CM and Pichler H (2007) Lipid requirements for endocytosis in yeast. Biochim. Biophys. Acta 1771, 442–454.

Souza CM, Schwabe TM, Pichler H, Ploier B, Leitner E, Guan XL, Wenk MR, Riezman I and Riezman H (2011) A stable yeast strain efficiently producing cholesterol instead of ergosterol is functional for tryptophan uptake, but not weak organic acid resistance. Metab. Eng., doi:10.1016/j.ymben.2011.06.006.

Stolterfoht H (2014) TLC based Screening of Sterol O-Acyltransferases. ACIB protocol

Taylor MS, Ruch TR, Hsiao PY, Hwang Y, Zhang P, Dai L, Huang CR, Berndsen CE, Kim MS, Pandey A, Wolberger C, Marmorstein R, Machamer C, Boeke JD and Cole PA (2013). Architectural organization of the metabolic regulatory enzyme ghrelin O-acyltransferase. J Biol Chem. 2013 Nov 8;288(45):32211-28. doi: 10.1074/jbc.M113.510313. Epub 2013 Sep 17.

Te Welscher YM, ten Napel HH, Balague MM, Souza CM, Riezman H, de Kruijff B and Breukink E (2008) Natamycin blocks fungal growth by binding specifically to ergosterol without permeabilizing the membrane. J. Biol. Chem. 283, 6393–6401.

Trenin AS (2013) [Microbial metabolites that inhibit sterol biosynthesis, their chemical diversity and characteristics of mode of action]. Bioorganicheskaya Khimiya, 2013, Vol. 39, No. 6, pp. 633–657. Published in Russian.

Volland C, Urban-Grimal D, Géraud G and Haguenauer-Tsapis R (1994) Endocytosis and degradation of the yeast uracil permease under adverse conditions. The Journal of biological chemistry, vol. 269, no. 13, pp. 9833–41.

Wagner A, Grillitsch K, Leitner E and Daum G (2009) Mobilization of steryl esters from lipid particles of the yeast Saccharomyces cerevisiae. Biochimica et biophysica acta, vol. 1791, no. 2, pp. 118–24, Feb. 2009.

Wriessnegger T and Pichler H (2013) Yeast metabolic engineering-targeting sterol metabolism and terpenoid formation. Prog Lipid Res. 2013 Jul;52(3):277-93.

Yang H, Bard M, Bruner DA, Gleeson A, Deckelbaum RJ, Aljinovic G, Pohl TM, Rothstein R and Sturley SL (1996) Sterol esterification in yeast: a two-gene process.," Science (New York, N.Y.), vol. 272, no. 5266, pp. 1353–6, May 1996.

Yue S, Li J, Lee SY, Lee HJ, Shao T, Song B, Cheng L, Masterson TA, Liu X, Ratliff TL and Cheng JX (2014) Cholesteryl Ester Accumulation Induced by PTEN Loss and PI3K/AKT Activation Underlies Human Prostate Cancer Aggressiveness. Cell Metabolism, 19(3), 393–406.

Zhang M, Wu JF, Chen WJ, Tang SL, Mo ZC, Tang YY, Li Y, Wang JL, Liu XY, Peng J, Chen K, He PP, Lv YC, Ouyang XP, Yao F, Tang DP, Cayabyab FS, Zhang DW, Zheng XL, Tian GP and Tang CK (2014). MicroRNA-27a/b regulates cellular cholesterol efflux, influx and esterification/hydrolysis in THP-1 macrophages. Atherosclerosis 2014;234:54-64.

Zhang Y, Yu C, Liu J, Spencer TA, Chang CC and Chang TY (2003) Cholesterol is superior to 7-ketocholesterol or 7 alpha-hydroxycholesterol as an allosteric activator for acyl-coenzyme A:cholesterol acyltransferase 1. J Biol Chem. 2003;14:11642–11647.

Zweytick D, Leitner E, Kohlwein SD, Yu Chunjiang, Rothblatt J and Daum G (2000) Contribution of Are1p and Are2p to steryl ester synthesis in the yeast Saccharomyces cerevisiae. Eur. J. Biochem. 267, 1075-1082.

APPENDIX

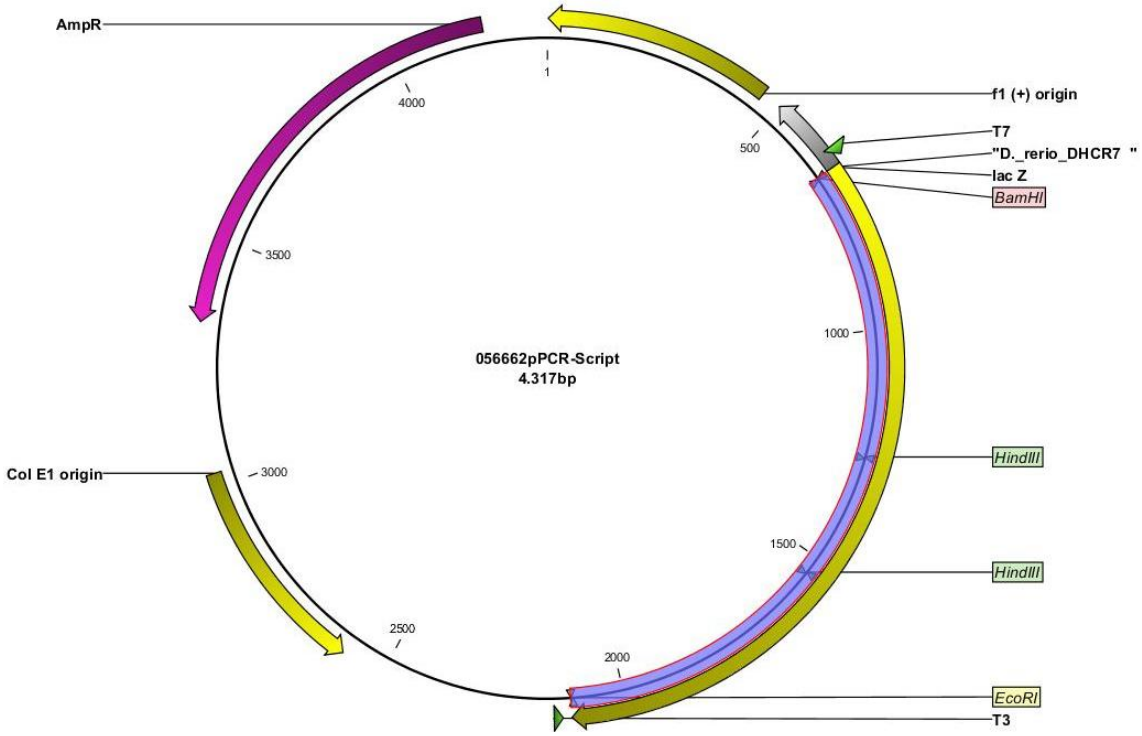

Figure 35: Schematic view of cloning vector 056662pPCR-Script. Purple shaded area corresponds to CDS of *DHCR7*. Synthetic gene 056662 (*DHCR7*) was assembled from synthetic oligonucleotides by GENEART GmbH.

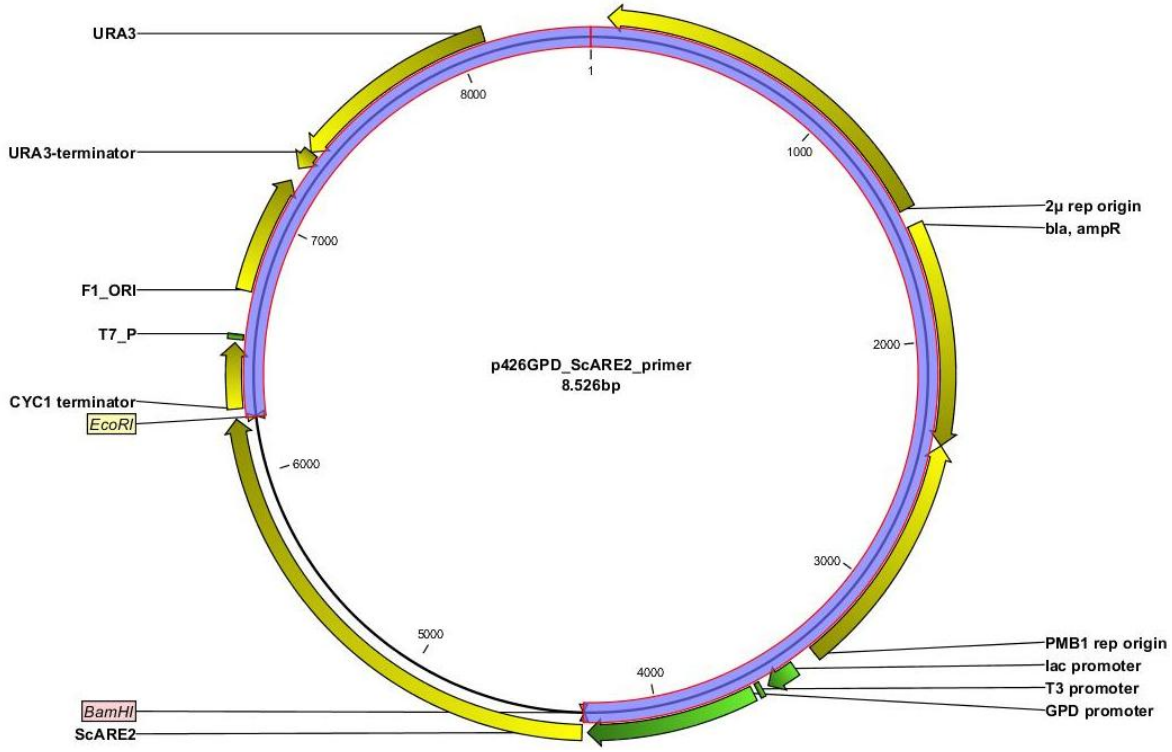

Figure 36: Schematic view of expression vector p426GPD_ARE2. Purple shaded area corresponds to vector backbone used for ligation after double digest.

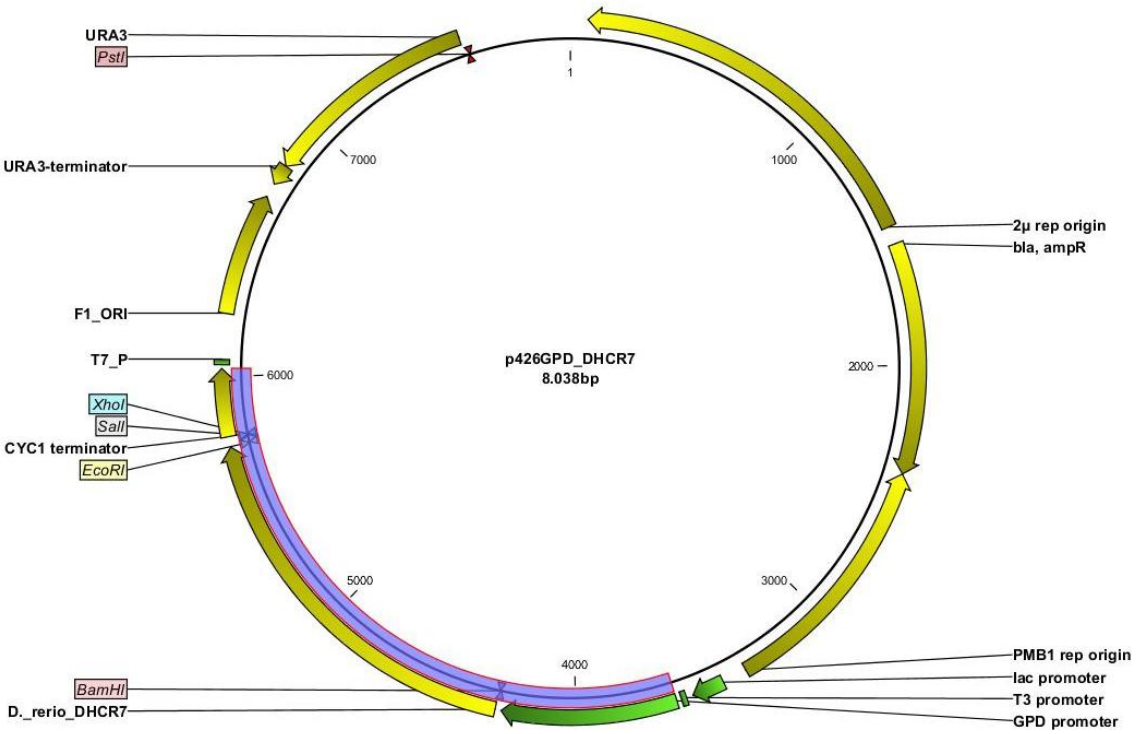

Figure 37: Schematic view of expression vector p426GPD_DHCR7. Purple shaded area corresponds to the sequence used for the *7R-fragment* PCR product containing *TDH3* promoter, *DHCR7* coding sequence and *CYC1* terminator.

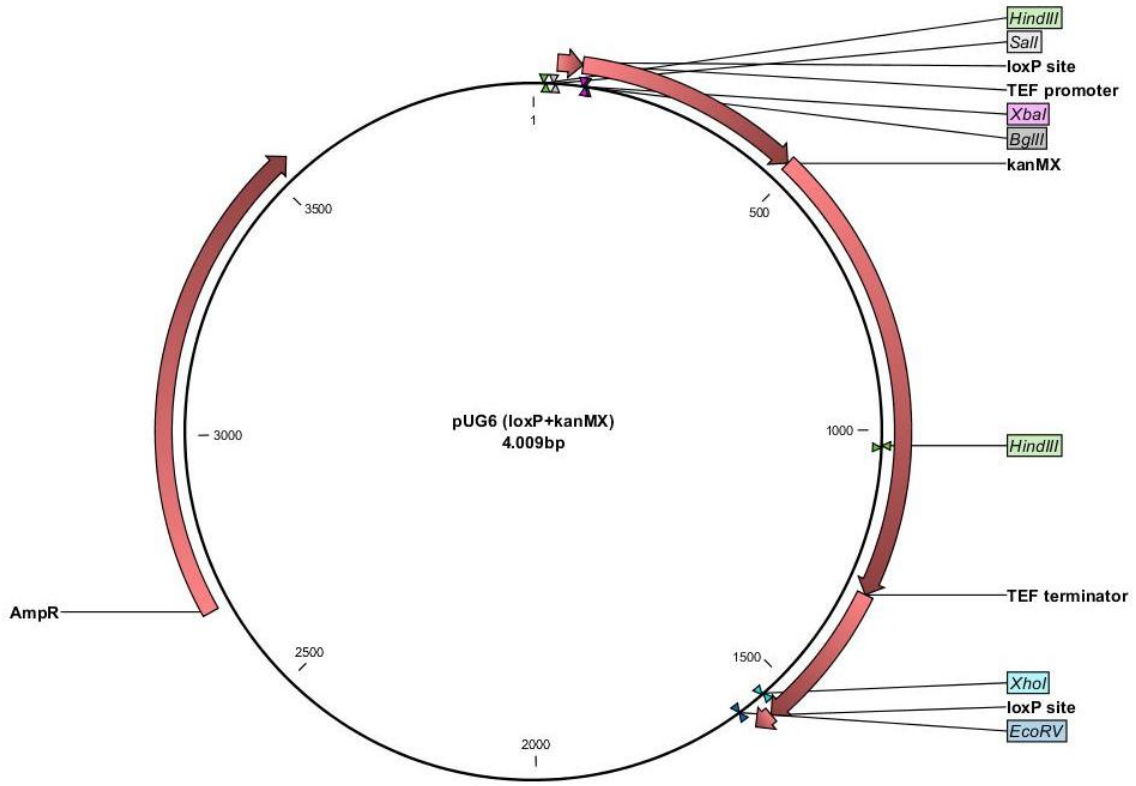

Figure 38: Schematic view of expression vector pUG6.

Table 16: Total sterol analysis by GC-MS measurement. Ergosta-compounds are not included into sum of area peaks.

sample	retention time	area	% of total area
BA-C I a	26.097	85299348	99.16
	26.210	448593	0.52
	26.330	866090	
	26.769	525519	
	26.928	270500	0.31
	27.432	26538367	
	27.650	738571	
	27.878	756429	
		86018441	
BA-C I b	26.104	86833960	99.22
	26.217	433692	0.50
	26.337	950782	
	26.774	538983	
	26.925	247901	0.28
	27.431	25991100	
	27.660	753996	
	27.878	820519	
		87515553	
BA-C II a	26.112	95110147	99.21
	26.217	509412	0.53
	26.334	1055177	
	26.778	582995	
	26.934	252382	0.26
	27.441	32661095	
	27.662	819965	
	27.876	798012	
		95871941	
BA-C II b	26.110	94436002	99.41
	26.219	357391	0.38
	26.332	667180	
	26.780	608401	
	26.931	203128	0.21
	27.433	34449781	
	27.665	963881	
	27.880	798435	
		94996521	
BA-C III a	26.124	115930433	99.35
	26.216	514364	0.44
	26.332	1038604	
	26.779	858679	
	26.931	247590	0.21
	27.442	39219873	
	27.663	1120460	
	27.881	1091386	
		116692387	
BA-C III b	26.112	94897440	99.19
	26.223	536304	0.56
	26.343	870309	
	26.780	691828	
	26.929	236097	0.25
	27.435	31498212	
	27.660	906065	
	27.884	762608	
		95669841	